

MULTISCALE ANALYSIS OF HETEROGENEOUS MEDIA  
FOR LOCAL AND NONLOCAL CONTINUUM THEORIES

A Dissertation

Submitted to the Graduate Faculty of the  
Louisiana State University and  
Agricultural and Mechanical College  
in partial fulfillment of the  
requirements for the degree of  
Doctor of Philosophy

in

The Department of Mathematics

by

Bacim Alali

B.S., Yarmouk University, 1998

M.S., Louisiana State University, 2005

August 2008

# Dedication

*To my father Qassim Alali and my mother Wedad Alali.*

*To my wife Zubieda and my sons Ahmed and Ibrahim.*

*To my sisters Tharwat, Maysoon, and Aya.*

*To my brothers Feras, Walid, Abdulkareem, and Ismael.*

*To my teacher and friend Othman Malhas.*

# Acknowledgments

All praise is due to God, the Lord of the Worlds.

I would like to express my sincere gratitude to my research advisor Professor Robert Lipton, who has been extremely generous with his insight and knowledge. He has also supported me financially through several grants. All of his help and guidance made this possible.

I am very grateful for the financial support given to me by different organizations throughout my time at LSU. This work has been funded by grants from the National Science Foundation, the Air Force Office of Scientific Research, and The Boeing Company.

I am grateful for all the help that I have received from the faculty members and fellow students at the mathematics department. I am particularly grateful to professors Neubrandner, Oxley, Richardson, Shipman, and Wolenski for their help and support.

I would like to thank Dr. Stewart Silling, Sandia National Laboratories, and Dr. Abe Askari, The Boeing Company, for the insightful discussions and helpful comments.

I would like to express my sincere gratitude to my undergraduate mathematics teacher Professor Othman Malhas, who had a major influence on me. I am deeply grateful for his encouragement and faith in me. I would like to thank my friend Hatem Zeine for his support during my time at Zeine Technological Applications, and for the stimulating and insightful discussions throughout the years.

Finally, I am forever grateful to my family for their prayers, love, and encouragement.

# Table of Contents

Dedication .....	ii
Acknowledgments .....	iii
List of Figures .....	viii
Abstract .....	ix
Introduction .....	1
<b>Chapter 1: Optimal Lower Bounds on Local Stress and Strain Fields in Random Media .....</b>	<b>5</b>
1.1 Introduction .....	5
1.2 Elastic Boundary Value Problem for Heterogeneous Media .....	7
<b>Chapter 2: Optimal Lower Bounds on the Local Stress Inside Ran- dom Composites .....</b>	<b>12</b>
2.1 Hydrostatic Applied Stress .....	12
2.1.1 Optimal Lower Bounds on the Local Stress Inside Material One .....	13
2.1.2 Optimal Lower Bounds on the Local Stress Inside Material Two .....	13
2.1.3 Optimal Lower Bounds on the $L^\infty$ Norm of the Local Stress	14
2.2 Deviatoric Applied Stress .....	14
2.2.1 Optimal Lower Bounds on the Moments of the Local Stress Inside the Phase with Higher Shear Modulus .....	15
2.2.2 Optimal Lower Bounds on the $L^\infty$ Norm of the Local Stress	15
2.3 Lower Bounds on the Local Stress that are Optimal for a Special Class of Imposed Macroscopic Stress States .....	16
2.3.1 Optimal Lower Bounds on the Local Stress Inside Material One for $\mu_1 = \mu_2$ .....	17
2.3.2 Optimal Lower Bounds on the Local Stress Inside Material Two for $\mu_1 = \mu_2$ .....	18
2.3.3 Optimal Lower Bounds on the Local Von Mises Equivalent Stress Inside Material One .....	18
2.3.4 Optimal Lower Bounds on the Local Von Mises Equivalent Stress Inside Material Two .....	19
2.4 Optimal Lower Bounds for General Imposed Macroscopic Stresses and $\mu_1 = \mu_2$ .....	19
2.4.1 Optimal Lower Bounds on the Local Hydrostatic Stress with $\mu_1 = \mu_2$ for Media Subjected to a General Imposed Stress ..	20

2.4.2	Optimal Lower Bounds on the $L^\infty$ Norm of the Local Hydrostatic Stress with $\mu_1 = \mu_2$ for Media Subjected to a General Imposed Stress . . . . .	20
2.5	Optimal Lower Bounds for General Imposed Macroscopic Stresses and $\kappa_1 = \kappa_2$ . . . . .	21
2.5.1	Optimal Lower Bounds on the Moments of the Local Von Mises Equivalent Stress Inside the Material with Greater Shear Modulus for $\kappa_1 = \kappa_2$ . . . . .	21
2.5.2	Optimal Lower Bounds on the $L^\infty$ Norm of the Von Mises Equivalent Stress for $\kappa_1 = \kappa_2$ . . . . .	22

**Chapter 3: Optimal Lower Bounds on the Local Strain Inside Random Composites . . . . . 23**

3.1	Imposed Hydrostatic Macroscopic Strain . . . . .	23
3.1.1	Optimal Lower Bounds on the Moments of the Local Strain in Material One . . . . .	24
3.1.2	Optimal Lower Bounds on the Moments of the Local Strain in Material Two . . . . .	24
3.1.3	Optimal Lower Bounds on the $L^\infty$ Norm of the Local Strain . . . . .	25
3.2	Deviatoric Applied Strain . . . . .	25
3.2.1	Optimal Lower Bounds on the Moments of the Local Strain Inside the Phase with Higher Shear Modulus . . . . .	26
3.3	Lower Bounds on the Local Strain that are Optimal for a Special Class of Imposed Macroscopic Strain States . . . . .	26
3.3.1	Optimal Lower Bounds on the Local Strain Inside Material One with $\mu_1 = \mu_2$ . . . . .	27
3.3.2	Optimal Lower Bounds on the Local Strain Inside Material Two with $\mu_1 = \mu_2$ . . . . .	28
3.3.3	Optimal Lower Bounds on the Deviatoric Component of the Local Strain Inside Material One . . . . .	28
3.3.4	Optimal Lower Bounds on the Deviatoric Component of the Local Strain Inside Material Two . . . . .	29
3.4	Optimal Lower Bounds for General Imposed Macroscopic Strains and $\mu_1 = \mu_2$ . . . . .	29
3.4.1	Optimal Lower Bounds on the Local Hydrostatic Strain Inside Material One with $\mu_1 = \mu_2$ for Media Subjected to a General Imposed Strain . . . . .	29
3.4.2	Optimal Lower Bounds on the Local Hydrostatic Strain Inside Material Two with $\mu_1 = \mu_2$ for Media Subjected to a General Imposed Strain . . . . .	30
3.4.3	Optimal Lower Bounds on the $L^\infty$ Norm of the Local Hydrostatic Strain for Composites Subjected to a General Imposed Strain and $\mu_1 = \mu_2$ . . . . .	30

3.5	Optimal Lower Bounds for General Imposed Macroscopic Strains and $\kappa_1 = \kappa_2$ . . . . .	31
3.5.1	Optimal Lower Bounds on the Moments of the Deviatoric Component of the Local Strain for a General Imposed Macroscopic Strain and $\kappa_1 = \kappa_2$ . . . . .	31
<b>Chapter 4: Lower Bounds on Local Stress and Strain Fields . . . . .</b>		<b>32</b>
4.1	Lower Bounds on Local Stress Fields . . . . .	32
4.1.1	Hydrostatic Applied Stress . . . . .	32
4.1.2	Deviatoric Applied Stress . . . . .	33
4.1.3	Lower Bounds on Stress Fields Subject to General Imposed Macroscopic Stresses and $\mu_1 = \mu_2$ . . . . .	36
4.1.4	Lower Bounds on Stress Fields Subject to General Imposed Macroscopic Stresses and $\kappa_1 = \kappa_2$ . . . . .	39
4.1.5	Form of $C^e$ for Mixtures of Two Elastically Isotropic Materials with Common Bulk Modulus. . . . .	40
4.1.6	Proof of (4.18) . . . . .	41
4.2	Lower Bounds on Local Strain Fields . . . . .	42
4.2.1	Hydrostatic Applied Strain . . . . .	42
4.2.2	Deviatoric Applied Strain . . . . .	42
4.2.3	Lower Bounds on the Local Strain for General Imposed Macroscopic Strains and $\mu_1 = \mu_2$ . . . . .	44
4.2.4	Lower Bounds on the Local Von Mises Strain for General Imposed Strains and $\kappa_1 = \kappa_2$ . . . . .	46
4.2.5	Proof of (4.65) . . . . .	47
<b>Chapter 5: Microstructures That Support Optimal Local Fields . .</b>		<b>48</b>
5.1	The Coated Sphere Construction and Optimal Lower Bounds on Local Stress and Strain Fields . . . . .	48
5.2	The Stress and Strain Fields Inside Simple Laminates and Optimal Bounds on Local Fields . . . . .	52
5.3	The Confocal Ellipsoid Assemblage and Optimal Lower Bounds on Local Stress and Strain Fields for Subsets of Imposed Macroscopic Loads . . . . .	57
<b>Chapter 6: Multiscale Analysis of Heterogeneous Media in the Peridynamic Formulation . . . . .</b>		<b>60</b>
6.1	Introduction . . . . .	60
6.2	The Peridynamic Formulation of Continuum Mechanics . . . . .	62
6.3	Three Peridynamic Models of Fiber-Reinforced Materials . . . . .	64
<b>Chapter 7: Multiscale Analysis Method for the Short-Range and Long-Range Bond Model . . . . .</b>		<b>70</b>
7.1	First Case . . . . .	71
7.1.1	The Macroscopic Equation . . . . .	72

7.1.2	The Cell–Problem . . . . .	72
7.1.3	Downscaling . . . . .	73
7.2	Second Case . . . . .	73
7.2.1	The Macroscopic Equation . . . . .	74
7.2.2	The Cell–Problem . . . . .	74
7.2.3	Downscaling . . . . .	75
7.3	Third Case . . . . .	75
7.3.1	The Macroscopic Equation . . . . .	75
7.3.2	The Cell–Problem . . . . .	76
7.3.3	Downscaling . . . . .	76
7.4	Fourth Case . . . . .	77
7.4.1	The Macroscopic Equation . . . . .	77
7.4.2	The Cell–Problem . . . . .	78
7.4.3	Downscaling . . . . .	78
<b>Chapter 8: Existence and Uniqueness Results for the Peridynamic Equation . . . . .</b>		<b>80</b>
<b>Chapter 9: Two-Scale Convergence and the Two-Scale Limit Equation . . . . .</b>		<b>87</b>
9.1	Two-Scale Convergence . . . . .	87
9.2	The Two-Scale Limit Equation . . . . .	89
<b>Chapter 10: The Macroscopic Equation and Downscaling . . . . .</b>		<b>104</b>
10.1	Derivation of the Macroscopic Equation . . . . .	104
10.2	Justifying the Downscaling Step . . . . .	106
10.2.1	First Case . . . . .	109
10.2.2	Second Case . . . . .	111
10.2.3	Third and Fourth Cases . . . . .	114
<b>Chapter 11: Fluctuating Long-Range Bond Model . . . . .</b>		<b>116</b>
11.1	Existence and Uniqueness Results . . . . .	118
11.2	Multiscale Analysis Using the Semigroups Approach . . . . .	121
11.2.1	Proof of (11.45) and (11.46) . . . . .	128
<b>References . . . . .</b>		<b>131</b>
<b>Vita . . . . .</b>		<b>137</b>

# List of Figures

5.1	Hashin-Shtrikman coated cylinder assemblage. . . . .	49
5.2	A rank-one layered material. . . . .	56
6.1	Fiber-reinforced composite. . . . .	62
6.2	New and old bond and displacements within the peridynamic horizon. . . . .	63
6.3	(a) Composite cube $Y$ . (b) Cross-section of $Y$ along the fiber direction. . . . .	65
6.4	Long-range bonds (horizon $\gamma$ ) and short-range bonds (horizon $\varepsilon\delta$ ). . . . .	67

# Abstract

The dissertation provides new multiscale methods for the analysis of heterogeneous media.

The first part of the dissertation treats heterogeneous media using the theory of linear elasticity. In this context, a methodology is presented for bounding the higher  $L^p$  norms,  $2 \leq p \leq \infty$ , of the local stress and strain fields inside random elastic media. Optimal lower bounds that are given in terms of the applied loading and the volume (area) fractions for random two-phase composites are presented. These bounds provide a means to measure load transfer across length scales relating the excursions of the local fields to applied loads.

The second part of the dissertation treats heterogeneous media using the peridynamic formulation of nonlocal continuum mechanics. In this context, a multiscale analysis method is presented for capturing the dynamics inside fiber-reinforced composites at both the structural scale and the microscopic scale. The method provides a multiscale numerical method with a cost that is much less than solving the full micro-scale model over the entire macroscopic domain.

# Introduction

This dissertation focuses on micromechanics, which is the analysis of multi-phase materials for which the length scales of the individual phases are small relative to characteristic length scales describing the greater body. The aim of micromechanics is to relate the gross macroscopical behavior of heterogeneous media to the details of their microscopical constitution<sup>1</sup>.

Many composite structures are hierarchical in nature and are made up of sub-structures distributed across several length scales. Examples include fiber reinforced laminates as well as naturally occurring structures like bone. From the perspective of failure initiation it is crucial to quantify the load transfer between length scales. It is common knowledge that the load transfer can result in local fields that are significantly greater than the applied macroscopic forces. The distribution of local fields is of great fundamental and practical importance in understanding many material properties<sup>2</sup>, such as breakdown phenomena [37] and the nonlinear behavior of composites [36].

This work focuses on the behavior of local fields in composite media. The analysis is carried out in the context of classical linear elasticity and in the context of the peridynamic theory of nonlocal continuum mechanics, recently introduced by Silling [62]. The goal in both cases is to compute the local field fluctuations about average macroscopic fields inside heterogeneous media.

In the first part of this dissertation, Chapters 1–5 , composites made from two linear isotropic elastic materials are considered. It is assumed that only the volume (area) fraction and elastic properties of each elastic material are known. Quantities

---

<sup>1</sup>Markov and Preziosi [45]

<sup>2</sup>Torquato [71]

useful for the study of load transfer include higher order moments of the stress and strain fields inside the composite. The higher moments are sensitive to local field concentrations generated by the interaction between the microstructure and the macroscopic load. These quantities have seen extensive application in the theoretical analysis of material failure, see [32]. In this work optimal lower bounds on the higher moments of the local stress and strain fields are established for several loading conditions. These bounds provide the minimum amount of local field amplification that can be expected from this class of composites.

The cases covered by this analysis do not yet provide the full story but they are significant and necessary for further developments in this area. The cases covered by this analysis include:

- Optimal lower bounds on the higher order moments and the  $L^\infty$  norm of the local stress and strain fields when the applied macroscopic loading is hydrostatic.
- Optimal lower bounds on the higher order moments and the  $L^\infty$  norm of the local stress and strain fields when the applied macroscopic loading is deviatoric.
- Optimal lower bounds on the higher order moments of the hydrostatic component of the local stress and strain fields for general applied macroscopic loading when the bulk moduli of the two materials are the same.
- Optimal lower bounds on the higher order moments and the  $L^\infty$  norm of the Von Mises equivalent stress and the deviatoric component of the strain for general applied macroscopic loading when the shear moduli of the two materials are the same.

- Optimal lower bounds on the higher order moments of the local stress and strain fields for a subspace of mixed mode loading characterized by a special dimensionless group of material parameters when the shear moduli of the two materials are the same.

The microgeometries that attain these bounds depend upon the macroscopic loading and material properties. Several distinguished parameter regimes are identified where the optimal configurations are given by layered materials, Hashin and Shtrikman coated sphere (cylinder) assemblages [27], or coated confocal ellipsoid (ellipse) assemblages [48, 68]. It is well-known that these microgeometries give extreme effective properties, see for example [2]. In this analysis, it is shown that these microgeometries give extreme field properties.

The second part of this dissertation, Chapters 6–11, aims at developing multi-scale analysis method for heterogeneous media in the peridynamic formulation of continuum mechanics. The peridynamic formulation is a nonlocal theory in which particles in a continuum interact with each other across a finite distance, as in molecular dynamics. The equation of motion in this theory is an integral equation, which does not include the spatial derivatives of the displacement field, rather than a partial differential equation as in the classical theory. These features allow for the damage to be incorporated at the level of these particle-interactions, so localization and fracture occur as a natural outgrowth of the equation of motion and constitutive models<sup>3</sup>.

Some theoretical aspects of peridynamic theory such as the motion of phase boundaries, nonlinear dispersion relations, and the dynamics of an infinite bar has been described in [11, 67, 73, 75]. A description of a meshfree numerical imple-

---

<sup>3</sup>Silling and Askari [65]

mentation for the peridynamic formulation is given in [65], where bond failure is related to the classical energy release rate in brittle fracture. The method is used in [66] to simulate the tearing of nonlinear membranes and failure of nanofiber networks. The numerical solution of the peridynamic equation, has been also studied in [13, 20]. Well-posedness of the linear peridynamic equation has been addressed in [13, 14]. In [15], it has been shown that the integral operator in the linear peridynamic equation of motion applied on a smooth function becomes in the limit of vanishing non-locality just the differential operator of the Navier equation of linear elasticity.

This work focuses on multiscale analysis of heterogeneous media using the peridynamic formulation. The objective is to capture the dynamics in composites at both the macroscopic scale and the microscopic scale with a cost that is much less than the cost of full microscale solvers. Capturing load transfer in the peridynamic context provides the ground work for understanding multiscale aspects of failure propagation inside heterogeneous media.

# Chapter 1

## Optimal Lower Bounds on Local Stress and Strain Fields in Random Media

### 1.1 Introduction

Over the last century major strides have been made in the characterization of effective constitutive laws relating average fluxes and gradients inside heterogeneous media see for example [25, 46, 48, 50, 60, 70, 71]. However the knowledge of effective properties alone are not sufficient for the quantitative description of load transfer across length scales. Suitable mathematical quantities need to be invoked that are sensitive to the presence of zones of high field values inside heterogeneous media. Such quantities include the  $L^p$  norms of the deviatoric and hydrostatic components of the local stress and strain. In this work we develop new methods for bounding the  $L^p$  norms of the local stress and strain in terms of the applied loading for  $2 \leq p \leq \infty$ . The bounds provide a means to measure load transfer across length scales relating the excursions of the local fields to the applied macroscopic loading. Earlier work along these lines has been carried out for uniform applied hydrostatic stress and strain and for uniform applied electric fields in random heterogeneous media see, [41] and [42], and [40]. Those efforts deliver optimal lower bounds on the  $L^p$  norms for the hydrostatic components of local stress and strain fields as well as the magnitude of the local electric field for all  $p$  in the range  $2 \leq p \leq \infty$ . In this treatment we build upon the earlier analysis and develop optimal lower bounds on the hydrostatic and deviatoric components of the local stress and strain fields for a ladder of progressively more complicated macroscopic load cases. In addition we provide optimal bounds on the sum of the magnitudes of both hydrostatic and deviatoric parts of the local stress and strain. The analysis is carried out for random

two phase linearly elastic composites made from two isotropic elastic materials in prescribed proportions. The bounds derived here quantify the minimum amount of stress and strain amplification that can be expected from this class of composites.

In this work we focus on lower bounds for the basic reason that volume constraints alone do not preclude the existence of microstructures with rough interfaces for which the  $L^p$  norms of local fields are divergent see [49], [17], and also [35]. It is now well known that finite upper bounds on the integral norms of local fields should be expected once one enforces a sufficient regularity of the interface separating two elastic materials, see [7], [8], [39], and [38].

Higher  $L^p$  norms of local fields are often used to describe phenomena related to failure initiation inside heterogeneous media. In the applications the  $L^\infty$  norm of the local field is used to describe the strength domain for both elastic–perfectly plastic, periodic fiber reinforced composites [23] and for random, rigid–perfectly plastic composites and polycrystals see for example [69], [61], [54], [59], [58], [19] [22], [33], [51]. For  $p < \infty$  the  $L^p$  norm of the local Von Mises stress is used in the description of failure probabilities see [3], [32], and [31].

We conclude noting that earlier work related to local field properties examines the stress field around a single inclusion subjected to a remote constant stress at infinity [74]. In that work an optimal lower bound is presented for the supremum of the maximum principal stress for a simply connected stiff inclusion embedded in an infinite elastic host. For a range of remote stresses it was shown that the class of optimal inclusion shapes are given by the ellipsoids. The more recent work presented in [24] provides an optimal lower bound on the supremum of the maximum principal stress for two-dimensional periodic composites consisting of a single simply connected stiff inclusion in the period cell. The bound is given in terms of the area fraction of the included phase and the eigenvalues of the average

uniform stress applied to the composite. For an explicit range of prescribed average stress the optimal inclusions are found to be given by the Vigdergauz [72] shapes. Recently the work of [28] builds on the earlier work of [41, 42] and develops lower bounds on the  $L^p$  norm of the local fields for statistically isotropic two-phase composites. However to date those bounds have been shown to be optimal only for  $p = 2$ , their optimality for  $p > 2$  remains to be seen. Optimal upper and lower bounds on the  $L^2$  norm of local gradient fields are given in [43].

The first part of the dissertation, Chapters 1-5, is organized as follows. In the next section we present the boundary value problem for two-phase elasticity. Chapters 2 and 3 provide lower bounds for a ladder of load cases of increasing generality. These lower bounds are derived in Chapter 4. The optimal microstructures that attain the lower bounds are introduced and discussed in Chapter 5.

In this part of the dissertation, we will adopt the notation of bold-face letters for vectors consistent with convention used in the Mechanics literature. For completeness we also introduce the following notation. The rank one matrix formed by taking the outer product of two unit vectors  $\mathbf{a}$  and  $\mathbf{b}$  is denoted by  $\mathbf{a} \otimes \mathbf{b}$  with elements  $(\mathbf{a} \otimes \mathbf{b})_{ij} = a_i b_j$ . The symmetric part of this matrix is denoted by  $\mathbf{a} \odot \mathbf{b}$  with elements  $(\mathbf{a} \odot \mathbf{b})_{ij} = (a_i b_j + a_j b_i)/2$ .

## 1.2 Elastic Boundary Value Problem for Heterogeneous Media

In this section we present the canonical boundary value problem used to describe elastic fields inside heterogeneous materials, [21], [30], [71], see also [48]. The heterogeneous medium occupies  $\mathbf{R}^d$ ,  $d = 2, 3$  and is composed of two elastically isotropic materials with elasticity tensors denoted by  $C^1$  and  $C^2$ . The bulk and shear moduli of material one and two are denoted by  $\kappa_1$  and  $\mu_1$ , and  $\kappa_2$  and  $\mu_2$  respectively. The geometry inside the heterogeneous material is specified by

the indicator functions of phase one and two given by  $\chi_1(\mathbf{x})$  and  $\chi_2(\mathbf{x})$ . Here  $\chi_1(\mathbf{x})$  takes the value 1 in phase one and zero outside and  $\chi_2(\mathbf{x}) = 1 - \chi_1(\mathbf{x})$ . The elastic tensor associated with the two phase medium is denoted by  $C(\mathbf{x})$  and  $C(\mathbf{x}) = \chi_1(\mathbf{x})C^1 + \chi_2(\mathbf{x})C^2$ .

The mean value of a field on  $\mathbf{R}^d$  is defined to be the limit of averages of the field over progressively larger volumes [21], [30], [71]. We denote the cube of side length  $r$  centered at a point  $\mathbf{x}$  by  $Q(r, \mathbf{x})$ . The mean value of a field  $f$  is given by

$$\langle f \rangle(\mathbf{x}) = \lim_{r \rightarrow \infty} \frac{1}{r^d} \int_{Q(r, \mathbf{x})} f(\mathbf{y}) d\mathbf{y}. \quad (1.1)$$

In what follows we will simply write  $\langle f \rangle$  to denote the mean value of a field. The medium is assumed statistically homogeneous in the sense that the mean values  $\langle \chi_1 \rangle$ ,  $\langle \chi_2 \rangle$  together with all higher order correlation functions are constants and do not depend on the centers of the cubes over which the averages are taken [71]. The volume (area) fractions of phase one and two are defined to be

$$\theta_1 = \langle \chi_1 \rangle \quad \text{and} \quad \theta_2 = \langle \chi_2 \rangle \quad (1.2)$$

and  $\theta_1 + \theta_2 = 1$ .

We impose a constant strain  $\bar{\epsilon}$  on the heterogeneous material and we seek a local elastic strain field  $\epsilon(\mathbf{x})$  of the form

$$\epsilon(\mathbf{x}) = \bar{\epsilon} + \hat{\epsilon}(\mathbf{x}) \quad (1.3)$$

where the fluctuation  $\hat{\epsilon}(\mathbf{x})$  satisfies  $\langle \hat{\epsilon} \rangle = 0$ . Hence  $\langle \epsilon \rangle$  is a constant function and  $\langle \epsilon \rangle = \bar{\epsilon}$ . The fluctuation is given in terms of the displacement field  $\hat{\mathbf{u}}$  with  $\hat{\epsilon}_{ij}(\mathbf{x}) = (\partial_j \hat{u}_i(\mathbf{x}) + \partial_i \hat{u}_j(\mathbf{x}))/2$  and we impose the condition  $\langle \hat{\mathbf{u}} \rangle(0) = 0$ . The fluctuation  $\hat{\mathbf{u}}$  satisfies  $\int_S (|\hat{\mathbf{u}}|^2 + |\hat{\epsilon}|^2) d\mathbf{x} < \infty$  for any bounded subset  $S$  of  $\mathbf{R}^d$ ,  $d = 2, 3$ . The local stress inside the composite is given by  $\sigma(\mathbf{x}) = C(\mathbf{x})\epsilon(\mathbf{x})$  and the equation of elastic

equilibrium inside each phase is given by

$$\operatorname{div} \sigma = 0. \quad (1.4)$$

It is assumed that there is perfect contact across interfaces separating the two materials. The traction at an interface with unit normal vector  $\mathbf{n}$  is denoted by the product  $\sigma \mathbf{n}$  and is the vector with components given by  $[\sigma \mathbf{n}]_i = \sigma_{ij} n_j$ , where summation is taken over repeated indices. Perfect contact implies that both the displacement  $\hat{\mathbf{u}}$  and traction  $\sigma \mathbf{n}$  are continuous across the two phase interface, i.e.,

$$\hat{\mathbf{u}}|_1 = \hat{\mathbf{u}}|_2, \quad (1.5)$$

$$\sigma|_1 \mathbf{n} = \sigma|_2 \mathbf{n}. \quad (1.6)$$

Here  $\mathbf{n}$  is the unit normal to the interface pointing into material 2 and the subscripts indicate the side of the interface that the displacement and traction fields are evaluated on.

The existence of the solution  $\hat{\mathbf{u}}$  follows from the Lax-Milgram Lemma [21], [30]. The boundary value problem just described is known to hold for almost every realization of a random two-phase medium associated with a stationary ergodic random elasticity field see, [55], [21], [30] and also [48], [71].

For this case the macroscopic constitutive law is given by the constant effective elasticity tensor  $C^e$  relating the mean stress to the mean strain

$$\langle \sigma \rangle_{ij} = C_{ijkl}^e \bar{\epsilon}_{kl}, \quad (1.7)$$

where repeated indices indicate summation. The effective elastic tensor is defined in terms of the solutions of six basis problems for three dimensional elasticity and three basis problems for two-dimensional elasticity. For three dimensional elastic problems we fix an orthonormal basis  $\mathbf{e}^1, \mathbf{e}^2, \mathbf{e}^3$  For  $i \leq j$  and  $i = 1, 2, 3$  we choose

as our constant strains  $\bar{\epsilon}^{ij} = \mathbf{e}^i \odot \mathbf{e}^j$ . The local strain fluctuation associated with  $\bar{\epsilon}^{ij}$  is denoted by  $\hat{\epsilon}^{ij}(\mathbf{x})$  and the formula for the effective elasticity tensor is given by

$$C_{ijkl}^e = \langle C_{mnop}(\bar{\epsilon}_{op}^{ij} + \hat{\epsilon}_{op}^{ij})\bar{\epsilon}_{mn}^{kl} \rangle. \quad (1.8)$$

The imposed strain  $\bar{\epsilon}$  is regarded as a macroscopic quantity and is referred to as the imposed macroscopic strain. The fields  $\sigma(\mathbf{x})$ ,  $\epsilon(\mathbf{x})$  provide the local response to the imposed macroscopic strain. The stress and strain fields  $\sigma(\mathbf{x})$ ,  $\epsilon(\mathbf{x})$  also give the local response to an imposed macroscopic stress  $\bar{\sigma} = \langle \sigma \rangle$ . This follows immediately by fixing  $\bar{\sigma}$  and choosing  $\bar{\epsilon}$  according to  $\bar{\epsilon}_{ij} = (C^e)_{ijkl}^{-1} \bar{\sigma}_{kl}$ .

In what follows we consider all statistically homogeneous configurations of two materials for which the volume fractions  $\theta_1$  and  $\theta_2$  are prescribed. The objective is to provide explicit optimal lower bounds on the local stress and strain in terms of the volume fractions, the elastic constants of the two materials, and the imposed macroscopic stress and strain  $\bar{\sigma}$  and  $\bar{\epsilon}$ .

We describe the various components of stress and strain tensors used in the bounds. Stress and strain tensor fields are represented by  $d \times d$  symmetric matrix valued fields with respect to a fixed coordinate system in  $\mathbf{R}^d$ ,  $d = 2, 3$ . Let  $\psi(\mathbf{x})$  and  $\eta(\mathbf{x})$  be two symmetric  $d \times d$  matrix valued fields defined on  $\mathbf{R}^d$ . Contractions of two  $d \times d$  matrix valued fields  $\psi$  and  $\eta$  are given by  $\psi : \eta = \psi_{ij}\eta_{ij}$  and  $|\psi|^2 = \psi : \psi$ . Products of fourth order tensors  $C$  and matrices  $\psi$  are written as  $C\psi$  and are given by  $[C\psi]_{ij} = C_{ijkl}\psi_{kl}$ ; and products of matrices  $\eta$  with vectors  $\mathbf{v}$  are given by  $[\eta\mathbf{v}]_i = \eta_{ij}v_j$ . The fourth order identity map on the space of  $d \times d$  matrices is denoted by  $\mathbf{I}$  and  $\mathbf{I}_{ijkl} = 1/2(\delta_{ik}\delta_{jl} + \delta_{il}\delta_{jk})$ . The projection onto the hydrostatic part of  $\psi(\mathbf{x})$  is denoted by  $\mathbf{\Pi}^H$  and is given explicitly by

$$\mathbf{\Pi}_{ijkl}^H = \frac{1}{d}\delta_{ij}\delta_{kl} \quad \text{and} \quad \mathbf{\Pi}^H\psi(\mathbf{x}) = \frac{\text{tr}\psi(\mathbf{x})}{d}I. \quad (1.9)$$

The projection onto the deviatoric part of  $\psi(\mathbf{x})$  is denoted by  $\mathbf{\Pi}^D$  and  $\mathbf{I} = \mathbf{\Pi}^H + \mathbf{\Pi}^D$ . When  $\psi(\mathbf{x})$  represents the local stress tensor, the well known Von Mises equivalent stress is given by  $|\mathbf{\Pi}^D\psi(\mathbf{x})|$ .

The isotropic elasticity tensor associated with each component material acts on strain fields and is written as

$$C^i = 2\mu_i\mathbf{\Pi}^D + d\kappa_i\mathbf{\Pi}^H, \text{ for } i = 1, 2, \quad (1.10)$$

where  $d = 2$  for planar elastic problems and  $d = 3$  for the three dimensional problem.

In what follows we will display lower bounds on the  $L^p$  norms of the local hydrostatic components of stress and strain given by  $\langle\chi_i(\mathbf{x})|\mathbf{\Pi}^H\sigma(\mathbf{x})|^p\rangle^{1/p}$  and  $\langle\chi_i(\mathbf{x})|\mathbf{\Pi}^H\epsilon(\mathbf{x})|^p\rangle^{1/p}$ , the  $L^p$  norm of the local deviatoric components  $\langle\chi_i(\mathbf{x})|\mathbf{\Pi}^D\sigma(\mathbf{x})|^p\rangle^{1/p}$  and  $\langle\chi_i(\mathbf{x})|\mathbf{\Pi}^D\epsilon(\mathbf{x})|^p\rangle^{1/p}$ , and the  $L^p$  norm of the full local stress and strain  $\langle\chi_i(\mathbf{x})|\sigma(\mathbf{x})|^p\rangle^{1/p}$  and  $\langle\chi_i(\mathbf{x})|\epsilon(\mathbf{x})|^p\rangle^{1/p}$ . The  $L^\infty$  norm of the magnitude of a quantity  $q$  taken over  $\mathbb{R}^d$  is denoted by  $\|q\|_\infty$ . The bounds will be derived for the full interval  $2 \leq p \leq \infty$ .

# Chapter 2

## Optimal Lower Bounds on the Local Stress Inside Random Composites

We present new optimal lower bounds on the local stress for a ladder of progressively more general sets of imposed macroscopic stress. As we progress to more general load cases we will apply additional hypotheses on the shear and bulk moduli of the constituent materials. In this section we provide lower bounds for the following applied macroscopic load cases: 1) lower bounds on the full local stress for imposed hydrostatic stresses, 2) lower bounds on the full local stress inside the material with larger shear modulus for elastic problems with imposed shear stress, 3) lower bounds on the full local stress for  $\mu_1 = \mu_2$ , that are seen to be optimal for a special class of imposed macroscopic stresses, 4) lower bounds on the local Von Mises equivalent stress that are optimal for a similar special class of imposed macroscopic stress fields, and 5) lower bounds on the hydrostatic and deviatoric components of the local stress for the full set of imposed macroscopic stresses subject to the hypotheses  $\mu_1 = \mu_2$  and  $\kappa_1 = \kappa_2$  respectively.

In what follows will adopt the notation  $\kappa_+ = \max\{\kappa_1, \kappa_2\}$ ,  $\mu_+ = \max\{\mu_1, \mu_2\}$ ,  $\kappa_- = \min\{\kappa_1, \kappa_2\}$ , and  $\mu_- = \min\{\mu_1, \mu_2\}$ .

### 2.1 Hydrostatic Applied Stress

In this section we consider imposed macroscopic stresses that are hydrostatic, i.e., of the form  $\bar{\sigma} = \bar{p}I$  where  $\bar{p}$  is a constant and  $I$  is the  $d \times d$  identity matrix. Here it is assumed that the elastic materials inside the heterogeneous medium are well-ordered i.e.,  $(\mu_1 - \mu_2)(\kappa_1 - \kappa_2) > 0$ . Without loss of generality we will suppose in this section that  $\mu_1 > \mu_2$  and  $\kappa_1 > \kappa_2$ . We present lower bounds that are optimal for all imposed hydrostatic stresses. The configurations that attain the bounds are given

by the Hashin-Shtrikman coated sphere and (cylinder) assemblages. We describe the construction of the coated sphere assemblage made from a core of material one with a coating of material two. We note that the coated cylinder assemblage is constructed similarly. One considers  $\mathbb{R}^3$  filled with a space-filling assemblage of spheres with sizes ranging down to the infinitesimal. Inside each sphere one places a smaller concentric sphere filled with “core” material one and the surrounding annulus is filled with the coating material two. The volume fractions of material one and two is taken to be the same for all of the coated spheres.

We begin by presenting optimal lower bounds on the moments of the local stress inside material one.

### 2.1.1 Optimal Lower Bounds on the Local Stress Inside Material One

Consider any heterogeneous medium with volume (area) fraction of materials one and two given by  $\theta_1$  and  $\theta_2$ , then for an imposed hydrostatic macroscopic stress  $\bar{\sigma} = \bar{p}I$  the local stress inside material one satisfies

$$\langle \chi_1 |\sigma(\mathbf{x})|^r \rangle^{1/r} \geq \theta_1^{1/r} \frac{\kappa_1 \kappa_2 + 2 \frac{d-1}{d} \mu_2 \kappa_1}{\kappa_1 \kappa_2 + 2 \frac{d-1}{d} \mu_2 (\theta_1 \kappa_1 + \theta_2 \kappa_2)} |\bar{p}|, \text{ for } 2 \leq r \leq \infty. \quad (2.1)$$

Moreover for  $d = 2(3)$  and for every  $r$  in  $2 \leq r \leq \infty$  the lower bound is attained by the local stress inside the coated cylinder (sphere) assemblage with core of material one and coating of material two.

A similar result holds for the local stress inside material two.

### 2.1.2 Optimal Lower Bounds on the Local Stress Inside Material Two

Consider any heterogeneous medium with volume (area) fraction of materials one and two given by  $\theta_1$  and  $\theta_2$ , then for an imposed hydrostatic macroscopic stress

$\bar{\sigma} = \bar{p}I$  the local stress inside material two satisfies

$$\langle \chi_2 |\sigma(\mathbf{x})|^r \rangle^{1/r} \geq \theta_2^{1/r} \frac{\kappa_1 \kappa_2 + 2 \frac{d-1}{d} \mu_2 \kappa_2}{\kappa_1 \kappa_2 + 2 \frac{d-1}{d} \mu_2 (\theta_1 \kappa_1 + \theta_2 \kappa_2)} |\bar{p}|, \text{ for } 2 \leq r \leq \infty. \quad (2.2)$$

Moreover for  $d = 2(3)$  and for every  $r$  in  $2 \leq r \leq \infty$  the lower bound is attained by the local stress inside the coated cylinder (sphere) assemblage with core of material two and coating of material one.

The optimal lower bound on the  $L^\infty$  norm of the magnitude of the local stress inside a random composite is given by the following result.

### 2.1.3 Optimal Lower Bounds on the $L^\infty$ Norm of the Local Stress

Consider any heterogeneous medium with volume (area) fraction of materials one and two given by  $\theta_1$  and  $\theta_2$ , then for an imposed hydrostatic macroscopic stress  $\bar{\sigma} = \bar{p}I$  the stress field inside the composite satisfies

$$\|\sigma(\mathbf{x})\|_\infty \geq \frac{\kappa_1 \kappa_2 + 2 \frac{d-1}{d} \mu_2 \kappa_1}{\kappa_1 \kappa_2 + 2 \frac{d-1}{d} \mu_2 (\theta_1 \kappa_1 + \theta_2 \kappa_2)} |\bar{p}|. \quad (2.3)$$

Moreover for  $d = 2(3)$  and for every  $r$  in  $2 \leq r \leq \infty$  the lower bound is attained by the local stress inside the coated cylinder (sphere) assemblage with core of material one and coating of material two.

## 2.2 Deviatoric Applied Stress

In this section we consider imposed macroscopic stresses that are purely deviatoric, i.e.,  $\bar{\sigma} = \bar{\sigma}^D$ , where  $\mathbf{\Pi}^D \bar{\sigma}^D = \bar{\sigma}^D$ . For two dimensional elastic problems any deviatoric stress tensor can be expressed as the symmetric tensor product of two orthogonal unit vectors  $\mathbf{a}$  and  $\mathbf{b}$ , i.e.,  $\bar{\sigma}^D = s(\mathbf{a} \odot \mathbf{b})$ . Here  $s$  is an arbitrary scalar. In three dimensions this type of stress tensor is referred to as a pure shear stress. For two-dimensional elastic problems we present lower bounds on the local stress that are optimal for all applied deviatoric stresses and for three dimensional problems

we show that the lower bounds are optimal for any imposed pure shear stress. The bounds are attained by simple laminates made by alternately layering material one with material two in the proportions  $\theta_1$  and  $\theta_2$  respectively. The direction normal to the layers is denoted by  $\mathbf{n}$ . The optimal choice of layer direction is given by  $\mathbf{n} = \mathbf{a}$  or  $\mathbf{n} = \mathbf{b}$ .

For a deviatoric macroscopic stress, we first present optimal lower bounds on the local stress inside the component material with the larger shear modulus. Here we denote the volume (area) fraction and indicator function of the material with the larger shear modulus by  $\theta_+$  and  $\chi_+$  respectively.

### 2.2.1 Optimal Lower Bounds on the Moments of the Local Stress Inside the Phase with Higher Shear Modulus

Consider any heterogeneous medium with area (volume) fraction of materials one and two given by  $\theta_1$  and  $\theta_2$ , then for an imposed deviatoric macroscopic stress  $\bar{\sigma}^D = s(\mathbf{a} \odot \mathbf{b})$  the stress field inside the material with larger shear modulus satisfies

$$\langle \chi_+ |\sigma(\mathbf{x})|^r \rangle^{1/r} \geq \theta_+^{1/r} |\bar{\sigma}^D|, \text{ for } 2 \leq r \leq \infty. \quad (2.4)$$

For  $d = 2, 3$  and for every  $2 \leq r \leq \infty$  the lower bound (2.4) is attained by a simple laminate. The vector normal to the layer interface for the optimal laminate is chosen according to  $\mathbf{n} = \mathbf{a}$  or  $\mathbf{n} = \mathbf{b}$ .

The optimal lower bound on the  $L^\infty$  norm of the magnitude of the local stress inside a random composite is given by the following result.

### 2.2.2 Optimal Lower Bounds on the $L^\infty$ Norm of the Local Stress

Consider any heterogeneous medium with area (volume) fraction of materials one and two given by  $\theta_1$  and  $\theta_2$ , then for an imposed deviatoric macroscopic stress

$\bar{\sigma}^D = s(\mathbf{a} \odot \mathbf{b})$  the stress field inside the composite satisfies

$$\|\sigma(\mathbf{x})\|_\infty \geq |\bar{\sigma}^D|. \quad (2.5)$$

For  $d = 2, 3$  the lower bound (2.5) is attained by a simple laminate with  $\mathbf{n} = \mathbf{a}$  or  $\mathbf{n} = \mathbf{b}$ .

### 2.3 Lower Bounds on the Local Stress that are Optimal for a Special Class of Imposed Macroscopic Stress States

In this section we start by considering heterogeneous materials made from two elastic materials sharing the same shear modulus, i.e.,  $\mu_1 = \mu_2 = \mu$ . We present new lower bounds on the full local stress field that hold for every imposed macroscopic stress  $\bar{\sigma}$ . The lower bounds are shown to be optimal for special subsets  $\mathcal{S}_1, \mathcal{S}_2$  of imposed macroscopic stresses. The subsets  $\mathcal{S}_1, \mathcal{S}_2$  are given by the set of imposed constant stresses for which one can construct a confocal ellipsoid (ellipse) assemblage that has a constant and purely hydrostatic stress and strain field inside the core phase of the confocal ellipsoid assemblage [24, 48].

We describe the construction of a confocal-ellipsoid assemblage with a core of material one and a coating of material two noting that the confocal ellipse assemblage is constructed in a similar way. Consider  $\mathbb{R}^3$  filled with a space-filling assemblage of ellipsoids. Here, all ellipsoids have the same shape and orientation of axes and differ only in their size. Inside each ellipsoid, one places a smaller confocal-ellipsoid filled with material one and the surrounding coating is filled with material two. We call these coated ellipsoids. The part of  $\mathbb{R}^3$  not covered by the coated ellipsoids has zero measure. The volume fractions of materials one and two are the same for each coated ellipsoid in the assemblage. The confocal ellipse assemblage is constructed similarly.

The set  $\mathcal{S}_1$  of applied stresses is given explicitly by the parametric representation [48]

$$\bar{\sigma} = \left( \frac{\kappa_2(\kappa_1 + 2\frac{(d-1)\mu}{d})}{\kappa_1 - \kappa_2} + \frac{2\theta_1\mu(d-1)}{d} \right) I + 2\mu\theta_2(M - \frac{1}{d}I), \quad (2.6)$$

where  $M$  ranges over the totality of positive semidefinite  $d \times d$  matrices with unit trace. For each  $\bar{\sigma}$  in  $\mathcal{S}_1$  one can construct a confocal ellipsoid assemblage with a core of material one and a coating of material two such that the local stress inside the core is constant and hydrostatic. We note here that the set  $\mathcal{S}_1$  is convex. The analogous parameterization of the set of imposed stresses for which the local stress is constant and hydrostatic for confocal ellipsoids with a core of material two is obtained by interchanging subscripts one and two in (2.6). This set of macroscopic stresses is denoted by  $\mathcal{S}_2$ .

The optimal lower bound on the moments of the local stress inside a random composite is given by the following result.

### 2.3.1 Optimal Lower Bounds on the Local Stress Inside Material One for $\mu_1 = \mu_2$

Consider any heterogeneous medium with volume (area) fraction of materials one and two given by  $\theta_1$  and  $\theta_2$ , then for any imposed macroscopic stress  $\bar{\sigma}$  the stress field inside material one satisfies

$$\langle \chi_1(\mathbf{x}) |\sigma(\mathbf{x})|^r \rangle^{1/r} \geq \theta_1^{1/r} \frac{\kappa_1\kappa_2 + 2\frac{d-1}{d}\mu\kappa_1}{\kappa_1\kappa_2 + 2\frac{d-1}{d}\mu(\theta_1\kappa_1 + \theta_2\kappa_2)} |\mathbf{\Pi}^H \bar{\sigma}|, \quad \text{for } 2 \leq r \leq \infty. \quad (2.7)$$

Moreover for  $d = 2, 3$  and for every  $r$  in  $2 \leq r \leq \infty$ , when  $\bar{\sigma}$  lies in the set  $\mathcal{S}_1$  the lower bound (2.7) is attained by the local stress inside material one for the confocal-ellipse (confocal-ellipsoid) assemblage associated with  $\bar{\sigma}$ .

A similar result holds for local stress fields inside material two.

### 2.3.2 Optimal Lower Bounds on the Local Stress Inside Material Two for $\mu_1 = \mu_2$

Consider any heterogeneous medium with volume (area) fraction of materials one and two given by  $\theta_1$  and  $\theta_2$ , then for any imposed macroscopic stress field  $\bar{\sigma}$  the stress field inside material two satisfies

$$\langle \chi_2(\mathbf{x}) |\sigma(\mathbf{x})|^r \rangle^{1/r} \geq \theta_2^{1/r} \frac{\kappa_1 \kappa_2 + 2 \frac{d-1}{d} \mu \kappa_2}{\kappa_1 \kappa_2 + 2 \frac{d-1}{d} \mu (\theta_1 \kappa_1 + \theta_2 \kappa_2)} |\mathbf{\Pi}^H \bar{\sigma}|, \text{ for } 2 \leq r \leq \infty. \quad (2.8)$$

Moreover for  $d = 2, 3$  and for every  $r$  in  $2 \leq r \leq \infty$ , when  $\bar{\sigma}$  lies in the set  $\mathcal{S}_2$ , the lower bound (2.8) is attained by the local stress field inside material two for the confocal-ellipse (confocal-ellipsoid) assemblage with core of material two associated with  $\bar{\sigma}$ .

We conclude this subsection by considering the two trivial lower bounds on the moments of the local Von Mises equivalent stress given by  $\langle \chi_1(\mathbf{x}) |\mathbf{\Pi}^D \sigma(\mathbf{x})|^r \rangle^{1/r} \geq 0$  and  $\langle \chi_2(\mathbf{x}) |\mathbf{\Pi}^D \sigma(\mathbf{x})|^r \rangle^{1/r} \geq 0$ . In what follows we make no hypothesis on the bulk and shear moduli of the component materials and point out that the trivial bounds are optimal for two subsets of imposed stresses  $\bar{\sigma}$ . The subsets are denoted by  $\hat{\mathcal{S}}_1$  and  $\hat{\mathcal{S}}_2$  and these sets correspond to the sets  $\mathcal{S}_1$  and  $\mathcal{S}_2$  with  $\mu = \mu_2$  and  $\mu = \mu_1$  respectively.

### 2.3.3 Optimal Lower Bounds on the Local Von Mises Equivalent Stress Inside Material One

Consider any heterogeneous medium with volume (area) fraction of materials one and two given by  $\theta_1$  and  $\theta_2$ , then for any imposed macroscopic stress  $\bar{\sigma}$  it is evident that the stress field inside material one satisfies

$$\langle \chi_1(\mathbf{x}) |\mathbf{\Pi}^D \sigma(\mathbf{x})|^r \rangle^{1/r} \geq 0, \text{ for } 2 \leq r \leq \infty. \quad (2.9)$$

Moreover for  $d = 2, 3$  and for every  $r$  in  $2 \leq r \leq \infty$ , when  $\bar{\sigma}$  lies in the set  $\hat{\mathcal{S}}_1$  the lower bound (2.9) is attained by the local Von Mises stress inside material one for the confocal-ellipse (confocal-ellipsoid) assemblage associated with  $\bar{\sigma}$ .

A similar result holds for local stress fields inside material two.

### 2.3.4 Optimal Lower Bounds on the Local Von Mises Equivalent Stress Inside Material Two

Consider any heterogeneous medium with volume (area) fraction of materials one and two given by  $\theta_1$  and  $\theta_2$ , then for any imposed macroscopic stress field  $\bar{\sigma}$  it is evident that the stress field inside material two satisfies

$$\langle \chi_2(\mathbf{x}) |\mathbf{\Pi}^D \sigma(\mathbf{x})|^r \rangle^{1/r} \geq 0, \text{ for } 2 \leq r \leq \infty. \quad (2.10)$$

Moreover for  $d = 2, 3$  and for every  $r$  in  $2 \leq r \leq \infty$ , when  $\bar{\sigma}$  lies in the set  $\hat{\mathcal{S}}_2$ , the lower bound (2.10) is attained by the local Von Mises stress field inside material two for the confocal-ellipse (confocal-ellipsoid) assemblage with core of material two associated with  $\bar{\sigma}$ .

## 2.4 Optimal Lower Bounds for General Imposed Macroscopic Stresses and $\mu_1 = \mu_2$

In this section we consider two-phase heterogeneous media subject to a general imposed macroscopic stress  $\bar{\sigma}$ . We suppose that the two materials share the same shear modulus  $\mu = \mu_1 = \mu_2$ , and we present optimal lower bounds on the hydrostatic part of the local stress.

The first result is a lower bound on all moments of the local hydrostatic stress inside each material.

### 2.4.1 Optimal Lower Bounds on the Local Hydrostatic Stress with $\mu_1 = \mu_2$ for Media Subjected to a General Imposed Stress

Consider any heterogeneous medium with volume (area) fraction of materials one and two given by  $\theta_1$  and  $\theta_2$ , then for any imposed macroscopic stress  $\bar{\sigma}$  the hydrostatic component of the local stress field inside the  $i$ -th material,  $i = 1, 2$ , satisfy

$$\langle \chi_i |\mathbf{\Pi}^H \sigma(\mathbf{x})|^r \rangle^{1/r} \geq \theta_i^{1/r} \frac{\kappa_1 \kappa_2 + 2 \frac{d-1}{d} \mu \kappa_i}{\kappa_1 \kappa_2 + 2 \frac{d-1}{d} \mu (\theta_1 \kappa_1 + \theta_2 \kappa_2)} |\mathbf{\Pi}^H \bar{\sigma}|, \text{ for } 2 \leq r \leq \infty. \quad (2.11)$$

Moreover for  $d = 2, 3$ , the lower bound (2.11) is attained for every  $r$  in  $2 \leq r \leq \infty$  by the local hydrostatic stress field inside laminates made from layering the two materials in the prescribed proportions  $\theta_1$  and  $\theta_2$ . Here the layering can be made along any direction  $\mathbf{n}$ .

The next result provides a lower bound on the  $L^\infty$  norm of the local stress inside the heterogeneous medium.

### 2.4.2 Optimal Lower Bounds on the $L^\infty$ Norm of the Local Hydrostatic Stress with $\mu_1 = \mu_2$ for Media Subjected to a General Imposed Stress

Consider any heterogeneous medium with volume (area) fraction of materials one and two given by  $\theta_1$  and  $\theta_2$ , then for any imposed macroscopic stress  $\bar{\sigma}$  the hydrostatic component of the local stress field satisfies

$$\|\mathbf{\Pi}^H \sigma(\mathbf{x})\|_\infty \geq \frac{\kappa_1 \kappa_2 + 2 \frac{d-1}{d} \mu \kappa_+}{\kappa_1 \kappa_2 + 2 \frac{d-1}{d} \mu (\theta_1 \kappa_1 + \theta_2 \kappa_2)} |\mathbf{\Pi}^H \bar{\sigma}|. \quad (2.12)$$

Moreover for  $d = 2, 3$ , the lower bound (2.12) is attained by the local hydrostatic stress field inside a simply layered material. Here the layering can be made along any direction  $\mathbf{n}$ .

## 2.5 Optimal Lower Bounds for General Imposed Macroscopic Stresses and $\kappa_1 = \kappa_2$

In this section we consider two-phase heterogeneous media subject to any imposed macroscopic stress  $\bar{\sigma}$ . We suppose that the two materials share the same bulk modulus, i.e.,  $\kappa = \kappa_1 = \kappa_2$ , and we present optimal lower bounds on the local Von Mises equivalent stress.

The first result is a lower bound on all moments of the local Von Mises equivalent stress inside the material with greater shear stiffness. To expedite the presentation we denote the indicator function of and proportion of the material with greater shear modulus by  $\chi_+$  and  $\theta_+$  respectively.

### 2.5.1 Optimal Lower Bounds on the Moments of the Local Von Mises Equivalent Stress Inside the Material with Greater Shear Modulus for $\kappa_1 = \kappa_2$

Consider any heterogeneous medium with volume (area) fraction of materials one and two given by  $\theta_1$  and  $\theta_2$ , then for any imposed macroscopic stress  $\bar{\sigma}$  the local Von Mises stress field inside the material with larger shear modulus satisfies

$$\langle \chi_+ |\mathbf{\Pi}^D \sigma(\mathbf{x})|^r \rangle^{1/r} \geq \theta_+^{1/r} |\mathbf{\Pi}^D \bar{\sigma}|, \text{ for } 2 \leq r \leq \infty. \quad (2.13)$$

For  $d = 2$  let  $\psi_1, \psi_2$  be an orthonormal system of eigenvectors for  $\bar{\sigma}$ . Then for every  $r$  in  $2 \leq r \leq \infty$ , the lower bound (2.13) is attained by the local Von Mises stress inside a simple laminate with layer normal  $\mathbf{n} = \frac{\psi_1 + \psi_2}{\sqrt{2}}$ . Here the deviatoric projection of the local stress inside this laminate is uniform and given by  $\mathbf{\Pi}^D \sigma(\mathbf{x}) = \mathbf{\Pi}^D \bar{\sigma}$ . For  $d = 3$  the explicit solution for the stress field inside a simple layered material shows that this is not the case see, Section 5.2.

The next result provides a lower bound on the  $L^\infty$  norm of the local Von Mises equivalent stress inside the heterogeneous material.

### 2.5.2 Optimal Lower Bounds on the $L^\infty$ Norm of the Von Mises Equivalent Stress for $\kappa_1 = \kappa_2$

Consider any heterogeneous medium with volume (area) fraction of materials one and two given by  $\theta_1$  and  $\theta_2$ , then for any imposed macroscopic stress  $\bar{\sigma}$  the local Von Mises equivalent stress inside the medium satisfies

$$\|\mathbf{\Pi}^D \sigma(\mathbf{x})\|_\infty \geq |\mathbf{\Pi}^D \bar{\sigma}|. \quad (2.14)$$

For  $d = 2$ , the lower bound (2.14) is attained by the local Von Mises stress inside a simple laminate with layer normal  $\mathbf{n} = \frac{\psi_1 + \psi_2}{\sqrt{2}}$ .

# Chapter 3

## Optimal Lower Bounds on the Local Strain Inside Random Composites

We present optimal lower bounds for the local strain that are given in terms of the applied loads, material properties, and volume fractions of the constituent materials. As in the previous section we provide new optimal bounds for a ladder of progressively more general sets of imposed macroscopic loads. As we progress to more general imposed macroscopic strains we will apply additional hypotheses on the shear and bulk moduli of the constituent materials. In this section we provide lower bounds for the following applied macroscopic load cases: 1) lower bounds on the full local strain for imposed hydrostatic macroscopic strains, 2) lower bounds on the full local strain inside the material with larger shear modulus for elastic problems with imposed macroscopic shear strains, 3) lower bounds on the full local strain for  $\mu_1 = \mu_2$ , that are seen to be optimal for a special class of applied macroscopic strains, 4) lower bounds on the local deviatoric component of the strain that are optimal for a special class of applied macroscopic strains, and 5) lower bounds on the hydrostatic and deviatoric components of the local strain for the full set of imposed macroscopic strains subject to the hypotheses  $\mu_1 = \mu_2$  and  $\kappa_1 = \kappa_2$  respectively.

### 3.1 Imposed Hydrostatic Macroscopic Strain

In this section we consider imposed macroscopic strains that are hydrostatic, i.e., of the form  $\bar{\epsilon} = \bar{p}I$  where  $\bar{p}$  is a constant and  $I$  is the  $d \times d$  identity matrix. Here it is assumed that the elastic materials inside the heterogeneous medium are well-ordered i.e.,  $(\mu_1 - \mu_2)(\kappa_1 - \kappa_2) > 0$  and without loss of generality we will suppose in this section that  $\mu_1 > \mu_2$  and  $\kappa_1 > \kappa_2$ . We present lower bounds that are optimal

for all applied hydrostatic stresses. The configurations that attain the bounds are given by the Hashin-Shtrikman coated sphere and (cylinder) assemblages.

We start by presenting optimal lower bounds on the moments of the local strain inside material one.

### 3.1.1 Optimal Lower Bounds on the Moments of the Local Strain in Material One

Consider any heterogeneous medium with volume (area) fraction of materials one and two given by  $\theta_1$  and  $\theta_2$ , then for an imposed hydrostatic macroscopic strain  $\bar{\epsilon} = \bar{p}I$  the local strain field inside material one satisfies

$$\langle \chi_1(\mathbf{x}) |\epsilon(\mathbf{x})|^r \rangle^{1/r} \geq \theta_1^{1/r} \frac{\kappa_2 + 2^{\frac{d-1}{d}} \mu_2}{\theta_1 \kappa_2 + \theta_2 \kappa_1 + 2^{\frac{d-1}{d}} \mu_2} |\bar{p}|, \text{ for } 2 \leq r \leq \infty, \quad (3.1)$$

Moreover for  $d = 2(3)$  and for every  $r$  in  $2 \leq r \leq \infty$  the lower bound is attained by the local strain inside the coated cylinder (sphere) assemblage with core of material one and coating of material two.

A similar result holds for the local strain field inside material two.

### 3.1.2 Optimal Lower Bounds on the Moments of the Local Strain in Material Two

Consider any heterogeneous medium with volume (area) fraction of materials one and two given by  $\theta_1$  and  $\theta_2$ , then for an imposed hydrostatic macroscopic strain  $\bar{\epsilon} = \bar{p}I$  the local strain field inside material two satisfies

$$\langle \chi_2(\mathbf{x}) |\epsilon(\mathbf{x})|^r \rangle^{1/r} \geq \theta_2^{1/r} \frac{\kappa_1 + 2^{\frac{d-1}{d}} \mu_1}{\theta_1 \kappa_2 + \theta_2 \kappa_1 + 2^{\frac{d-1}{d}} \mu_1} |\bar{p}|, \text{ for } 2 \leq r \leq \infty, \quad (3.2)$$

Moreover for  $d = 2(3)$  and for every  $r$  in  $2 \leq r \leq \infty$  the lower bound is attained by the local strain inside the coated cylinder (sphere) assemblage with core of material two and coating of material one.

The optimal lower bound on the  $L^\infty$  norm of the magnitude of the local strain inside a random composite is given by the following result.

### 3.1.3 Optimal Lower Bounds on the $L^\infty$ Norm of the Local Strain

Consider any heterogeneous medium with volume (area) fraction of materials one and two given by  $\theta_1$  and  $\theta_2$ , then for an imposed hydrostatic macroscopic strain  $\bar{\epsilon} = \bar{p}I$  the local strain field inside the composite satisfies

$$\|\epsilon(\mathbf{x})\|_{L^\infty(Q)} \geq \frac{\kappa_1 + 2\frac{d-1}{d}\mu_1}{\theta_1\kappa_2 + \theta_2\kappa_1 + 2\frac{d-1}{d}\mu_1} |\bar{p}| \quad (3.3)$$

Moreover for  $d = 2$  the lower bound is attained by the local strain inside the coated cylinder assemblage with core of material two and coating of material one.

For  $d = 3$  and if the elastic materials satisfy  $(\kappa_1 + \kappa_2) - 9(\kappa_1 - \kappa_2) + 16\mu_1 \geq 0$ , then the lower bound is attained by the local strain inside the coated sphere assemblage with core of material two and coating of material one.

## 3.2 Deviatoric Applied Strain

In this section the imposed macroscopic strains are taken to be purely deviatoric, i.e.,  $\mathbf{\Pi}^D \bar{\epsilon}^D = \bar{\epsilon}^D$ . For two dimensional elastic problems the deviatoric strain tensor can be expressed as the symmetric tensor product of two orthogonal unit vectors  $\mathbf{a}$  and  $\mathbf{b}$ , i.e.,  $\bar{\epsilon}^D = \varepsilon(\mathbf{a} \odot \mathbf{b})$ , where  $\varepsilon$  is an arbitrary scalar. In three dimensions this type of strain tensor is referred to as a pure shear strain. For two-dimensional elastic problems we present lower bounds on the local strain that are optimal for all applied deviatoric strains and for three dimensional problems we show that the lower bounds are optimal for any imposed pure shear strain. The bounds are attained by simple laminates made by layering material one with material two in the proportions  $\theta_1$  and  $\theta_2$  respectively. The direction normal to the layers is denoted by  $\mathbf{n}$ . The optimal choice of layer direction is given by  $\mathbf{n} = \mathbf{a}$  or  $\mathbf{n} = \mathbf{b}$ .

We present optimal lower bounds on the local strain inside the component material with the larger shear modulus. The volume fraction and indicator functions associated with material having larger shear modulus are denoted by  $\theta_+$  and  $\chi_+$ .

### 3.2.1 Optimal Lower Bounds on the Moments of the Local Strain Inside the Phase with Higher Shear Modulus

Consider any heterogeneous medium with area (volume) fraction of materials one and two given by  $\theta_1$  and  $\theta_2$ , then for an imposed deviatoric macroscopic strain  $\bar{\epsilon}^D = \epsilon(\mathbf{a} \odot \mathbf{b})$  the strain field inside the material with larger shear modulus satisfies

$$\langle \chi_+(\mathbf{x}) |\epsilon(\mathbf{x})|^r \rangle^{1/r} \geq \theta_+^{1/r} \frac{\mu_-}{\theta_1 \mu_2 + \theta_2 \mu_1} |\bar{\epsilon}^D|, \text{ for } 2 \leq r \leq \infty. \quad (3.4)$$

Moreover for  $d = 2, 3$ , the lower bound (3.4) is attained by the strain field inside a simple laminate for every  $r$  in  $2 \leq r \leq \infty$ . Here the layering direction in the optimal laminate is given by  $\mathbf{n} = \mathbf{a}$  or  $\mathbf{n} = \mathbf{b}$ .

## 3.3 Lower Bounds on the Local Strain that are Optimal for a Special Class of Imposed Macroscopic Strain States

In this section we start by considering heterogeneous materials made from two elastic materials sharing the same shear modulus, i.e.,  $\mu_1 = \mu_2 = \mu$ . We present new lower bounds on the full local strain field that hold for every applied macroscopic strain  $\bar{\epsilon}$ . The lower bounds are shown to be optimal for special subsets  $\mathcal{E}_1, \mathcal{E}_2$  of applied strains. The subsets  $\mathcal{E}_1, \mathcal{E}_2$  correspond the set of imposed constant strains for which one can construct a confocal ellipsoid assemblage that has constant and purely hydrostatic stress and strain fields inside the core phase of the confocal ellipsoid assemblage [24, 48].

The set  $\mathcal{E}_1$  of applied strains is given explicitly by the parametric representation developed in [48]

$$\bar{\epsilon} = \left( \frac{d\kappa_2 + \frac{(d-1)\mu}{d}}{d^2(\kappa_1 - \kappa_2)} \right) I + \theta_2 M, \quad (3.5)$$

where  $M$  ranges over the totality of positive semidefinite  $d \times d$  matrices with unit trace. For each  $\bar{\epsilon}$  in  $\mathcal{E}_1$  one can construct a confocal ellipsoid assemblage with core material one and coating material two such that the local strain inside the core is constant and hydrostatic. We note here that the set  $\mathcal{E}_1$  is convex. The analogous parameterization of the set of imposed strains for which the local strain is constant and hydrostatic for suitably constructed confocal ellipsoids with core two is obtained by interchanging subscripts one and two in (3.5). The associated set of macroscopic strains is denoted by  $\mathcal{E}_2$ .

We present optimal lower bounds on the local strain inside material one that hold for all composites with  $\mu = \mu_1 = \mu_2$ .

### 3.3.1 Optimal Lower Bounds on the Local Strain Inside Material One with $\mu_1 = \mu_2$

Consider any heterogeneous medium with area (volume) fraction of materials one and two given by  $\theta_1$  and  $\theta_2$ , then for any imposed macroscopic strain  $\bar{\epsilon}$  the strain field inside material one satisfies

$$\langle \chi_1(\mathbf{x}) |\epsilon(\mathbf{x})|^r \rangle^{1/r} \geq \theta_1^{1/r} \frac{\kappa_2 + 2\frac{d-1}{d}\mu}{\theta_1\kappa_2 + \theta_2\kappa_1 + 2\frac{d-1}{d}\mu} |\mathbf{\Pi}^H \bar{\epsilon}|, \text{ for } 2 \leq r \leq \infty. \quad (3.6)$$

Moreover for  $d = 2(3)$  and for every  $r$  in  $2 \leq r \leq \infty$  if  $\bar{\epsilon}$  lies in  $\mathcal{E}_1$  the lower bound is attained by the local strain inside the confocal ellipsoid (ellipse) assemblage.

A similar result holds for the strain fields inside materials two.

### 3.3.2 Optimal Lower Bounds on the Local Strain Inside Material Two with $\mu_1 = \mu_2$

Consider any heterogeneous medium with area (volume) fraction of materials one and two given by  $\theta_1$  and  $\theta_2$ , then for any imposed macroscopic strain  $\bar{\epsilon}$  the strain field inside material two satisfies

$$\langle \chi_2(\mathbf{x}) |\epsilon(\mathbf{x})|^r \rangle^{1/r} \geq \theta_2^{1/r} \frac{\kappa_1 + 2\frac{d-1}{d}\mu}{\theta_1\kappa_2 + \theta_2\kappa_1 + 2\frac{d-1}{d}\mu} |\mathbf{\Pi}^H \bar{\epsilon}|, \text{ for } 2 \leq r \leq \infty. \quad (3.7)$$

Moreover for  $d = 2(3)$  and for every  $r$  in  $2 \leq r \leq \infty$  if  $\bar{\epsilon}$  lies in  $\mathcal{E}_2$  the lower bound is attained by the local strain inside the confocal ellipsoid (ellipse) assemblage.

We conclude this subsection by considering the two trivial lower bounds on the moments of the deviatoric component of the local strain given by

$\langle \chi_1(\mathbf{x}) |\mathbf{\Pi}^D \epsilon(\mathbf{x})|^r \rangle^{1/r} \geq 0$  and  $\langle \chi_2(\mathbf{x}) |\mathbf{\Pi}^D \epsilon(\mathbf{x})|^r \rangle^{1/r} \geq 0$ . In what follows we make no hypothesis on the bulk and shear moduli of the component materials and point out that the trivial bounds are optimal for two subsets of imposed macroscopic strains  $\bar{\epsilon}$ . The subsets are denoted by  $\hat{\mathcal{E}}_1$  and  $\hat{\mathcal{E}}_2$  and these sets correspond to  $\mathcal{E}_1$  and  $\mathcal{E}_2$  with  $\mu = \mu_2$  and  $\mu = \mu_1$  respectively.

### 3.3.3 Optimal Lower Bounds on the Deviatoric Component of the Local Strain Inside Material One

Consider any heterogeneous medium with volume (area) fraction of materials one and two given by  $\theta_1$  and  $\theta_2$ , then for any imposed macroscopic strain  $\bar{\epsilon}$  it is evident that the strain field inside material one satisfies

$$\langle \chi_1(\mathbf{x}) |\mathbf{\Pi}^D \epsilon(\mathbf{x})|^r \rangle^{1/r} \geq 0, \text{ for } 2 \leq r \leq \infty. \quad (3.8)$$

Moreover for  $d = 2(3)$  and for every  $r$  in  $2 \leq r \leq \infty$  if  $\bar{\epsilon}$  lies in  $\hat{\mathcal{E}}_1$  the lower bound is attained by the local strain inside the confocal ellipsoid (ellipse) assemblage with a core of material one.

A similar result holds for strain fields inside material two.

### 3.3.4 Optimal Lower Bounds on the Deviatoric Component of the Local Strain Inside Material Two

Consider any heterogeneous medium with volume (area) fraction of materials one and two given by  $\theta_1$  and  $\theta_2$ , then for any imposed macroscopic strain  $\bar{\epsilon}$  it is evident that the strain field inside material two satisfies

$$\langle \chi_2(\mathbf{x}) |\mathbf{\Pi}^D \epsilon(\mathbf{x})|^r \rangle^{1/r} \geq 0, \quad \text{for } 2 \leq r \leq \infty. \quad (3.9)$$

For  $d = 2(3)$  and for every  $r$  in  $2 \leq r \leq \infty$  if  $\bar{\epsilon}$  lies in  $\hat{\mathcal{E}}_2$  the lower bound is attained by the local strain inside the confocal ellipsoid (ellipse) assemblage with a core of material two.

## 3.4 Optimal Lower Bounds for General Imposed Macroscopic Strains and $\mu_1 = \mu_2$

In this section we consider two-phase heterogeneous media subject to a general imposed macroscopic strain  $\bar{\epsilon}$ . We suppose that the two materials share the same shear modulus  $\mu = \mu_1 = \mu_2$ , and we present optimal lower bounds on the hydrostatic part of the local strain.

The first result is a lower bound on all moments of the local hydrostatic strain inside each material.

### 3.4.1 Optimal Lower Bounds on the Local Hydrostatic Strain Inside Material One with $\mu_1 = \mu_2$ for Media Subjected to a General Imposed Strain

Consider any heterogeneous medium with volume (area) fraction of materials one and two given by  $\theta_1$  and  $\theta_2$ , then for any imposed macroscopic strain  $\bar{\epsilon}$  the hydrostatic component of the local strain field inside material one satisfies

$$\langle \chi_1(\mathbf{x}) |\mathbf{\Pi}^H \epsilon(\mathbf{x})|^r \rangle^{1/r} \geq \theta_1^{1/r} \frac{\kappa_2 + 2 \frac{d-1}{d} \mu}{\theta_1 \kappa_2 + \theta_2 \kappa_1 + 2 \frac{d-1}{d} \mu} |\mathbf{\Pi}^H \bar{\epsilon}|, \quad \text{for } 2 \leq r \leq \infty. \quad (3.10)$$

Moreover for  $d = 2(3)$  and for  $2 \leq r \leq \infty$  the lower bound (3.10) is attained by any simple layering of the two materials along any direction  $\mathbf{n}$ .

A similar result holds for strain fields inside material two.

### 3.4.2 Optimal Lower Bounds on the Local Hydrostatic Strain Inside Material Two with $\mu_1 = \mu_2$ for Media Subjected to a General Imposed Strain

Consider any heterogeneous medium with volume (area) fraction of materials one and two given by  $\theta_1$  and  $\theta_2$ , then for any imposed macroscopic strain  $\bar{\epsilon}$  the hydrostatic component of the local strain field inside material two satisfies

$$\langle \chi_2(\mathbf{x}) |\mathbf{\Pi}^H \epsilon(\mathbf{x})|^r \rangle^{1/r} \geq \theta_2^{1/r} \frac{\kappa_1 + 2 \frac{d-1}{d} \mu}{\theta_1 \kappa_2 + \theta_2 \kappa_1 + 2 \frac{d-1}{d} \mu} |\mathbf{\Pi}^H \bar{\epsilon}|, \text{ for } 2 \leq r \leq \infty. \quad (3.11)$$

Moreover for  $d = 2(3)$ , the lower bound (3.11) is attained by any simple layering of the two materials along any direction  $\mathbf{n}$ .

The next result provides an optimal result on the  $L^\infty$  norm of the local strain inside a heterogeneous medium.

### 3.4.3 Optimal Lower Bounds on the $L^\infty$ Norm of the Local Hydrostatic Strain for Composites Subjected to a General Imposed Strain and $\mu_1 = \mu_2$

Consider any heterogeneous medium with volume (area) fraction of materials one and two given by  $\theta_1$  and  $\theta_2$ , then for any imposed macroscopic strain  $\bar{\epsilon}$  the hydrostatic component of the local strain field satisfies

$$\|\mathbf{\Pi}^H \epsilon(\mathbf{x})\|_\infty \geq \frac{\kappa_+ + 2 \frac{d-1}{d} \mu}{\theta_1 \kappa_2 + \theta_2 \kappa_1 + 2 \frac{d-1}{d} \mu} |\mathbf{\Pi}^H \bar{\epsilon}|. \quad (3.12)$$

Moreover for  $d = 2(3)$ , the lower bound (3.12) is attained by any simple layering of the two materials along any direction  $\mathbf{n}$ .

## 3.5 Optimal Lower Bounds for General Imposed Macroscopic Strains and $\kappa_1 = \kappa_2$

In this section we consider two-phase heterogeneous media subjected to any imposed macroscopic strain  $\bar{\epsilon}$ . We suppose that the two materials share the same bulk moduli, i.e.,  $\kappa = \kappa_1 = \kappa_2$ . For this case we present optimal lower bounds on the moments of the deviatoric component of the local strain inside the material possessing the largest shear modulus.

### 3.5.1 Optimal Lower Bounds on the Moments of the Deviatoric Component of the Local Strain for a General Imposed Macroscopic Strain and $\kappa_1 = \kappa_2$

Consider any heterogeneous medium with volume (area) fraction of materials one and two given by  $\theta_1$  and  $\theta_2$ , then for any imposed macroscopic strain  $\bar{\epsilon}$  the deviatoric component of the local strain inside the material with the largest shear stiffness satisfies

$$\langle \chi_+(\mathbf{x}) |\mathbf{\Pi}^D \epsilon(\mathbf{x})|^r \rangle^{1/r} \geq \theta_+^{1/r} \frac{\mu_-}{\theta_1 \mu_2 + \theta_2 \mu_1} |\mathbf{\Pi}^D \bar{\epsilon}|, \text{ for } 2 \leq r \leq \infty. \quad (3.13)$$

For  $d = 2$  let  $\psi_1, \psi_2$  be the orthonormal system of eigenvectors for  $\bar{\epsilon}$  then for  $2 \leq r \leq \infty$  the lower bound (3.13) is attained by the deviatoric component of the local strain inside a simple layered material with layer normal  $\mathbf{n} = \frac{\psi_1 + \psi_2}{\sqrt{2}}$ .

# Chapter 4

## Lower Bounds on Local Stress and Strain Fields

In this chapter, we derive the lower bounds on the local stress and strain inside the composite presented in Chapters 2 and 3.

The lower bounds on the local stress and strain are established with the aid of two elementary inequalities that follow immediately from Jensen's inequality. Let  $\psi(\mathbf{x})$  be a symmetric  $d \times d$  matrix valued field defined on  $\mathbf{R}^d$ . Then

$$\langle \chi_i(\mathbf{x})\psi(\mathbf{x}) : \psi(\mathbf{x}) \rangle \geq \frac{1}{\theta_i} |\langle \chi_i(\mathbf{x})\psi(\mathbf{x}) \rangle|^2 \quad (4.1)$$

and

$$\langle \psi(\mathbf{x}) : \psi(\mathbf{x}) \rangle \geq |\langle \psi(\mathbf{x}) \rangle|^2 \quad (4.2)$$

These inequalities are strict in that equality holds in (4.1) only if  $\psi(\mathbf{x})$  is constant on the set of points where  $\chi_i = 1$  and in (4.2) only if  $\psi(\mathbf{x})$  is constant everywhere.

Lower bounds on the local stress are derived in the first subsection and lower bounds on the local strain are derived in the second subsection.

### 4.1 Lower Bounds on Local Stress Fields

#### 4.1.1 Hydrostatic Applied Stress

In this section the imposed macroscopic stress is taken to be hydrostatic, i.e.,  $\bar{\sigma} = \bar{p}I$  and the two materials are well ordered. With out loss of generality we make the choice  $\mu_1 > \mu_2$  and  $\kappa_1 > \kappa_2$ . For heterogeneous media with prescribed volume (area) fractions of material one and two the lower bounds on the hydrostatic component of the local stress are given by [42]

$$\langle \chi_1(\mathbf{x}) |\mathbf{\Pi}^H \sigma(\mathbf{x})|^r \rangle^{1/r} \geq \theta_1^{1/r} \frac{\kappa_1 \kappa_2 + 2 \frac{d-1}{d} \mu_2 \kappa_1}{\kappa_1 \kappa_2 + 2 \frac{d-1}{d} \mu_2 (\theta_1 \kappa_1 + \theta_2 \kappa_2)} |\bar{p}|, \text{ for } 2 \leq r \leq \infty, \quad (4.3)$$

$$\langle \chi_2(\mathbf{x}) |\mathbf{\Pi}^H \sigma(\mathbf{x})|^r \rangle^{1/r} \geq \theta_2^{1/r} \frac{\kappa_1 \kappa_2 + 2 \frac{d-1}{d} \mu_2 \kappa_2}{\kappa_1 \kappa_2 + 2 \frac{d-1}{d} \mu_2 (\theta_1 \kappa_1 + \theta_2 \kappa_2)} |\bar{p}|, \text{ for } 2 \leq r \leq \infty. \quad (4.4)$$

and

$$\| |\mathbf{\Pi}^H \sigma(\mathbf{x})| \|_\infty \geq \frac{\kappa_1 \kappa_2 + 2 \frac{d-1}{d} \mu_2 \kappa_1}{\kappa_1 \kappa_2 + 2 \frac{d-1}{d} \mu_2 (\theta_1 \kappa_1 + \theta_2 \kappa_2)} |\bar{p}|. \quad (4.5)$$

It is pointed out that one also has lower bounds on the hydrostatic component of the local stress for the non-well ordered case [42].

The lower bounds (2.1), (2.2), (2.3) follow immediately noting that the full local stress  $|\sigma(\mathbf{x})|$  is given by  $|\sigma(\mathbf{x})| = (|\mathbf{\Pi}^H \sigma(\mathbf{x})|^2 + |\mathbf{\Pi}^D \sigma(\mathbf{x})|^2)^{1/2}$  so  $|\sigma(\mathbf{x})| \geq |\mathbf{\Pi}^H \sigma(\mathbf{x})|$ . In Section 5.2 we establish the optimality of these lower bounds for the well ordered case.

### 4.1.2 Deviatoric Applied Stress

In what follows we make no assumption on the relative magnitudes of the component bulk moduli. We examine the local stress field inside the material with larger shear modulus and without loss of generality we suppose that the shear modulus of material one is greater than that of material two, i.e.,  $\mu_1 > \mu_2$ . We derive new lower bounds on the local stress inside material one that hold for any imposed macroscopic deviatoric stress. In subsequent sections these lower bounds are shown to be optimal for imposed macroscopic deviatoric stresses in two dimensions and for imposed macroscopic stresses that are pure shear stresses in three dimensions.

The local stress inside material one satisfies the following estimate

$$\langle \chi_1 \sigma(\mathbf{x}) : \sigma(\mathbf{x}) \rangle \geq \frac{1}{\theta_1} |\langle \chi_1 \sigma(\mathbf{x}) \rangle|^2, \quad (4.6)$$

which can be seen by taking  $\psi = \sigma$  in Eq. (4.1). Because of orthogonality, we see that

$$|\langle \chi_1 \sigma(\mathbf{x}) \rangle|^2 = |\langle \chi_1 \mathbf{\Pi}^D \sigma(\mathbf{x}) \rangle|^2 + |\langle \chi_1 \mathbf{\Pi}^H \sigma(\mathbf{x}) \rangle|^2$$

Thus Eq. (4.6) becomes

$$\langle \chi_1 \sigma(\mathbf{x}) : \sigma(\mathbf{x}) \rangle \geq \frac{1}{\theta_1} |\langle \chi_1 \mathbf{\Pi}^D \sigma(\mathbf{x}) \rangle|^2 \quad (4.7)$$

The average stress inside material one can be written as

$$\begin{aligned} \langle \chi_1 \sigma(\mathbf{x}) \rangle &= \langle \chi_1 C(\mathbf{x}) \epsilon(\mathbf{x}) \rangle \\ &= C^1 \langle \chi_1 \epsilon(\mathbf{x}) \rangle. \end{aligned} \quad (4.8)$$

Averaging the local stress-strain relation  $\sigma(\mathbf{x}) = C(\mathbf{x})\epsilon(\mathbf{x})$  and applying the definition of the effective elastic tensor gives

$$\begin{aligned} \bar{\sigma} = C^e \bar{\epsilon} &= \langle ((C^2 + \chi_1(C^1 - C^2)) \epsilon(\mathbf{x})) \rangle \\ &= C^2 \bar{\epsilon} + (C^1 - C^2) \langle \chi_1 \epsilon(\mathbf{x}) \rangle. \end{aligned} \quad (4.9)$$

Using Eq. (4.9) the deviatoric part of the average macroscopic stress can be written as

$$\mathbf{\Pi}^D \bar{\sigma} = 2\mu_2 \mathbf{\Pi}^D \bar{\epsilon} + 2(\mu_1 - \mu_2) \langle \chi_1 \mathbf{\Pi}^D \epsilon(\mathbf{x}) \rangle \quad (4.10)$$

We apply the deviatoric projection on both sides of equation Eq. (4.8) to find that

$$\langle \chi_1 \mathbf{\Pi}^D \sigma(\mathbf{x}) \rangle = 2\mu_1 \langle \chi_1 \mathbf{\Pi}^D \epsilon(\mathbf{x}) \rangle \quad (4.11)$$

Solving for  $\langle \chi_1 \mathbf{\Pi}^D \epsilon(\mathbf{x}) \rangle$  in Eq. (4.10) and substituting in Eq. (4.11), one obtains

$$\langle \chi_1 \mathbf{\Pi}^D \sigma(\mathbf{x}) \rangle = \frac{2\mu_1 \mu_2}{\mu_1 - \mu_2} \left( \frac{1}{2\mu_2} \mathbf{\Pi}^D \bar{\sigma} - \mathbf{\Pi}^D \bar{\epsilon} \right) \quad (4.12)$$

From Eq. (1.7) it follows that

$$\mathbf{\Pi}^D \bar{\epsilon} = \mathbf{\Pi}^D (C^e)^{-1} \bar{\sigma} \quad (4.13)$$

Up to this point we have assumed that the imposed macroscopic stress was given by an arbitrary  $d \times d$  matrix. From now on in this subsection we will assume that the imposed macroscopic stress is taken to be deviatoric for both two and three dimensional elastic problems, i.e.,

$$\bar{\sigma} = \sigma^D = \mathbf{\Pi}^D \bar{\sigma}^D \quad (4.14)$$

From Eqs. (4.12) and (4.13), one obtains

$$\langle \chi_1 \mathbf{\Pi}^D \sigma(\mathbf{x}) \rangle = \frac{2\mu_1\mu_2}{\mu_1 - \mu_2} \left( \frac{1}{2\mu_2} \mathbf{\Pi}^D \bar{\sigma} - \mathbf{\Pi}^D (C^e)^{-1} \bar{\sigma} \right) \quad (4.15)$$

$$= \frac{2\mu_1\mu_2}{\mu_1 - \mu_2} \left( \frac{1}{2\mu_2} \mathbf{\Pi}^D - \mathbf{\Pi}^D (C^e)^{-1} \right) \mathbf{\Pi}^D \bar{\sigma}, \quad (4.16)$$

where in the second equality we used the assumption that  $\bar{\sigma}$  is deviatoric.

We apply Cauchy-Schwarz inequality to find that

$$|\langle \chi_1 \mathbf{\Pi}^D \sigma(\mathbf{x}) \rangle|^2 \geq \left( \frac{2\mu_1\mu_2}{\mu_1 - \mu_2} \right)^2 \frac{\left( \frac{1}{2\mu_2} \mathbf{\Pi}^D \bar{\sigma} : \mathbf{\Pi}^D \bar{\sigma} - ((C^e)^{-1} \mathbf{\Pi}^D \bar{\sigma} : \mathbf{\Pi}^D \bar{\sigma}) \right)^2}{|\mathbf{\Pi}^D \bar{\sigma}|^2}. \quad (4.17)$$

The effective elasticity tensor  $C^e$  satisfies the following well known estimate, see [56]

$$(C^e)^{-1} \bar{\sigma} : \bar{\sigma} \leq (\theta_1 (C^1)^{-1} + \theta_2 (C^2)^{-1}) \bar{\sigma} : \bar{\sigma} \quad (4.18)$$

From Eq. (4.18) one obtains

$$\begin{aligned} (C^e)^{-1} \mathbf{\Pi}^D \bar{\sigma} : \mathbf{\Pi}^D \bar{\sigma} &\leq (\theta_1 (C^1)^{-1} + \theta_2 (C^2)^{-1}) \mathbf{\Pi}^D \bar{\sigma} : \mathbf{\Pi}^D \bar{\sigma} \\ &= \left( \frac{\theta_1}{2\mu_1} + \frac{\theta_2}{2\mu_2} \right) |\mathbf{\Pi}^D \bar{\sigma}|^2 \end{aligned} \quad (4.19)$$

after a straightforward calculation. It now easily follows from Eq. (4.19) that

$$\begin{aligned} \frac{1}{2\mu_2} \mathbf{\Pi}^D \bar{\sigma} : \mathbf{\Pi}^D \bar{\sigma} - (C^e)^{-1} \mathbf{\Pi}^D \bar{\sigma} : \mathbf{\Pi}^D \bar{\sigma} &\geq \left( \frac{1}{2\mu_2} - \left( \frac{\theta_1}{2\mu_1} + \frac{\theta_2}{2\mu_2} \right) \right) |\mathbf{\Pi}^D \bar{\sigma}|^2 \\ &= \frac{\theta_1 (\mu_1 - \mu_2)}{2\mu_1\mu_2} |\mathbf{\Pi}^D \bar{\sigma}|^2 \end{aligned} \quad (4.20)$$

Because  $\mu_1 > \mu_2$ , and after some simplification, we obtain from Eqs. (4.44) and (4.20) that

$$|\langle \chi_1 \mathbf{\Pi}^D \sigma(\mathbf{x}) \rangle|^2 \geq \theta_1^2 |\mathbf{\Pi}^D \bar{\sigma}|^2 \quad (4.21)$$

and it follows from Eq. (4.43) that

$$\begin{aligned} \langle \chi_1 |\mathbf{\Pi}^D \sigma(\mathbf{x})|^2 \rangle &= \\ \langle \chi_1 \mathbf{\Pi}^D \sigma(\mathbf{x}) : \sigma(\mathbf{x}) \rangle &\geq \theta_1 |\mathbf{\Pi}^D \bar{\sigma}|^2. \end{aligned} \quad (4.22)$$

An application of Hölder's inequality to the left hand side of (4.22) delivers

$$\langle \chi_1 |\mathbf{\Pi}^D \sigma(\mathbf{x})|^r \rangle^{1/r} \geq \theta_1^{1/r} |\mathbf{\Pi}^D \bar{\sigma}|, \text{ for } 2 \leq r \leq \infty \quad (4.23)$$

From the orthogonality of the projections  $\mathbf{\Pi}^H$  and  $\mathbf{\Pi}^D$  it is evident that

$$\begin{aligned} |\chi_1 \sigma(\mathbf{x})|^2 &= |\chi_1 \mathbf{\Pi}^D \sigma(\mathbf{x})|^2 + |\chi_1 \mathbf{\Pi}^H \sigma(\mathbf{x})|^2 \\ &\geq |\chi_1 \mathbf{\Pi}^D \sigma(\mathbf{x})|^2 \end{aligned} \quad (4.24)$$

and it follows that

$$\langle \chi_1 |\sigma(\mathbf{x})|^r \rangle^{1/r} \geq \langle \chi_1 |\mathbf{\Pi}^D \sigma(\mathbf{x})|^r \rangle^{1/r}, \text{ for } 2 \leq r \leq \infty. \quad (4.25)$$

The bound (2.4) now follows immediately from Eqs. (4.25) and (4.23). Substitution of  $\psi(\mathbf{x}) = \sigma(\mathbf{x})$  into (4.2) and (4.24) gives

$$\|\sigma(\mathbf{x})\|_\infty \geq \sqrt{\langle |\sigma(\mathbf{x})|^2 \rangle} \geq |\mathbf{\Pi}^D(\bar{\sigma})| \quad (4.26)$$

and (2.5) follows.

### 4.1.3 Lower Bounds on Stress Fields Subject to General Imposed Macroscopic Stresses and $\mu_1 = \mu_2$

In this section no constraints are placed on the imposed macroscopic stress. The imposed macroscopic stress can be any constant  $d \times d$  stress tensor,  $d = 2, 3$ .

In what follows we suppose the two component materials share the same shear modulus, i.e.,  $\mu = \mu_1 = \mu_2$ . We will derive new lower bounds on the local stress inside material one that hold for any imposed macroscopic stress. In subsequent sections the lower bounds on the full local stress are shown to be optimal for special sets  $\mathcal{S}_1$  and  $\mathcal{S}_2$  and the lower bounds on the hydrostatic component of the local stress is shown to be optimal for all imposed macroscopic stresses.

From Eqs. (4.8) and (4.9) and since  $\mu_1 = \mu_2$ , one obtains

$$\langle \chi_1 \mathbf{\Pi}^H \sigma(\mathbf{x}) \rangle = \frac{\kappa_1}{\kappa_1 - \kappa_2} (\mathbf{\Pi}^H \bar{\sigma} - d\kappa_2 \mathbf{\Pi}^H \bar{\epsilon}) \quad (4.27)$$

The hydrostatic stress inside material one satisfies the following estimate

$$\langle \chi_1 \mathbf{\Pi}^H \sigma(\mathbf{x}) : \sigma(\mathbf{x}) \rangle \geq \frac{1}{\theta_1} |\langle \chi_1 \mathbf{\Pi}^H \sigma(\mathbf{x}) \rangle|^2, \quad (4.28)$$

which can be seen by taking  $\psi = \mathbf{\Pi}^H \sigma$  in Eq. (4.1).

For a composite consisting of two isotropic phases of equal shear moduli ( $\mu_1 = \mu_2 = \mu$ ), Hill's relation [29] shows that the effective elasticity tensor  $C^e$  is given by

$$C^e = 2\mu \mathbf{\Pi}^D + d\kappa^e \mathbf{\Pi}^H, \quad (4.29)$$

where

$$\kappa^e = (\theta_1 \kappa_1 + \theta_2 \kappa_2) - \frac{\theta_1 \theta_2 (\kappa_1 - \kappa_2)^2}{\theta_1 \kappa_2 + \theta_2 \kappa_1 + 2 \frac{d-1}{d} \mu} \quad (4.30)$$

From Eqs. (1.7) and (4.29), one obtains

$$\mathbf{\Pi}^H \bar{\epsilon} = \frac{1}{d\kappa^e} \mathbf{\Pi}^H \bar{\sigma} \quad (4.31)$$

Substituting in (4.27) one can write

$$\langle \chi_1 \mathbf{\Pi}^H \sigma(\mathbf{x}) \rangle = \frac{\kappa_1}{\kappa_1 - \kappa_2} \left(1 - \frac{\kappa_2}{\kappa^e}\right) \mathbf{\Pi}^H \bar{\sigma} \quad (4.32)$$

and from estimate (4.28), it follows that

$$\langle \chi_1 \mathbf{\Pi}^H \sigma(\mathbf{x}) : \sigma(\mathbf{x}) \rangle \geq \frac{\kappa_1^2}{\theta_1 (\kappa_1 - \kappa_2)^2} \left(1 - \frac{\kappa_2}{\kappa^e}\right)^2 |\mathbf{\Pi}^H \bar{\sigma}|^2 \quad (4.33)$$

Using the formula for  $\kappa^e$  given (4.30) we rewrite (4.33) as

$$\langle \chi_1 \mathbf{\Pi}^H \sigma(\mathbf{x}) : \sigma(\mathbf{x}) \rangle \geq \theta_1 \left( \frac{\kappa_1 \kappa_2 + 2 \frac{d-1}{d} \mu \kappa_1}{\kappa_1 \kappa_2 + 2 \frac{d-1}{d} \mu (\theta_1 \kappa_1 + \theta_2 \kappa_2)} \right)^2 |\mathbf{\Pi}^H \bar{\sigma}|^2. \quad (4.34)$$

For  $p$  and  $q$  such that  $p \geq 1$  and  $1/p + 1/q = 1$ , we apply Hölder's inequality to find that

$$\theta_1^{1/q} \langle \chi_1 |\mathbf{\Pi}^H \sigma(\mathbf{x})|^{2p} \rangle^{1/p} \geq \langle \chi_1 |\mathbf{\Pi}^H \sigma(\mathbf{x})|^2 \rangle \quad (4.35)$$

and hence the inequality

$$\langle \chi_1 |\mathbf{\Pi}^H \sigma(\mathbf{x})|^{2p} \rangle^{1/p} \geq \theta_1^{1/p} \left( \frac{\kappa_1 \kappa_2 + 2 \frac{d-1}{d} \mu \kappa_1}{\kappa_1 \kappa_2 + 2 \frac{d-1}{d} \mu (\theta_1 \kappa_1 + \theta_2 \kappa_2)} \right)^2 |\mathbf{\Pi}^H \bar{\sigma}|^2, \quad (4.36)$$

for  $1 \leq p \leq \infty$ .

Similar arguments give the bound

$$\langle \chi_2 \mathbf{\Pi}^H \sigma(\mathbf{x}) : \sigma(\mathbf{x}) \rangle \geq \theta_2 \left( \frac{\kappa_1 \kappa_2 + 2 \frac{d-1}{d} \mu \kappa_2}{\kappa_1 \kappa_2 + 2 \frac{d-1}{d} \mu (\theta_1 \kappa_1 + \theta_2 \kappa_2)} \right)^2 |\mathbf{\Pi}^H \bar{\sigma}|^2 \quad (4.37)$$

and it follows that

$$\langle \chi_2 |\mathbf{\Pi}^H \sigma(\mathbf{x})|^{2p} \rangle^{1/p} \geq \theta_2^{1/p} \left( \frac{\kappa_1 \kappa_2 + 2 \frac{d-1}{d} \mu \kappa_2}{\kappa_1 \kappa_2 + 2 \frac{d-1}{d} \mu (\theta_1 \kappa_1 + \theta_2 \kappa_2)} \right)^2 |\mathbf{\Pi}^H \bar{\sigma}|^2 \quad (4.38)$$

The bound (2.11) follows from Eqs. (4.36) and (4.38). The  $L^\infty$  bound, Eq. (2.12), follows from the bound (2.11) by taking  $r = \infty$  noting that

$$\|\mathbf{\Pi}^H \sigma(\mathbf{x})\|_\infty \geq \|\chi_i \mathbf{\Pi}^H \sigma(\mathbf{x})\|_\infty \text{ for } i = 1, 2.$$

To establish the bounds (2.7) and (2.8), we observe that because of orthogonality one obtains

$$|\sigma(\mathbf{x})|^2 = |\mathbf{\Pi}^H \sigma(\mathbf{x})|^2 + |\mathbf{\Pi}^D \sigma(\mathbf{x})|^2 \geq |\mathbf{\Pi}^H \sigma(\mathbf{x})|^2 \quad (4.39)$$

From Eq. (4.39) one can easily show that for  $i = 1, 2$

$$\langle \chi_i(\mathbf{x}) |\sigma(\mathbf{x})|^r \rangle^{1/r} \geq \langle |\mathbf{\Pi}^H \sigma(\mathbf{x})|^r \rangle^{1/r} \quad (4.40)$$

The bounds (2.7) and (2.8) follow from Eqs. (2.11) and (4.40).

#### 4.1.4 Lower Bounds on Stress Fields Subject to General Imposed Macroscopic Stresses and $\kappa_1 = \kappa_2$

In this subsection no constraints are placed on the imposed macroscopic stress. The imposed macroscopic stress can be any constant  $d \times d$  stress tensor,  $d = 2, 3$ . In what follows we suppose that the two component materials share the same bulk modulus, i.e.,  $\kappa = \kappa_1 = \kappa_2$  and we derive new lower bounds on the local Von Mises stress inside the material with greater shear stiffness. To fix ideas we suppose that material one has the greater shear stiffness, i.e.,  $\mu_1 > \mu_2$ . We will establish the lower bound Eq. (2.13) with the aid of the following observation whose proof is provided in Section 4.1.5.

For  $\kappa = \kappa_1 = \kappa_2$ , the effective elasticity tensor  $C^e$  can be written as

$$C^e = \mathbf{\Pi}^D C^e \mathbf{\Pi}^D + d\kappa \mathbf{\Pi}^H \quad (4.41)$$

and consequently

$$(C^e)^{-1} = (\mathbf{\Pi}^D C^e \mathbf{\Pi}^D)^{-1} + \frac{1}{d\kappa} \mathbf{\Pi}^H. \quad (4.42)$$

The Von Mises equivalent stress inside material one satisfies the following estimate

$$\langle \chi_1 \mathbf{\Pi}^D \sigma(\mathbf{x}) : \sigma(\mathbf{x}) \rangle \geq \frac{1}{\theta_1} |\langle \chi_1 \mathbf{\Pi}^D \sigma(\mathbf{x}) \rangle|^2, \quad (4.43)$$

which can be seen by taking  $\psi = \mathbf{\Pi}^D \sigma$  in Eq. (4.1).

We notice from Eq. (4.41) that  $C^e$  commutes with  $\mathbf{\Pi}^D$  which implies that  $(C^e)^{-1}$  commutes with  $\mathbf{\Pi}^D$ . Thus from Eq. (1.7) it follows that

$$\begin{aligned} \mathbf{\Pi}^D \bar{\epsilon} &= \mathbf{\Pi}^D (C^e)^{-1} \bar{\sigma} \\ &= (C^e)^{-1} \mathbf{\Pi}^D \bar{\sigma} \end{aligned}$$

Thus Eq. (4.12) becomes

$$\langle \chi_1 \mathbf{\Pi}^D \sigma(\mathbf{x}) \rangle = \frac{2\mu_1\mu_2}{\mu_1 - \mu_2} \left( \frac{1}{2\mu_2} \mathbf{\Pi}^D \bar{\sigma} - (C^e)^{-1} \mathbf{\Pi}^D \bar{\sigma} \right) \quad (4.44)$$

We apply Cauchy-Schwarz inequality to find that

$$|\langle \chi_1 \mathbf{\Pi}^D \sigma(\mathbf{x}) \rangle|^2 \geq \left( \frac{2\mu_1\mu_2}{\mu_1 - \mu_2} \right)^2 \frac{\left( \frac{1}{2\mu_2} \mathbf{\Pi}^D \bar{\sigma} : \mathbf{\Pi}^D \bar{\sigma} - ((C^e)^{-1} \mathbf{\Pi}^D \bar{\sigma} : \mathbf{\Pi}^D \bar{\sigma})^2 \right)}{|\mathbf{\Pi}^D \bar{\sigma}|^2} \quad (4.45)$$

With (4.45) in hand we proceed as in Section 5.1.2 to discover

$$|\langle \chi_1 \mathbf{\Pi}^D \sigma(\mathbf{x}) \rangle|^2 \geq \theta_1^2 |\mathbf{\Pi}^D \bar{\sigma}|^2 \quad (4.46)$$

and it follows from Eq. (4.43) that

$$\langle \chi_1 \mathbf{\Pi}^D \sigma(\mathbf{x}) : \sigma(\mathbf{x}) \rangle \geq \theta_1 |\mathbf{\Pi}^D \bar{\sigma}|^2. \quad (4.47)$$

The bounds (2.13) and (2.14) now follow from Hölder's inequality and arguments identical to those of Section (4.1.3).

The bound (2.14) follows directly from

$$\|\mathbf{\Pi}^D \sigma(\mathbf{x})\|_\infty \geq \sqrt{\langle \mathbf{\Pi}^D \sigma(\mathbf{x}) : \sigma(\mathbf{x}) \rangle} \geq |\mathbf{\Pi}^D \bar{\sigma}|, \quad (4.48)$$

where the last inequality is a consequence of Eq. (4.2).

#### 4.1.5 Form of $C^e$ for Mixtures of Two Elastically Isotropic Materials with Common Bulk Modulus.

In this section, we show that when  $\kappa = \kappa_1 = \kappa_2$ , the effective elasticity tensor  $C^e$  can be written as

$$C^e = \mathbf{\Pi}^D C^e \mathbf{\Pi}^D + d\kappa \mathbf{\Pi}^H.$$

Let  $\bar{\epsilon} = \langle \epsilon \rangle$ . Then since the two materials are isotropic and  $\kappa_1 = \kappa_2 = \kappa$  one obtains

$$\begin{aligned} C^e \bar{\epsilon} &= \langle C(\mathbf{x}) \epsilon(\mathbf{x}) \rangle \\ &= \langle 2\mu(\mathbf{x}) \mathbf{\Pi}^D \epsilon(\mathbf{x}) \rangle + \langle d\kappa \mathbf{\Pi}^H \epsilon(\mathbf{x}) \rangle \\ &= \mathbf{\Pi}^D \langle 2\mu(\mathbf{x}) \epsilon(\mathbf{x}) \rangle + d\kappa \mathbf{\Pi}^H \bar{\epsilon}. \end{aligned} \quad (4.49)$$

Since  $\mathbf{\Pi}^H \mathbf{\Pi}^D = 0$ , one obtains from Eq. (4.49) that

$$\mathbf{\Pi}^H C^e \bar{\epsilon} = d \kappa \mathbf{\Pi}^H \bar{\epsilon}. \quad (4.50)$$

For a deviatoric uniform field  $\bar{\epsilon} = \mathbf{\Pi}^D \bar{\epsilon}$ , it follows from Eq. (4.49) that

$$C^e \mathbf{\Pi}^D \bar{\epsilon} = \mathbf{\Pi}^D \langle 2\mu(\mathbf{x}) \epsilon(\mathbf{x}) \rangle \quad (4.51)$$

Thus for any two uniform strain fields  $\xi$  and  $\eta$

$$C^e \mathbf{\Pi}^D \xi : \mathbf{\Pi}^H \eta = \mathbf{\Pi}^H C^e \mathbf{\Pi}^D \xi : \eta = 0 \quad (4.52)$$

and using this observation one finds that

$$\begin{aligned} C^e \xi : \eta &= C^e (\mathbf{\Pi}^D \xi + \mathbf{\Pi}^H \xi) : (\mathbf{\Pi}^D \eta + \mathbf{\Pi}^H \eta) \\ &= C^e \mathbf{\Pi}^D \xi : \mathbf{\Pi}^D \eta + C^e \mathbf{\Pi}^H \xi : \mathbf{\Pi}^H \eta \\ &= \mathbf{\Pi}^D C^e \mathbf{\Pi}^D \xi : \eta + \mathbf{\Pi}^H C^e \mathbf{\Pi}^H \xi : \eta \end{aligned} \quad (4.53)$$

From Eq. (4.50) one obtains

$$\mathbf{\Pi}^H C^e \mathbf{\Pi}^H \xi : \eta = d \kappa \mathbf{\Pi}^H \xi : \eta \quad (4.54)$$

Thus Eq. (4.53) becomes

$$C^e \xi : \eta = (\mathbf{\Pi}^D C^e \mathbf{\Pi}^D + \mathbf{\Pi}^H) \xi : \eta \quad (4.55)$$

from which the result follows.

#### 4.1.6 Proof of (4.18)

For completeness, we provide a proof for inequality (4.18) presented in Section 4.1.2.

The complementary energy  $(C^e)^{-1} \bar{\sigma} : \bar{\sigma}$  satisfies the following variational principle (see, for example [71])

$$(C^e)^{-1} \bar{\sigma} : \bar{\sigma} = \inf_{\tau} \langle C^{-1} \tau : \tau \rangle \quad (4.56)$$

where  $\tau$  satisfies  $\nabla \cdot \tau = 0$ ,  $\langle \tau \rangle = \bar{\sigma}$ , and  $\tau = \tau^T$ . Taking the trial field  $\bar{\sigma}$  in the variational principle above, one obtains

$$(C^e)^{-1} \bar{\sigma} : \bar{\sigma} \leq \langle C^{-1} \rangle \bar{\sigma} : \bar{\sigma}. \quad (4.57)$$

Inequality (4.18) follows from this observation and the fact that

$$\langle C^{-1} \rangle = \theta_1 (C^1)^{-1} + \theta_2 (C^2)^{-1}.$$

## 4.2 Lower Bounds on Local Strain Fields

### 4.2.1 Hydrostatic Applied Strain

In this section we suppose that the imposed macroscopic strain is hydrostatic, i.e.,  $\bar{\epsilon} = \bar{p}I$ . It is assumed that the elastic materials are well-ordered and we suppose that  $\mu_1 > \mu_2$  and  $\kappa_1 > \kappa_2$ . For this case the lower bounds on the hydrostatic component of the local strain are given by [41]

$$\langle \chi_1(\mathbf{x}) |\mathbf{\Pi}^H \epsilon(\mathbf{x})|^r \rangle^{1/r} \geq \theta_1^{1/r} \frac{\kappa_2 + 2 \frac{d-1}{d} \mu_2}{\theta_1 \kappa_2 + \theta_2 \kappa_1 + 2 \frac{d-1}{d} \mu_2} |\bar{p}|, \text{ for } 2 \leq r \leq \infty. \quad (4.58)$$

and

$$\langle \chi_2(\mathbf{x}) |\mathbf{\Pi}^H \epsilon(\mathbf{x})|^r \rangle^{1/r} \geq \theta_2^{1/r} \frac{\kappa_1 + 2 \frac{d-1}{d} \mu_1}{\theta_1 \kappa_2 + \theta_2 \kappa_1 + 2 \frac{d-1}{d} \mu_1} |\bar{p}|, \text{ for } 2 \leq r \leq \infty. \quad (4.59)$$

$$\|\mathbf{\Pi}^H \epsilon(\mathbf{x})\|_\infty \geq \frac{\kappa_1 + 2 \frac{d-1}{d} \mu_1}{\theta_1 \kappa_2 + \theta_2 \kappa_1 + 2 \frac{d-1}{d} \mu_1} |\bar{p}| \quad (4.60)$$

It is pointed out that similar bounds hold for the non-well ordered case [41].

The lower bounds (3.1) and (3.2) and (3.3) follow immediately noting that the norm of the local strain is given by

$$|\epsilon(\mathbf{x})| = (|\mathbf{\Pi}^H \epsilon(\mathbf{x})|^2 + |\mathbf{\Pi}^D \epsilon(\mathbf{x})|^2)^{1/2} \text{ so } |\epsilon(\mathbf{x})| \geq |\mathbf{\Pi}^H \epsilon(\mathbf{x})|.$$

### 4.2.2 Deviatoric Applied Strain

In what follows we make no assumption on the magnitudes of the bulk modulus of each component material. We examine the local strain field inside the material

with larger shear modulus and without loss of generality we suppose that  $\mu_1 > \mu_2$ . We derive new lower bounds on the local strain inside material one that hold for any imposed macroscopic deviatoric strain. In subsequent sections these lower bounds are shown to be optimal for imposed macroscopic deviatoric strains in two dimensions and for imposed macroscopic strains that are pure shear strains in three dimensions.

The local strain inside material one satisfies the following inequality

$$\begin{aligned} \langle \chi_1 \epsilon(\mathbf{x}) : \epsilon(\mathbf{x}) \rangle &\geq \frac{1}{\theta_1} |\langle \chi_1 \epsilon(\mathbf{x}) \rangle|^2 \\ &\geq \frac{1}{\theta_1} |\langle \chi_1 \mathbf{\Pi}^D \epsilon(\mathbf{x}) \rangle|^2, \end{aligned} \quad (4.61)$$

which can be seen by taking  $\psi = \epsilon$  in Eq. (4.1) and noting that

$$|\langle \chi_1 \epsilon \rangle|^2 = |\langle \chi_1 \mathbf{\Pi}^D \epsilon \rangle|^2 + |\langle \chi_1 \mathbf{\Pi}^D \bar{\epsilon} \rangle|^2.$$

We apply the deviatoric projection on both sides of equation Eq. (4.9) and solve for  $\langle \chi_1 \mathbf{\Pi}^D \epsilon(\mathbf{x}) \rangle$  to obtain

$$\langle \chi_1 \mathbf{\Pi}^D \epsilon(\mathbf{x}) \rangle = \frac{1}{2(\mu_1 - \mu_2)} \mathbf{\Pi}^D (C^e - C^2) \bar{\epsilon} \quad (4.62)$$

Now we apply the hypothesis that  $\bar{\epsilon}$  is deviatoric, i.e.,  $\bar{\epsilon} = \bar{\epsilon}^D = \mathbf{\Pi}^D \bar{\epsilon}^D$  and from Eq. (4.62) one obtains

$$\begin{aligned} \langle \chi_1 \mathbf{\Pi}^D \epsilon(\mathbf{x}) \rangle &= \frac{1}{2(\mu_1 - \mu_2)} (\mathbf{\Pi}^D C^e \bar{\epsilon} - 2\mu_2 \mathbf{\Pi}^D \bar{\epsilon}) \\ &= \frac{1}{2(\mu_1 - \mu_2)} (\mathbf{\Pi}^D C^e \mathbf{\Pi}^D \bar{\epsilon} - 2\mu_2 \mathbf{\Pi}^D \bar{\epsilon}). \end{aligned} \quad (4.63)$$

We apply the Cauchy-Schwarz inequality to find that

$$|\langle \chi_1 \mathbf{\Pi}^D \epsilon(\mathbf{x}) \rangle|^2 \geq \frac{1}{(2\mu_1 - 2\mu_2)^2} \frac{(C^e \mathbf{\Pi}^D \bar{\epsilon} : \mathbf{\Pi}^D \bar{\epsilon} - 2\mu_2 \mathbf{\Pi}^D \bar{\epsilon} : \mathbf{\Pi}^D \bar{\epsilon})^2}{|\mathbf{\Pi}^D \bar{\epsilon}|^2}. \quad (4.64)$$

The effective elasticity tensor satisfies the following well known estimate [56]

$$\begin{aligned} C^e \mathbf{\Pi}^D \bar{\epsilon} : \mathbf{\Pi}^D \bar{\epsilon} &\geq \langle C^{-1}(\mathbf{x}) \rangle^{-1} \mathbf{\Pi}^D \bar{\epsilon} : \mathbf{\Pi}^D \bar{\epsilon} \\ &= \frac{2\mu_1 \mu_2}{\theta_1 \mu_2 + \theta_2 \mu_1} |\mathbf{\Pi}^D \bar{\epsilon}|^2 \end{aligned} \quad (4.65)$$

Using Eq. (4.65) one obtains

$$C^e \mathbf{\Pi}^{D\bar{\epsilon}} : \mathbf{\Pi}^{D\bar{\epsilon}} - 2\mu_2 \mathbf{\Pi}^{D\bar{\epsilon}} : \mathbf{\Pi}^{D\bar{\epsilon}} \geq \frac{\theta_1 \mu_2 (\mu_1 - \mu_2)}{\theta_1 \mu_2 + \theta_2 \mu_1} |\mathbf{\Pi}^{D\bar{\epsilon}}|^2 \quad (4.66)$$

Because  $\mu_1 > \mu_2$ , and after some simplification, we obtain from Eqs. (4.82) and (4.83) that

$$|\langle \chi_1 \mathbf{\Pi}^D \epsilon(\mathbf{x}) \rangle|^2 \geq \frac{\theta_1^2 \mu_2^2}{(\theta_1 \mu_2 + \theta_2 \mu_1)^2} |\mathbf{\Pi}^{D\bar{\epsilon}}|^2 \quad (4.67)$$

and it follows from Eq. (4.61) that

$$\langle \chi_1 \epsilon(\mathbf{x}) : \epsilon(\mathbf{x}) \rangle \geq \theta_1 \frac{\mu_2^2}{(\theta_1 \mu_2 + \theta_2 \mu_1)^2} |\mathbf{\Pi}^{D\bar{\epsilon}}|^2 \quad (4.68)$$

The lower bound (3.4) now easily follows from application of Hölder's inequality to the left side of (4.68).

### 4.2.3 Lower Bounds on the Local Strain for General Imposed Macroscopic Strains and $\mu_1 = \mu_2$

The dilatational strain inside material one satisfies the following estimate

$$\langle \chi_1 \mathbf{\Pi}^H \epsilon(\mathbf{x}) : \epsilon(\mathbf{x}) \rangle \geq \frac{1}{\theta_1} |\langle \chi_1 \mathbf{\Pi}^H \epsilon(\mathbf{x}) \rangle|^2, \quad (4.69)$$

which can be seen by taking  $\psi = \mathbf{\Pi}^H \epsilon$  in Eq. (4.1).

From Eq. (4.9) and since  $\mu_1 = \mu_2$ , one obtains

$$C^e \bar{\epsilon} = C^2 \bar{\epsilon} + 2(\kappa_1 - \kappa_2) \mathbf{\Pi}^H \langle \chi_1 \epsilon(\mathbf{x}) \rangle \quad (4.70)$$

Substitution of (4.29) into (4.70) and solving for  $\mathbf{\Pi}^H \langle \chi_1 \epsilon(\mathbf{x}) \rangle$  gives

$$\mathbf{\Pi}^H \langle \chi_1 \epsilon(\mathbf{x}) \rangle = \frac{\kappa^e - \kappa_2}{\kappa_1 - \kappa_2} |\mathbf{\Pi}^H \bar{\epsilon}| \quad (4.71)$$

It follows from Eqs. (4.69) and (4.71) that

$$\langle \chi_1 \mathbf{\Pi}^H \epsilon(\mathbf{x}) : \epsilon(\mathbf{x}) \rangle \geq \frac{1}{\theta_1} \left( \frac{\kappa^e - \kappa_2}{\kappa_1 - \kappa_2} \right)^2 |\mathbf{\Pi}^H \bar{\epsilon}|^2. \quad (4.72)$$

Substitution of (4.30) into (4.72) gives

$$\langle \chi_1 \mathbf{\Pi}^H \epsilon(\mathbf{x}) : \epsilon(\mathbf{x}) \rangle \geq \theta_1 \left( \frac{\kappa_2 + 2 \frac{d-1}{d} \mu}{\theta_1 \kappa_2 + \theta_2 \kappa_1 + 2 \frac{d-1}{d} \mu} \right)^2 |\mathbf{\Pi}^H \bar{\epsilon}|^2. \quad (4.73)$$

For  $p$  and  $q$  such that  $p \geq 1$  and  $1/p + 1/q = 1$ , we apply Hölder's inequality to find that

$$\theta_1^{1/q} \langle \chi_1 |\mathbf{\Pi}^H \epsilon(\mathbf{x})|^{2p} \rangle^{1/p} \geq \langle \chi_1 |\mathbf{\Pi}^H \epsilon(\mathbf{x})|^2 \rangle \quad (4.74)$$

and hence the inequality

$$\langle \chi_1 |\mathbf{\Pi}^H \epsilon(\mathbf{x})|^{2p} \rangle^{1/p} \geq \theta_1^{1/p} \left( \frac{\kappa_2 + 2 \frac{d-1}{d} \mu}{\theta_1 \kappa_2 + \theta_2 \kappa_1 + 2 \frac{d-1}{d} \mu} \right)^2 |\mathbf{\Pi}^H \bar{\epsilon}|^2, \quad (4.75)$$

for  $1 \leq p \leq \infty$ , and the bound Eq. (3.10) follows.

Similar arguments give the bound

$$\langle \chi_2 \mathbf{\Pi}^H \epsilon(\mathbf{x}) : \epsilon(\mathbf{x}) \rangle \geq \theta_2 \left( \frac{\kappa_1 + 2 \frac{d-1}{d} \mu}{\theta_1 \kappa_2 + \theta_2 \kappa_1 + 2 \frac{d-1}{d} \mu} \right)^2 |\mathbf{\Pi}^H \bar{\epsilon}|^2 \quad (4.76)$$

and it follows that

$$\langle \chi_2 |\mathbf{\Pi}^H \epsilon(\mathbf{x})|^{2p} \rangle^{1/p} \geq \theta_2^{1/p} \left( \frac{\kappa_1 + 2 \frac{d-1}{d} \mu}{\theta_1 \kappa_2 + \theta_2 \kappa_1 + 2 \frac{d-1}{d} \mu} \right)^2 |\mathbf{\Pi}^H \bar{\epsilon}|^2 \quad (4.77)$$

from which the bound Eq. (3.11) follows. The  $L^\infty$  bound, Eq. (3.12), follows from the bounds (3.10) and (3.11) by taking  $r = \infty$  noting that

$$\|\mathbf{\Pi}^D \epsilon(\mathbf{x})\|_\infty \geq \|\chi_i \mathbf{\Pi}^D \epsilon(\mathbf{x})\|_\infty \text{ for } i = 1, 2.$$

To establish the bounds (3.6) and (3.7), we observe that because of orthogonality one obtains

$$|\epsilon(\mathbf{x})|^2 = |\mathbf{\Pi}^H \epsilon(\mathbf{x})|^2 + |\mathbf{\Pi}^D \epsilon(\mathbf{x})|^2 \geq |\mathbf{\Pi}^H \epsilon(\mathbf{x})|^2 \quad (4.78)$$

It easily follows from (4.78) that for  $i = 1, 2$

$$\langle \chi_i(\mathbf{x}) |\epsilon(\mathbf{x})|^r \rangle^{1/r} \geq \langle \chi_i(\mathbf{x}) |\mathbf{\Pi}^H \epsilon(\mathbf{x})|^r \rangle^{1/r} \quad (4.79)$$

The bounds (3.6) and (3.7) follow from Eqs. (3.10), (3.11), and (4.79).

#### 4.2.4 Lower Bounds on the Local Von Mises Strain for General Imposed Strains and $\kappa_1 = \kappa_2$

In this section we consider a composite in which  $\kappa_1 = \kappa_2 = \kappa$  and assume without loss of generality that  $\mu_1 > \mu_2$ . The Von Mises equivalent strain inside material one satisfies the following estimate

$$\langle \chi_1 \mathbf{\Pi}^D \epsilon(\mathbf{x}) : \epsilon(\mathbf{x}) \rangle \geq \frac{1}{\theta_1} |\langle \chi_1 \mathbf{\Pi}^D \epsilon(\mathbf{x}) \rangle|^2, \quad (4.80)$$

which can be seen by taking  $\psi = \mathbf{\Pi}^D \epsilon$  in Eq. (4.1).

Since  $\kappa_1 = \kappa_2$  the effective elastic tensor is of the form given by (4.41) so  $\mathbf{\Pi}^D$  commutes with  $C^e$ . Thus Eq. (4.62) becomes

$$\langle \chi_1 \mathbf{\Pi}^D \epsilon(\mathbf{x}) \rangle = \frac{1}{2(\mu_1 - \mu_2)} (C^e - 2\mu_2) \mathbf{\Pi}^D \bar{\epsilon} \quad (4.81)$$

and we apply the Cauchy-Schwarz inequality to find that

$$|\langle \chi_1 \mathbf{\Pi}^D \epsilon(\mathbf{x}) \rangle|^2 \geq \frac{1}{(2\mu_1 - 2\mu_2)^2} \frac{(C^e \mathbf{\Pi}^D \bar{\epsilon} : \mathbf{\Pi}^D \bar{\epsilon} - 2\mu_2 \mathbf{\Pi}^D \bar{\epsilon} : \mathbf{\Pi}^D \bar{\epsilon})^2}{|\mathbf{\Pi}^D \bar{\epsilon}|^2}. \quad (4.82)$$

Application of (4.65) to (4.82) gives.

$$C^e \mathbf{\Pi}^D \bar{\epsilon} : \mathbf{\Pi}^D \bar{\epsilon} - 2\mu_2 \mathbf{\Pi}^D \bar{\epsilon} : \mathbf{\Pi}^D \bar{\epsilon} \geq \frac{\theta_1 \mu_2 (\mu_1 - \mu_2)}{\theta_1 \mu_2 + \theta_2 \mu_1} |\mathbf{\Pi}^D \bar{\epsilon}|^2. \quad (4.83)$$

We easily see from Eqs. (4.82) and (4.83) that

$$|\langle \chi_1 \mathbf{\Pi}^D \epsilon(\mathbf{x}) \rangle|^2 \geq \frac{\theta_1^2 \mu_2^2}{(\theta_1 \mu_2 + \theta_2 \mu_1)^2} |\mathbf{\Pi}^D \bar{\epsilon}|^2 \quad (4.84)$$

and it follows from Eq. (4.80) that

$$\langle \chi_1 \mathbf{\Pi}^D \epsilon(\mathbf{x}) : \epsilon(\mathbf{x}) \rangle \geq \theta_1 \frac{\mu_2^2}{(\theta_1 \mu_2 + \theta_2 \mu_1)^2} |\mathbf{\Pi}^D \bar{\epsilon}|^2. \quad (4.85)$$

The bound (3.13) follows immediately from Hölder's inequality applied to the left hand side of (4.85).

### 4.2.5 Proof of (4.65)

For completeness, we provide a proof for inequality (4.65) presented in Section 4.2.2.

The effective elastic energy satisfies

$$C^e \bar{\epsilon} : \bar{\epsilon} = \langle C(\mathbf{x}) \epsilon(\mathbf{x}) : \epsilon(\mathbf{x}) \rangle. \quad (4.86)$$

Applying Legendre transform to the local elastic energy in the right-hand side of Eq. (4.86) one obtains

$$C^e \bar{\epsilon} : \bar{\epsilon} \geq \langle 2\epsilon(\mathbf{x}) : \eta(\mathbf{x}) - C^{-1}(\mathbf{x})\eta(\mathbf{x}) : \eta(\mathbf{x}) \rangle, \quad (4.87)$$

for all  $Q$ -periodic symmetric  $d \times d$  tensors  $\eta \in L^2(Q)$ . Setting  $\eta$  equal a constant deviator  $\bar{\eta} = \mathbf{\Pi}^D \bar{\eta}$ , inequality (4.87) becomes

$$\begin{aligned} C^e \bar{\epsilon} : \bar{\epsilon} &\geq 2\bar{\epsilon} : \mathbf{\Pi}^D \bar{\eta} - \langle C^{-1}(\mathbf{x}) \rangle \mathbf{\Pi}^D \bar{\eta} : \mathbf{\Pi}^D \bar{\eta} \\ &= 2\bar{\epsilon} : \mathbf{\Pi}^D \bar{\eta} - \left( \frac{\theta_1}{2\mu_1} + \frac{\theta_2}{2\mu_2} \right) \mathbf{\Pi}^D \bar{\eta} : \mathbf{\Pi}^D \bar{\eta}. \end{aligned} \quad (4.88)$$

Optimizing over  $\bar{\eta}$  gives

$$C^e \bar{\epsilon} : \bar{\epsilon} \geq \frac{2\mu_1\mu_2}{\theta_1\mu_2 + \theta_2\mu_1} |\bar{\epsilon}|^2, \quad (4.89)$$

from which inequality (4.65) follows by setting  $\bar{\epsilon} = \mathbf{\Pi}^D \bar{\epsilon}$ .

# Chapter 5

## Microstructures That Support Optimal Local Fields

It is well known that the coated sphere, coated ellipsoid and laminated microstructures possess optimal effective elastic properties, for reviews of the literature see [48] and [71]. In the following sections we show that these microstructures possess optimal local field properties as well.

### 5.1 The Coated Sphere Construction and Optimal Lower Bounds on Local Stress and Strain Fields

In this section, it is shown that the lower bounds presented in Sections (2.1) and (3.1) are attained by the stress and strain fields inside the Hashin-Shtrikman [26, 27] coated cylinder and sphere assemblages, see Figure 5.1. We introduce the normalized  $L^p$  norm of a field  $f$  over a domain  $S$  by  $(|S|^{-1} \int_S |f(\mathbf{x})|^p d\mathbf{x})^{1/p}$ . One striking feature of the fields inside the coated sphere and cylinder assemblage is that the normalized  $L^p$  norm of the local stress or strain taken over a prototypical coated cylinder or sphere is the same as the  $L^p$  norm of the whole assemblage. Thus the  $L^p$  norms of local fields inside these assemblages are obtained by computing the  $L^p$  norm of a prototypical coated sphere or disk. Assuming that the applied field  $\bar{\sigma}$  is hydrostatic, the stress field inside a prototypical coated sphere (cylinder) centered at the origin with core of material one and coating of material two in Hashin-Shtrikman assemblage, is given by

$$\sigma = \begin{cases} B_1 \bar{\sigma} - B_2 \left( \frac{d\hat{\mathbf{x}} \otimes \hat{\mathbf{x}} - I}{|\mathbf{x}|^d} \right) \bar{\sigma}, & a < |\mathbf{x}| \leq b \\ B_3 \bar{\sigma}, & |\mathbf{x}| \leq a \end{cases} \quad (5.1)$$

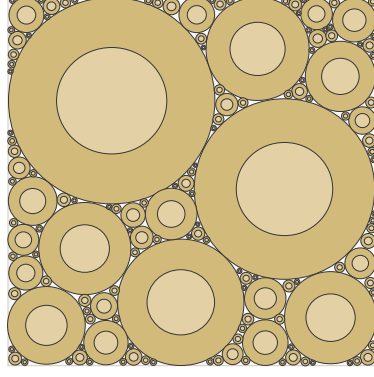


FIGURE 5.1. Hashin-Shtrikman coated cylinder assemblage.

where  $\hat{\mathbf{x}} = \mathbf{x}/|\mathbf{x}|$ ,  $a$  and  $b$  are the inner and outer radii of the coated sphere (cylinder), and the constants  $B_1, B_2, B_3$  are given by

$$B_1 = \frac{\kappa_1 \kappa_2 + 2 \frac{d-1}{d} \mu_2 \kappa_2}{\kappa_1 \kappa_2 + 2 \frac{d-1}{d} \mu_2 (\theta_1 \kappa_1 + \theta_2 \kappa_2)}, \quad (5.2)$$

$$B_2 = \frac{-2 \mu_2 a^d (\kappa_1 - \kappa_2)}{d(\kappa_1 \kappa_2 + 2 \frac{d-1}{d} \mu_2 (\theta_1 \kappa_1 + \theta_2 \kappa_2))}, \quad (5.3)$$

$$B_3 = \frac{\kappa_1 \kappa_2 + 2 \frac{d-1}{d} \mu_2 \kappa_1}{\kappa_1 \kappa_2 + 2 \frac{d-1}{d} \mu_2 (\theta_1 \kappa_1 + \theta_2 \kappa_2)}. \quad (5.4)$$

We notice from Eq. (5.1) that the stress field inside the core material (material one) is hydrostatic, thus

$$\langle \chi_1(\mathbf{x}) |\sigma(\mathbf{x})|^r \rangle^{1/r} = \langle \chi_1(\mathbf{x}) |\mathbf{\Pi}^H \sigma(\mathbf{x})|^r \rangle^{1/r} \quad (5.5)$$

On the other hand, as reported by Lipton [42], the local hydrostatic stress inside this microstructure attains the lower bound (4.3). Optimality of the lower bound (2.1) follows from these observations. Similar arguments show the lower bound (2.2) is attained by the stress field inside material two of a coated sphere (cylinder) assemblage with core of material two and coating of material one.

Next we show that the  $L^\infty$  bound (2.3) is attained by the stress field inside the coated sphere (cylinder) assemblage. One uses equations (5.1)-(5.4) to compute

the maximum stress inside each material. It is found that

$$\|\chi_1|\sigma|\|_\infty = \frac{\kappa_1\kappa_2 + 2\frac{d-1}{d}\mu_2\kappa_1}{\kappa_1\kappa_2 + 2\frac{d-1}{d}\mu_2(\theta_1\kappa_1 + \theta_2\kappa_2)} |\bar{\sigma}| \quad (5.6)$$

$$\|\chi_2|\sigma|\|_\infty = \frac{\sqrt{(\kappa_1\kappa_2 + 2\frac{d-1}{d}\mu_2\kappa_2)^2 + \frac{2}{d}(\mu_2(\kappa_1 - \kappa_2))^2}}{\kappa_1\kappa_2 + 2\frac{d-1}{d}\mu_2(\theta_1\kappa_1 + \theta_2\kappa_2)} |\bar{\sigma}| \quad (5.7)$$

Let  $D = 2\frac{d-1}{d}$ . Then a straightforward calculation shows that

$$\begin{aligned} \|\chi_1|\sigma|\|_\infty^2 - \|\chi_2|\sigma|\|_\infty^2 &= \frac{1}{(\kappa_1\kappa_2 + D\mu_2(\theta_1\kappa_1 + \theta_2\kappa_2))^2} |\bar{\sigma}|^2 \times \\ &\quad (\kappa_1 - \kappa_2) \left( \mu_2^2 \left( (D^2 + \frac{2}{d})\kappa_2 + (D^2 - \frac{2}{d})\kappa_1 \right) + 2D\mu_2\kappa_1\kappa_2 \right). \end{aligned} \quad (5.8)$$

Since  $\kappa_1 \geq \kappa_2$  and  $D^2 - \frac{2}{d} \geq 0$  for  $d = 2, 3$ , it follows from Eq. (5.8) that

$\|\sigma\|_{L^\infty(Q_1)}^2 \geq \|\sigma\|_{L^\infty(Q_2)}^2$  and hence

$$\|\sigma\|_\infty = \|\chi_1|\sigma|\|_\infty = \frac{\kappa_1\kappa_2 + 2\frac{d-1}{d}\mu_2\kappa_1}{\kappa_1\kappa_2 + 2\frac{d-1}{d}\mu_2(\theta_1\kappa_1 + \theta_2\kappa_2)} |\bar{\sigma}| \quad (5.9)$$

and it is evident that the local stress attains the bound (2.3).

Next we assume that the applied field  $\bar{\epsilon}$  is hydrostatic, the strain field inside a prototypical coated sphere (cylinder) with core of material two and coating of material one in Hashin-Shtrikman assemblage, is given by

$$\epsilon = \begin{cases} A_1 \bar{\epsilon} - A_2 \left( \frac{d\hat{\mathbf{x}} \otimes \hat{\mathbf{x}} - I}{|\mathbf{x}|^d} \right) \bar{\epsilon}, & a < |\mathbf{x}| \leq b \\ A_3 \bar{\epsilon}, & |\mathbf{x}| \leq a \end{cases} \quad (5.10)$$

and the constants  $A_1, A_2, A_3$  are given by

$$A_1 = \frac{\kappa_2 + 2\frac{d-1}{d}\mu_1}{\theta_1\kappa_2 + \theta_2\kappa_1 + 2\frac{d-1}{d}\mu_1}, \quad (5.11)$$

$$A_2 = \frac{-a^d(\kappa_2 - \kappa_1)}{\theta_1\kappa_2 + \theta_2\kappa_1 + 2\frac{d-1}{d}\mu_1}, \quad (5.12)$$

$$A_3 = \frac{\kappa_1 + 2\frac{d-1}{d}\mu_1}{\theta_1\kappa_2 + \theta_2\kappa_1 + 2\frac{d-1}{d}\mu_1}. \quad (5.13)$$

We see from Eq. (5.10) that the strain field inside the core material (material two) is hydrostatic, thus

$$\langle \chi_2(\mathbf{x}) |\epsilon(\mathbf{x})|^r \rangle^{1/r} = \langle \chi_2(\mathbf{x}) |\mathbf{\Pi}^H \epsilon(\mathbf{x})|^r \rangle^{1/r} \quad (5.14)$$

On the other hand this microstructure attains the lower bound (4.59) see [41]. Optimality of the lower bound (3.2) follows from these observations. Similar arguments show the lower bound (3.1) is attained by the strain field inside material one of a coated sphere (cylinder) assemblage with core of material one and coating of material two.

To show that the strain field inside the coated sphere (cylinder) assemblage attains the  $L^\infty$  bound (3.3) we use equations (5.10)-(5.13) to compute the maximum strain inside each material. It is found that

$$\|\chi_1|\epsilon|\|_\infty = \frac{\sqrt{(\kappa_2 + 2\frac{d-1}{d}\mu_1)^2 + \frac{d}{2}(\kappa_1 - \kappa_2)^2}}{\theta_1\kappa_2 + \theta_2\kappa_1 + 2\frac{d-1}{d}\mu_1} |\bar{\epsilon}| \quad (5.15)$$

$$\|\chi_2|\epsilon|\|_\infty = \frac{\kappa_1 + 2\frac{d-1}{d}\mu_1}{\theta_1\kappa_2 + \theta_2\kappa_1 + 2\frac{d-1}{d}\mu_1} |\bar{\epsilon}| \quad (5.16)$$

A straightforward calculation shows that

$$\|\chi_2|\epsilon|\|_\infty^2 - \|\chi_1|\epsilon|\|_\infty^2 = (\kappa_1 - \kappa_2) \left( (\kappa_1 + \kappa_2) - \frac{d}{2}(\kappa_1 - \kappa_2) + 4\frac{d-1}{d}\mu_1 \right) \times \frac{1}{(\theta_1\kappa_2 + \theta_2\kappa_1 + 2\frac{d-1}{d}\mu_1)^2} |\bar{\epsilon}|^2. \quad (5.17)$$

It follows from Eq. (5.17) that if  $d = 3$  and the elastic materials satisfy

$(\kappa_1 + \kappa_2) - \frac{3}{2}(\kappa_1 - \kappa_2) + \frac{8}{3}\mu_1 \geq 0$  or if  $d = 2$ , then  $\|\chi_2|\epsilon|\|_\infty \geq \|\chi_1|\epsilon|\|_\infty$  and hence

$$\|\epsilon|\|_\infty = \|\chi_2|\epsilon|\|_\infty = \frac{\kappa_1 + 2\frac{d-1}{d}\mu_1}{\theta_1\kappa_2 + \theta_2\kappa_1 + 2\frac{d-1}{d}\mu_1} |\bar{\epsilon}| \quad (5.18)$$

and it is evident that the bound (3.3) is attained by the local fields inside the coated sphere (cylinder) assemblage.

## 5.2 The Stress and Strain Fields Inside Simple Laminates and Optimal Bounds on Local Fields

For a two-phase simple laminate of two isotropic phases the local stress field is piecewise constant under uniform applied stress  $\bar{\sigma}$ . Thus

$$\begin{aligned}\bar{\sigma} &= \langle \chi_1(\mathbf{x})\sigma(\mathbf{x}) + \chi_2(\mathbf{x})\sigma(\mathbf{x}) \rangle \\ &= \theta_1\bar{\sigma}^1 + \theta_2\bar{\sigma}^2\end{aligned}\tag{5.19}$$

where  $\bar{\sigma}^i$  is the (constant) field inside the  $i$ -th phase. Since the stress field inside each phase satisfies the equation of elastic equilibrium Eq. (1.4) and from the continuity of the displacement  $\mathbf{u}$  and the traction  $\sigma\mathbf{n}$  across the two phase interface Eqs. (1.5) and (1.6), it follows that

$$\bar{\sigma}^1\mathbf{n} = \bar{\sigma}^2\mathbf{n}\tag{5.20}$$

$$(C^1)^{-1}\bar{\sigma}^1 - (C^2)^{-1}\bar{\sigma}^2 = \boldsymbol{\lambda} \odot \mathbf{n}\tag{5.21}$$

where  $\boldsymbol{\lambda}$  is a vector to be determined and  $\mathbf{n}$  is the layering direction of the laminate. Solution of the system of equations (5.19)–(5.21) delivers the local stress field inside each layer. The fields are given by

$$\bar{\sigma}^1 = \left( (C^1)^{-1} + \frac{\theta_1}{\theta_2}(C^2)^{-1} \right)^{-1} \left( \boldsymbol{\lambda} \odot \mathbf{n} + \frac{1}{\theta_2}(C^2)^{-1}\bar{\sigma} \right)\tag{5.22}$$

$$\bar{\sigma}^2 = \left( (C^2)^{-1} + \frac{\theta_2}{\theta_1}(C^1)^{-1} \right)^{-1} \left( -\boldsymbol{\lambda} \odot \mathbf{n} + \frac{1}{\theta_1}(C^1)^{-1}\bar{\sigma} \right)\tag{5.23}$$

and

$$\boldsymbol{\lambda} \odot \mathbf{n} = -A(\bar{\sigma}\mathbf{n} \odot \mathbf{n}) + \left( B(\bar{\sigma}\mathbf{n} \cdot \mathbf{n}) + C\frac{\text{tr}\bar{\sigma}}{d} \right) \mathbf{n} \odot \mathbf{n},\tag{5.24}$$

where

$$\begin{aligned}
A &= \frac{\Delta\mu}{\mu_1\mu_2} \\
B &= \Delta\mu \left( \frac{\langle\kappa\rangle \left(1 - \frac{2}{d}\right) + \langle\mu\rangle \frac{\kappa_1\kappa_2}{\mu_1\mu_2}}{2\mu_1\mu_2 \langle\kappa\rangle \left(1 - \frac{1}{d}\right) + \kappa_1\kappa_2 \langle\mu\rangle} \right) \\
C &= \frac{\Delta\mu \langle\kappa\rangle - \Delta\kappa \langle\mu\rangle}{2\mu_1\mu_2 \langle\kappa\rangle \left(1 - \frac{1}{d}\right) + \kappa_1\kappa_2 \langle\mu\rangle}, \tag{5.25}
\end{aligned}$$

where  $\langle\tilde{\mu}\rangle = \theta_1\mu_2 + \theta_2\mu_1$ , and  $\langle\tilde{\kappa}\rangle = \theta_1\kappa_2 + \theta_2\kappa_1$ . Here  $\Delta\mu = \mu_1 - \mu_2$ ,  $\Delta\kappa = \kappa_1 - \kappa_2$ ,  $\langle\mu\rangle = \theta_1\mu_1 + \theta_2\mu_2$ , and  $\langle\kappa\rangle = \theta_1\kappa_1 + \theta_2\kappa_2$ .

The local piece wise constant strain field inside each layer can be found in a similar way. For this case

$$\begin{aligned}
\bar{\epsilon} &= \langle\chi_1(\mathbf{x})\epsilon(\mathbf{x}) + \chi_2(\mathbf{x})\epsilon(\mathbf{x})\rangle \\
&= \theta_1\bar{\epsilon}^1 + \theta_2\bar{\epsilon}^2 \tag{5.26}
\end{aligned}$$

where  $\bar{\epsilon}^i$  is the (constant) field inside the  $i$ -th phase. Rewriting equations (5.20) and (5.21) in terms of the strain gives

$$(C^1\bar{\epsilon}^1)\mathbf{n} = (C^2\bar{\epsilon}^2)\mathbf{n} \tag{5.27}$$

$$\bar{\epsilon}^1 - \bar{\epsilon}^2 = \boldsymbol{\lambda} \odot \mathbf{n} \tag{5.28}$$

where  $\boldsymbol{\lambda}$  is a vector to be determined and  $\mathbf{n}$  is the layering direction of the laminate. Solution of the system of equations (5.26) – (5.28) delivers the local strain field inside each material. The strain fields are given by

$$\bar{\epsilon}^1 = \bar{\epsilon} + \theta_2\boldsymbol{\lambda} \odot \mathbf{n} \tag{5.29}$$

$$\bar{\epsilon}^2 = \bar{\epsilon} - \theta_1\boldsymbol{\lambda} \odot \mathbf{n} \tag{5.30}$$

and

$$\boldsymbol{\lambda} \odot \mathbf{n} = -A(\bar{\epsilon}\mathbf{n} \odot \mathbf{n}) + \left( B(\bar{\epsilon}\mathbf{n} \cdot \mathbf{n}) + C\frac{\text{tr}\bar{\epsilon}}{d} \right) \mathbf{n} \odot \mathbf{n} \tag{5.31}$$

Here

$$\begin{aligned}
A &= \frac{2\Delta\mu}{\langle\tilde{\mu}\rangle} \\
B &= \frac{2\Delta\mu(d\langle\tilde{\kappa}\rangle + (d-2)\langle\tilde{\mu}\rangle)}{\langle\tilde{\mu}\rangle((2d-2)\langle\tilde{\mu}\rangle + d\langle\tilde{\kappa}\rangle)} \\
C &= \frac{d(2\Delta\mu + d\Delta\kappa)}{(2d-2)\langle\tilde{\mu}\rangle + d\langle\tilde{\kappa}\rangle}.
\end{aligned} \tag{5.32}$$

where  $\langle\tilde{\mu}\rangle = \theta_1\mu_2 + \theta_2\mu_1$ , and  $\langle\tilde{\kappa}\rangle = \theta_1\kappa_2 + \theta_2\kappa_1$ .

We recall that both deviatoric applied stress in two dimensions as well as pure shear stresses in three dimensions can be expressed in the form  $\bar{\sigma} = s(\mathbf{a} \odot \mathbf{b})$  with  $\mathbf{a} \cdot \mathbf{b} = 0$ ,  $|\mathbf{a}| = 1$  and  $|\mathbf{b}| = 1$ . On choosing  $\mathbf{n} = \mathbf{a}$  or  $\mathbf{n} = \mathbf{b}$  in (5.24), one easily sees that that

$$\boldsymbol{\lambda} \odot \mathbf{n} = -\frac{\Delta\mu}{2\mu_1\mu_2} \bar{\sigma} \tag{5.33}$$

and it follows from Eqs. (5.22) and (5.23) that

$$\bar{\sigma}^1 = \bar{\sigma}^2 = \bar{\sigma} \tag{5.34}$$

From this observation it is evident that the stress field inside this simple laminate attains the bounds (2.4) and (2.5).

The deviatoric applied strain in two dimensions as well as pure shear strains in three dimensions also are expressed in the form  $\bar{\epsilon} = \varepsilon(\mathbf{a} \odot \mathbf{b})$  with  $\mathbf{a} \cdot \mathbf{b} = 0$ ,  $|\mathbf{a}| = 1$  and  $|\mathbf{b}| = 1$ . On choosing  $\mathbf{n} = \mathbf{a}$  or  $\mathbf{n} = \mathbf{b}$  in (5.31) one easily finds that

$$\boldsymbol{\lambda} \odot \mathbf{n} = -\frac{\Delta\mu}{\langle\tilde{\mu}\rangle} \bar{\epsilon} \tag{5.35}$$

and it follows from Eq. (5.29) that

$$\bar{\epsilon}^1 = \frac{\mu_2}{\langle\tilde{\mu}\rangle} \bar{\epsilon} \tag{5.36}$$

From this observation it is evident that the strain field inside this simple laminate attains the bound (3.4).

When both materials share the same shear modulus we find that the local hydrostatic stress and strain fields inside simple laminates have extremal properties. We demonstrate first that the lower bounds (2.11) and (2.12) are attained by the hydrostatic stress fields inside any simple laminate. For a simple laminate the stress field inside each material is constant hence both sides of inequality (4.28) are in fact equal and

$$\langle \chi_1 \mathbf{\Pi}^H \sigma(\mathbf{x}) : \sigma(\mathbf{x}) \rangle = \frac{1}{\theta_1} |\langle \chi_1 \mathbf{\Pi}^H \sigma(\mathbf{x}) \rangle|^2 = \theta_1 |\mathbf{\Pi}^H \bar{\sigma}^1|^2, \quad (5.37)$$

where  $\bar{\sigma}^1$  is the constant field inside material one. On the other hand, since  $\mu_1 = \mu_2$  one obtains from Eqs. (4.32) and (4.30) that

$$\frac{1}{\theta_1} |\langle \chi_1 \mathbf{\Pi}^H \sigma(\mathbf{x}) \rangle|^2 = \theta_1 \left( \frac{\kappa_1 \kappa_2 + 2 \frac{d-1}{d} \mu \kappa_1}{\kappa_1 \kappa_2 + 2 \frac{d-1}{d} \mu (\theta_1 \kappa_1 + \theta_2 \kappa_2)} \right)^2 |\mathbf{\Pi}^H \bar{\sigma}^1|^2. \quad (5.38)$$

Thus it follows from Eqs. (5.37) and (5.38) that the local hydrostatic stress inside a simply layered laminate attains the bound (2.11) when  $i = 1$ . Given  $\mu_1 = \mu_2$  these arguments show that if the stress field is constant inside material one then its hydrostatic part attains the lower bound (2.11). Similar arguments show the optimality of the bound (2.11) when  $i = 2$ . The fact that the hydrostatic stress inside a rank-one laminate attains the bound (2.11) for  $i = 1$  and  $i = 2$ , implies that it also attains the  $L^\infty$  bound (2.12).

We demonstrate that the lower bounds (3.10), (3.11) and (3.12) are attained by the hydrostatic strain fields inside any simple laminate. For a simple laminate the strain field inside each material is constant hence both sides of inequality (4.69) are in fact equal

$$\langle \chi_1 \mathbf{\Pi}^H \epsilon(\mathbf{x}) : \epsilon(\mathbf{x}) \rangle = \frac{1}{\theta_1} |\langle \chi_1 \mathbf{\Pi}^H \epsilon(\mathbf{x}) \rangle|^2 = \theta_1 |\mathbf{\Pi}^H \bar{\epsilon}^1|^2, \quad (5.39)$$



FIGURE 5.2. A rank-one layered material.

where  $\bar{\epsilon}^1$  is the constant field inside material one. On the other hand, since  $\mu_1 = \mu_2$  one observes that (4.71) and (4.30) imply

$$\frac{1}{\theta_1} |\langle \chi_1 \mathbf{\Pi}^H \epsilon(\mathbf{x}) \rangle|^2 = \theta_1 \left( \frac{\kappa_2 + 2\frac{d-1}{d}\mu}{\theta_1 \kappa_2 + \theta_2 \kappa_1 + 2\frac{d-1}{d}\mu} \right)^2 |\mathbf{\Pi}^H \bar{\epsilon}|^2. \quad (5.40)$$

It easily follows from (5.39) and (5.40) that the hydrostatic component of the local strain attains the lower bound (3.10). Given  $\mu_1 = \mu_2$  these arguments show that if the strain field is constant inside material one then its hydrostatic part attains the lower bound (3.10). Similar arguments show the optimality of the bound (3.11). The fact that the dilatational strain inside a rank-one laminate attains the two bounds (3.10) and (3.11), implies that it also attains the  $L^\infty$  bound (3.12).

We suppose that  $\kappa_1 = \kappa_2$ ,  $d = 2$  and we denote the orthonormal system of eigenvectors for a prescribed  $2 \times 2$  imposed macroscopic stress by  $\boldsymbol{\psi}^1, \boldsymbol{\psi}^2$ . We show that the lower bounds presented in Section (2.5) are attained by the stress fields inside a rank-one laminate with layering direction  $\mathbf{n} = \frac{1}{\sqrt{2}}(\boldsymbol{\psi}^1 + \boldsymbol{\psi}^2)$ , see Figure 5.2. Choosing  $\kappa_1 = \kappa_2$  and  $\mathbf{n} = \frac{1}{\sqrt{2}}(\boldsymbol{\psi}^1 + \boldsymbol{\psi}^2)$  in (5.24) gives

$$\boldsymbol{\lambda} \odot \mathbf{n} = -\frac{\Delta\mu}{2\mu_1\mu_2} \mathbf{\Pi}^D \bar{\sigma} \quad (5.41)$$

and it follows from Eqs. (5.22) and (5.23) that

$$\mathbf{\Pi}^D \bar{\sigma}^1 = \mathbf{\Pi}^D \bar{\sigma}^2 = \mathbf{\Pi}^D \bar{\sigma} \quad (5.42)$$

From this observation it is evident that the stress field inside this rank-one laminate attains the bounds (2.13) and (2.14).

A similar phenomena occurs for the local strain fields inside a simple laminate. As before suppose  $\kappa_1 = \kappa_2$ ,  $d = 2$  and denote the eigenvectors for an imposed  $2 \times 2$  macroscopic strain  $\bar{\epsilon}$  by  $\boldsymbol{\epsilon}^1$  and  $\boldsymbol{\epsilon}^2$ . We set  $\kappa_1 = \kappa_2$  and  $\mathbf{n} = \frac{1}{\sqrt{2}}(\boldsymbol{\epsilon}^1 + \boldsymbol{\epsilon}^2)$  in Eq. (5.31) to discover that

$$\boldsymbol{\lambda} \odot \mathbf{n} = -\frac{\Delta\mu}{\langle \tilde{\mu} \rangle} \boldsymbol{\Pi}^D \bar{\epsilon}. \quad (5.43)$$

It now follows from Eq. (5.29) that

$$\boldsymbol{\Pi}^D \bar{\epsilon}^{-1} = \frac{\mu_2}{\langle \tilde{\mu} \rangle} \boldsymbol{\Pi}^D \bar{\epsilon} \quad (5.44)$$

From this observation it is evident that the Von Mises equivalent strain field inside this rank-one laminate attains the bound (3.13).

### 5.3 The Confocal Ellipsoid Assemblage and Optimal Lower Bounds on Local Stress and Strain Fields for Subsets of Imposed Macroscopic Loads

In this section, it is shown that the lower bounds (2.7), (2.8), (2.9), and (2.10) are attained by the stress fields inside the confocal-ellipsoid and confocal-ellipse assemblages. Assuming that the uniform stress lies in  $\mathcal{S}_1$  it follows that there is a confocal-ellipse (confocal-ellipsoid) assemblage with core of material one and coating of material two associated with  $\bar{\sigma}$  such that the local stress inside the core material is constant and hydrostatic. Since the stress field inside material one of material two is constant, then it follows from earlier arguments that

$$\langle \chi_1 \boldsymbol{\Pi}^H \boldsymbol{\sigma}(\mathbf{x}) : \boldsymbol{\sigma}(\mathbf{x}) \rangle = \theta_1 \left( \frac{\kappa_1 \kappa_2 + 2 \frac{d-1}{d} \mu \kappa_1}{\kappa_1 \kappa_2 + 2 \frac{d-1}{d} \mu (\theta_1 \kappa_1 + \theta_2 \kappa_2)} \right)^2 |\boldsymbol{\Pi}^H \bar{\sigma}|^2. \quad (5.45)$$

On the other hand, since the stress field in material one is hydrostatic one sees that

$$\langle \chi_1 \mathbf{\Pi}^D \sigma(\mathbf{x}) : \sigma(\mathbf{x}) \rangle = 0 \quad (5.46)$$

and it is also evident that the lower bounds (2.9) are attained. From Eqs. (5.45) and (5.46), and the fact that  $\sigma(\mathbf{x}) = \mathbf{\Pi}^H \sigma(\mathbf{x}) + \mathbf{\Pi}^D \sigma(\mathbf{x})$  one obtains

$$\langle \chi_1 \sigma(\mathbf{x}) : \sigma(\mathbf{x}) \rangle = \theta_1 \left( \frac{\kappa_1 \kappa_2 + 2 \frac{d-1}{d} \mu \kappa_1}{\kappa_1 \kappa_2 + 2 \frac{d-1}{d} \mu (\theta_1 \kappa_1 + \theta_2 \kappa_2)} \right)^2 |\mathbf{\Pi}^H \bar{\sigma}|^2, \quad (5.47)$$

from which optimality of the bound (2.7) follows.

Identical arguments show that the local stress field inside material two of a confocal-ellipse (confocal-ellipsoid) assemblage with core of material two and coating of material one saturates the bounds (2.8) and (2.10).

A similar phenomena occurs for the local strain inside the confocal ellipse and confocal ellipsoid assemblage. Here we show that the lower bounds (3.6), (3.7), (3.8), and (3.9) are attained by the strain fields inside the confocal-ellipsoid and confocal-ellipse assemblages. Assuming that the uniform strain lies in  $\mathcal{E}_1$  it follows that there is a confocal-ellipse (confocal-ellipsoid) assemblage with core of material one and coating of material two associated with  $\bar{\epsilon}$  such that the local stress inside the core material is constant and hydrostatic. Since the strain field in material one of is constant, then it follows from earlier arguments that

$$\langle \chi_1 \mathbf{\Pi}^H \epsilon(\mathbf{x}) : \epsilon(\mathbf{x}) \rangle = \theta_1 \left( \frac{\kappa_2 + 2 \frac{d-1}{d} \mu}{\theta_1 \kappa_2 + \theta_2 \kappa_1 + 2 \frac{d-1}{d} \mu} \right)^2 |\mathbf{\Pi}^H \bar{\epsilon}|^2. \quad (5.48)$$

On the other hand, since the strain field in material one is hydrostatic one obtains

$$\langle \chi_1 \mathbf{\Pi}^D \epsilon(\mathbf{x}) : \epsilon(\mathbf{x}) \rangle = 0 \quad (5.49)$$

and it is also evident that the lower bounds (3.8) are attained. From Eqs. (5.48) and (5.49), and the fact that  $\epsilon(\mathbf{x}) = \mathbf{\Pi}^H \epsilon(\mathbf{x}) + \mathbf{\Pi}^D \epsilon(\mathbf{x})$  one obtains

$$\langle \chi_1 \epsilon(\mathbf{x}) : \epsilon(\mathbf{x}) \rangle = \theta_1 \left( \frac{\kappa_2 + 2 \frac{d-1}{d} \mu}{\theta_1 \kappa_2 + \theta_2 \kappa_1 + 2 \frac{d-1}{d} \mu} \right)^2 |\mathbf{\Pi}^H \bar{\epsilon}|^2, \quad (5.50)$$

from which optimality of the bound (3.6) follows.

Similar arguments show that the strain field in material two of a confocal-ellipse (confocal-ellipsoid) assemblage with core of material two and coating of material one attains the bounds (3.7) and (3.9).

# Chapter 6

## Multiscale Analysis of Heterogeneous Media in the Peridynamic Formulation

### 6.1 Introduction

The peridynamic formulation is a nonlocal continuum theory for deformable bodies that does not use the spatial derivatives of the displacement field. Interactions between material particles are characterized by a pairwise force field that acts across a finite *horizon*, see Section 6.2. The same equations of motion are applicable over the entire body and no special treatment is required near or at defects. These properties make it a potentially powerful tool to model problems that involve cracks, interfaces, and other defects, see [4, 5, 20, 63, 64, 65]. This work focuses on the multiscale analysis of heterogeneous media using the peridynamic formulation. The objective is to capture the dynamics inside composites at both the structural scale and the microscopic scale with a cost far below that of direct numerical simulation.

We consider particle or fiber reinforced composites. Here the characteristic length scale of the particle or fiber reinforced geometry is assumed to be very small relative to the length scale of the applied loads. The length scale of the microstructure is denoted by  $\varepsilon$ . We study three peridynamic models of fiber-reinforced materials. In the first model, which we call “the short-range bond model”, the peridynamic horizon is of the same length scale as that of the microstructure and the horizon approaches zero as  $\varepsilon$  goes to zero. In the second model, a long-range  $\varepsilon$ -independent pairwise force is added to the short-range pairwise force of the first model. Here the long-range pairwise force depends only on the relative position of the two particles and the associated peridynamic horizon is fixed and independent of the

microstructure length scale  $\varepsilon$ . We will refer to the second model as “the short-range and long-range bond model”. In the third model, we consider a long-range pairwise force that fluctuates with the microstructure. The peridynamic horizon in this model is fixed and independent of  $\varepsilon$ . This model will be called “the fluctuating long-range bond model”.

In all of these models, the peridynamic initial value problem is a partial integro-differential equation with rapidly-oscillating coefficients supplemented with initial conditions.

A multiscale analysis method is developed for the first two models. The concept of two-scale convergence, introduced by Nguetseng [53] and Allaire [1], is used as a tool to identify both the macroscopic and microscopic dynamics inside the composite. A downscaling method obtained through the use of Semigroup theory provides a strong convergence result which captures the micro-level fluctuations about the macroscopic displacement field. The downscaling step in the first model is complemented with error estimates for sufficiently regular initial data. This multiscale analysis is shown to provide the theoretical framework for an inexpensive multiscale numerical method for computing the deformation of fiber-reinforced composites in the presence of residual forces.

A multiscale analysis method is developed for the third model. The Semigroup theory of linear operators [16, 18] is utilized to identify both the macroscopic and microscopic dynamics of the composite. Downscaling and error estimates are provided for this model. Finally, an inexpensive multiscale numerical method is presented.

The second part of the dissertation, Chapters 6-11, is organized as follows. Section 6.2 provides an overview of the peridynamic formulation of continuum mechanics. In Section 6.3, we introduce three peridynamic models of fiber-reinforced

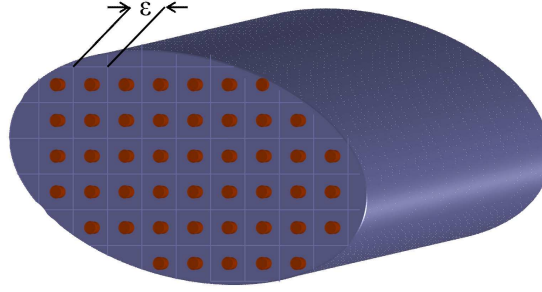


FIGURE 6.1. Fiber-reinforced composite.

composites. The results for the first two models are discussed and derived in Chapters 7-10. In Chapter 7, we present a multiscale analysis method for these two models. Chapter 8 provides uniqueness and existence results for the linear peridynamic initial-value problem (6.10)-(6.12). In Chapter 9, we review two-scale convergence and then use it to identify the two-scale asymptotic limit of (6.10)-(6.12). In Chapter 10, we build on the analysis provided in Chapter 9 to justify the results of Chapter 7. Chapter 11 is devoted to the third peridynamic model of fiber-reinforced composites. A multiscale analysis method is presented and justified for this model.

## 6.2 The Peridynamic Formulation of Continuum Mechanics

In the peridynamic theory, the time evolution of the displacement vector field  $u$ , in a heterogeneous medium, is given by the partial integro-differential equation

$$\rho(x) \partial_t^2 u(x, t) = \int_{H_x} f(u(\hat{x}, t) - u(x, t), \hat{x} - x, x) d\hat{x} + b(x, t), \quad (x, t) \in \Omega \times (0, T) \quad (6.1)$$

where  $H_x$  is a neighborhood of  $x$ ,  $\rho$  is the mass density,  $b$  is a prescribed loading force density field, and  $\Omega$  is a bounded set in  $\mathbb{R}^3$ . Here  $f$  denotes the pairwise force field whose value is the force vector (per unit volume squared) that the particle at  $\hat{x}$  exerts on the particle at  $x$ . For a homogeneous medium  $f$  is of the form  $f(u(\hat{x}, t) - u(x, t), \hat{x} - x)$ , i.e., it depends only on the relative position of the two

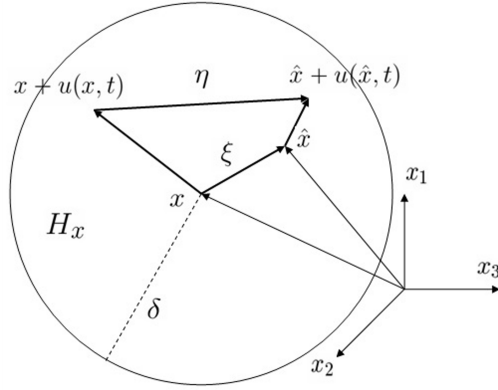


FIGURE 6.2. New and old bond and displacements within the peridynamic horizon.

particles. We will often refer to  $f$  as a *bond force*. Equation (6.1) is supplemented with initial conditions for  $u(x, 0)$  and  $\partial_t u(x, 0)$ . For the sake of simplicity, we assume constant mass density given by  $\rho(x) = 1$ . However, the removal of this hypothesis presents no barrier to the subsequent analysis. For the purposes of discussion it will be convenient to set

$$\xi = \hat{x} - x,$$

which represents the relative position of these two particles in the reference configuration, and

$$\eta = u(\hat{x}, t) - u(x, t),$$

which represents their relative displacement (see Figure 6.2). In the peridynamic formulation, it is assumed that for a given material there is a positive number  $\delta$ , called the horizon, such that

$$f(\eta, \xi, x) = 0, \text{ for } |\xi| > \delta.$$

The pairwise force field  $f$  is required to satisfy the following properties:

$$f(-\eta, -\xi, x + \xi) = -f(\eta, \xi, x) \tag{6.2}$$

which assures conservation of linear momentum, and

$$(\xi + \eta) \times f(\eta, \xi, x) = 0$$

which assures conservation of angular momentum.

A material is said to be *microelastic* if the pairwise force is derivable from a scalar *micropotential*  $\omega$

$$f(\eta, \xi, x) = \frac{\partial \omega}{\partial \eta}(\eta, \xi, x).$$

It can be shown that for a microelastic material the pairwise force is of the form (see [62])

$$f(\eta, \xi, x) = H(|\xi + \eta|, \xi, x)(\xi + \eta),$$

where  $H$  is a real-valued function. Finally, a material is linear if the associated bond force  $f(\eta, \xi, x)$  is linear in  $\eta$ .

In this treatment, all materials will be taken to be microelastic and linear.

### 6.3 Three Peridynamic Models of Fiber-Reinforced Materials

To fix ideas, we consider a periodic medium of unidirectional fiber-reinforced material. Here the pairwise force is given by the linearized version of the *bond-stretch model* proposed in [65]

$$f(\eta, \xi, x) = \alpha(x, x + \xi) \frac{\xi \otimes \xi}{|\xi|^3} \eta, \quad \text{for } \xi \in H_x.$$

Here  $\alpha$  is a real-valued function satisfying  $\alpha(x, \hat{x}) = \alpha(\hat{x}, x)$ . We will study three different peridynamic models for this composite. These models are distinct in the way the coefficient  $\alpha$  and the neighborhood set  $H_x$  are defined. We start by providing the mathematical description of the periodic microgeometry.

Let  $Y \subset \mathbb{R}^3$  be a unit cube and the local coordinates inside  $Y$  are denoted by  $y$  with the origin at the center of the unit cube. The unit cube is composed of a fiber

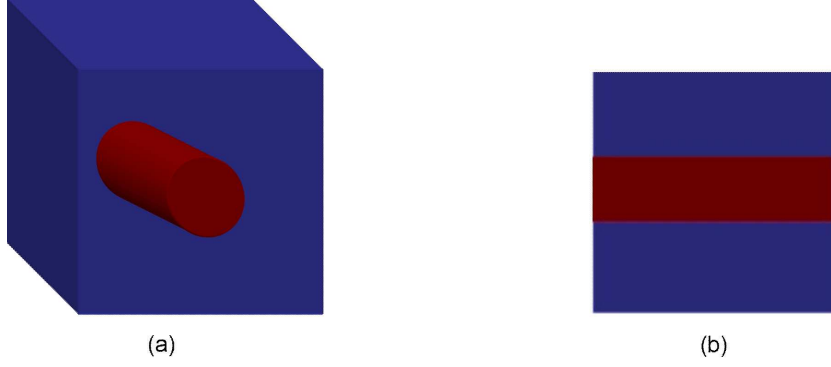


FIGURE 6.3. (a) Composite cube  $Y$ . (b) Cross-section of  $Y$  along the fiber direction.

which is surrounded by a second material called the matrix material, see Figure 6.3.

Let  $\chi_f$  denote the indicator function of the set occupied by the fiber material and  $\chi_m$  denote the the indicator function of the set occupied by the matrix material.

Here  $\chi_f$  is given by

$$\chi_f(y) = \begin{cases} 1, & y \text{ is in the fiber phase,} \\ 0, & \text{otherwise,} \end{cases}$$

and  $\chi_m$  is given by

$$\chi_m(y) = 1 - \chi_f(y).$$

We extend the functions  $\chi_f$  and  $\chi_m$  to  $\mathbb{R}^3$  by periodicity. For future reference, we denote by  $\theta_f$  and  $\theta_m$  the volume fractions of the fiber material and the matrix material, respectively. Here  $\theta_f = \int_Y \chi_f(y) dy$  and  $\theta_m = 1 - \theta_f$ . Also, we let  $n$  denote a unit vector parallel to the fiber direction.

In the first model, the short-range pairwise force is given by

$$f_{\text{short}}(\eta_y, \xi_y, y) = \begin{cases} \alpha(y, y + \xi_y) \frac{\xi_y \otimes \xi_y}{|\xi_y|^3} \eta_y, & |\xi_y| \leq \delta \\ 0, & \text{otherwise.} \end{cases} \quad (6.3)$$

where  $y \in Y$ ,  $\xi_y = \hat{y} - y$ ,  $\eta_y = u(\hat{y}, t) - u(y, t)$ , and  $\alpha$  is given by

$$\alpha(y, \hat{y}) = C_f \chi_f(y) \chi_f(\hat{y}) + C_m \chi_m(y) \chi_m(\hat{y}) + C_i (\chi_f(y) \chi_m(\hat{y}) + \chi_m(y) \chi_f(\hat{y})). \quad (6.4)$$

We note that (6.3)-(6.4) give the pairwise force on  $\mathbb{R}^3$  associated with a unit periodic geometry. In summary, the function  $\alpha$  in (6.4) is given by

$$\alpha(y, \hat{y}) = \begin{cases} C_f, & \text{if } y \text{ and } \hat{y} \text{ are in the fiber phase} \\ C_m, & \text{if } y \text{ and } \hat{y} \text{ are in the matrix phase} \\ C_i, & \text{otherwise.} \end{cases}$$

In equation (6.3), the peridynamic horizon  $\delta$  is chosen to be smaller than the fiber thickness in the unit cell. The material parameters  $C_f$  and  $C_m$  are intrinsic to each phase and can be determined through experiments. Bonds connecting particles in the different materials are characterized by  $C_i$ , which can be chosen such that  $C_f > C_i > C_m > 0$ , see [65].

The microgeometry associated with the length scale  $\varepsilon$  is obtained by rescaling the bond force  $f_{\text{short}}$  as follows. For  $x \in \Omega$ ,

$$f_{\text{short}}^\varepsilon(\eta, \xi, x) = \begin{cases} \frac{1}{\varepsilon^2} \alpha\left(\frac{x}{\varepsilon}, \frac{x + \xi}{\varepsilon}\right) \frac{\xi \otimes \xi}{|\xi|^3} \eta, & |\xi| \leq \varepsilon \delta \\ 0, & \text{otherwise.} \end{cases}$$

We see from (6.4) that  $\alpha\left(\frac{x}{\varepsilon}, \frac{\hat{x}}{\varepsilon}\right)$  is given by

$$\alpha\left(\frac{x}{\varepsilon}, \frac{\hat{x}}{\varepsilon}\right) = C_f \chi_f^\varepsilon(x) \chi_f^\varepsilon(\hat{x}) + C_m \chi_m^\varepsilon(x) \chi_m^\varepsilon(\hat{x}) + C_i (\chi_f^\varepsilon(x) \chi_m^\varepsilon(\hat{x}) + \chi_m^\varepsilon(x) \chi_f^\varepsilon(\hat{x})), \quad (6.5)$$

where  $\chi_f^\varepsilon(x) := \chi_f\left(\frac{x}{\varepsilon}\right)$  and  $\chi_m^\varepsilon(x) := \chi_m\left(\frac{x}{\varepsilon}\right)$ .

The peridynamic equation of motion for this model is given by

$$\partial_t^2 u^\varepsilon(x, t) = \int_{H_{\varepsilon\delta}(x)} \frac{1}{\varepsilon^2} \alpha\left(\frac{x}{\varepsilon}, \frac{\hat{x}}{\varepsilon}\right) \frac{(\hat{x} - x) \otimes (\hat{x} - x)}{|\hat{x} - x|^3} (u^\varepsilon(\hat{x}, t) - u^\varepsilon(x, t)) d\hat{x} + b\left(x, \frac{x}{\varepsilon}, t\right) \quad (6.6)$$

supplemented with initial conditions

$$u^\varepsilon(x, 0) = u^0\left(x, \frac{x}{\varepsilon}\right), \quad (6.7)$$

$$\partial_t u^\varepsilon(x, 0) = v^0\left(x, \frac{x}{\varepsilon}\right). \quad (6.8)$$

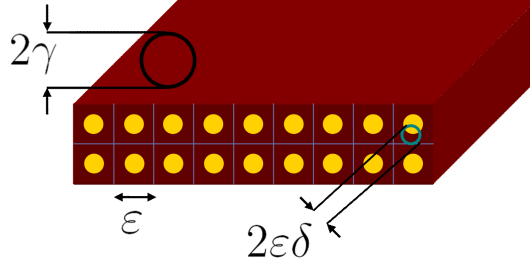


FIGURE 6.4. Long-range bonds (horizon  $\gamma$ ) and short-range bonds (horizon  $\varepsilon\delta$ ).

In what follows, we will denote by  $s$  a real number such that  $\frac{3}{2} < s < \infty$ . In (6.6)-(6.8),  $b(x, y, t)$  is in  $C([0, T]; L^s(\Omega \times Y)^3)$  and  $Y$ -periodic in  $y$  and  $u^0(x, y)$  and  $v^0(x, y)$  are in  $L^s(\Omega \times Y)^3$  and  $Y$ -periodic in  $y$ .

In the second model, the following long-range pairwise force is added to the short-range pairwise force of the first model (see Figure 6.4)

$$f_{\text{long}}(\eta, \xi) = \begin{cases} \lambda(\xi) \frac{\xi \otimes \xi}{|\xi|^3} \eta, & |\xi| \leq \gamma \\ 0, & \text{otherwise,} \end{cases}$$

where  $\gamma$  is a prescribed peridynamic horizon. Here  $\lambda$  is a real-valued function defined by

$$\lambda(\xi) = \begin{cases} C_f^M, & \nu_\xi \leq \frac{\pi}{2} \theta_f, \\ C_m^M, & \text{otherwise,} \end{cases} \quad (6.9)$$

where  $\nu_\xi$  denotes the angle between  $\xi$  and a line parallel to the fiber direction, with  $0 \leq \nu_\xi \leq \frac{\pi}{2}$ . The constants  $C_f^M$  and  $C_m^M$  are macroscopic parameters determined through experiments, see [65, 14].

Now the peridynamic equation of motion associated with the total pairwise force is given by

$$\begin{aligned}
\partial_t^2 u^\varepsilon(x, t) &= \int_{H_\gamma(x)} \lambda(\hat{x} - x) \frac{(\hat{x} - x) \otimes (\hat{x} - x)}{|\hat{x} - x|^3} (u^\varepsilon(\hat{x}, t) - u^\varepsilon(x, t)) d\hat{x} \\
&+ \int_{H_{\varepsilon\delta}(x)} \frac{1}{\varepsilon^2} \alpha\left(\frac{x}{\varepsilon}, \frac{\hat{x}}{\varepsilon}\right) \frac{(\hat{x} - x) \otimes (\hat{x} - x)}{|\hat{x} - x|^3} (u^\varepsilon(\hat{x}, t) - u^\varepsilon(x, t)) d\hat{x} \\
&+ b\left(x, \frac{x}{\varepsilon}, t\right),
\end{aligned} \tag{6.10}$$

supplemented with initial conditions

$$u^\varepsilon(x, 0) = u^0\left(x, \frac{x}{\varepsilon}\right), \tag{6.11}$$

$$\partial_t u^\varepsilon(x, 0) = v^0\left(x, \frac{x}{\varepsilon}\right). \tag{6.12}$$

**Remark 6.3.** The first model follows from the second model on setting  $\lambda = 0$ . Thus in Chapters 7-10, we will often present our results and analysis for the second model only.

In the third model, the pairwise force is given by

$$f(\eta_y, \xi_y, y) = \begin{cases} \alpha_L(y, y + \xi_y) \frac{\xi_y \otimes \xi_y}{|\xi_y|^3} \eta_y, & |\xi_y| \leq \delta \\ 0, & \text{otherwise,} \end{cases}$$

where  $y \in Y$  and  $\delta$  is a prescribed peridynamic horizon, and  $\alpha_L$  is given by

$$\alpha_L(y, y + \xi_y) = \begin{cases} C_f |\xi_y| \delta_n(\xi_y), & \text{if } y \text{ and } y + \xi_y \text{ are in the fiber phase,} \\ & \text{and } \xi_y \text{ is parallel to } n, \\ C_m |\xi_y|, & \text{otherwise.} \end{cases}$$

Here  $\delta_n$  is the Dirac delta distribution concentrated at a line parallel to  $n$ . The function  $\alpha_L$  can be written in terms of  $\chi_f$  as follows

$$\alpha_L(y, y + \xi_y) = C_f |\xi_y| \delta_n(\xi_y) \chi_f(y) \chi_f(y + \xi_y) + C_m |\xi_y| (1 - \delta_n(\xi_y)) \chi_f(y) \chi_f(y + \xi_y). \tag{6.13}$$

We note that in equation (6.13),  $\chi_f(y) = \chi_f(y + \xi_y)$  because  $y$  and  $y + \xi_y$  both lie on a line parallel to the fiber direction  $n$ .

The pairwise force defined on  $\Omega$  is given by

$$f^\varepsilon(\eta, \xi, x) = \begin{cases} \alpha_L^\varepsilon(x, x + \xi) \frac{\xi \otimes \xi}{|\xi|^3} \eta, & |\xi| \leq \delta \\ 0, & \text{otherwise,} \end{cases}$$

where  $\alpha_L^\varepsilon$  is defined by

$$\alpha_L^\varepsilon(x, x + \xi) = C_f |\xi| \delta_n(\xi) \chi_f^\varepsilon(x) + \varepsilon C_m |\xi| (1 - \delta_n(\xi) \chi_f^\varepsilon(x)). \quad (6.14)$$

The peridynamic equation of motion for this model is given by

$$\partial_t^2 u^\varepsilon(x, t) = \int_{H_\delta(x)} \alpha^\varepsilon(x, \hat{x}) \frac{(\hat{x} - x) \otimes (\hat{x} - x)}{|\hat{x} - x|^3} (u^\varepsilon(\hat{x}, t) - u^\varepsilon(x, t)) d\hat{x} \quad (6.15)$$

supplemented with initial data

$$u^\varepsilon(x, 0) = u^0(x), \quad (6.16)$$

$$\partial_t u^\varepsilon(x, 0) = v^0(x). \quad (6.17)$$

Here the initial data  $u^0$  and  $v^0$  are in  $L^p(\Omega)^3$  with  $1 \leq p < \infty$  and the loading force in equation (6.15) is zero.

# Chapter 7

## Multiscale Analysis Method for the Short-Range and Long-Range Bond Model

In this chapter, we present the multiscale analysis method for computing the deformation of fiber-reinforced composites modeled by the peridynamic formulation. This is done for the Short-Range and Long-Range Bond model described in Section 6.3. The method delivers a computationally inexpensive multiscale numerical method for analysis of these peridynamic models of fiber-reinforced materials. It consists of the following three steps.

(i) **Macroscopic Equation**

Compute the macroscopic or average displacement field by solving a peridynamic macroscopic equation.

(ii) **Cell-Problem**

Compute the micro-level mechanical responses by solving a peridynamic cell-problem.

(iii) **Downscaling**

The displacement field of the oscillatory peridynamic equation is given approximately by superimposing the rescaled micro-level mechanical responses over the average displacement field. The error in this approximation is shown to converge in norm to zero.

In the following sections, we consider four cases of initial and loading conditions. For each case, we present the macroscopic equation, the cell-problem, and the downscaling step. The results provided in this chapter are justified in Chapter 10.

For convenience, we introduce the following notation for the average of a periodic function. Let a function of the form  $p(y)$ ,  $p(x, y)$ , or  $p(x, y, t)$  be  $Y$ -periodic in the variable  $y$ . Its average over  $Y$  is denoted by

$$\begin{aligned}\bar{p} &= \int_Y p(y) dy, \\ \bar{p}(x) &= \int_Y p(x, y) dy, \text{ or} \\ \bar{p}(x, t) &= \int_Y p(x, y, t) dy,\end{aligned}$$

respectively. For future reference, we let

$$K = \int_{H_\gamma(x)} \lambda(\hat{x} - x) \frac{(\hat{x} - x) \otimes (\hat{x} - x)}{|\hat{x} - x|^3} d\hat{x}. \quad (7.1)$$

By the change of variables  $\xi = \hat{x} - x$ , it is easy to see that  $K$  is a constant matrix, which depends on the macroscopic parameters  $\gamma$ ,  $C_{\text{matrix}}^M$ , and  $C_{\text{fiber}}^M$ .

For future reference, we will adopt the notation  $L_{per}^p(Y)$  for the space of Lebesgue  $p$ -integrable functions which are  $Y$ -periodic. Similarly,  $C_{per}(Y)$  denotes the space of continuous  $Y$ -periodic functions. Also we denote by  $C^{0,\beta}(\bar{\Omega})$  the space of Hölder continuous functions with exponent  $\beta$ , where  $0 < \beta \leq 1$ .

## 7.1 First Case

In this section, the loading force and initial data are given by

$$b\left(x, \frac{x}{\varepsilon}, t\right) = l(x, t) + R\left(\frac{x}{\varepsilon}\right), \quad (7.2a)$$

$$u^0\left(x, \frac{x}{\varepsilon}\right) = u_0(x) + u_1\left(\frac{x}{\varepsilon}\right), \quad (7.2b)$$

$$v^0\left(x, \frac{x}{\varepsilon}\right) = v_0(x) + v_1\left(\frac{x}{\varepsilon}\right), \quad (7.2c)$$

where  $l \in C([0, T]; L^s(\Omega)^3)$ ,  $R$  is in  $L_{per}^s(Y)^3$  with  $\bar{R} = 0$ ,  $u_0$  and  $v_0$  are in  $L^s(\Omega)^3$ , and  $u_1$  and  $v_1$  are in  $L_{per}^s(Y)^3$  with  $\bar{u}_1 = \bar{v}_1 = 0$ . Here,  $R(\frac{x}{\varepsilon})$  can be interpreted as a residual force. For example, such forces can arise from the differences in thermal expansion between the two materials.

### 7.1.1 The Macroscopic Equation

The macroscopic or homogenized peridynamic equation is given by

$$\partial_t^2 u^H(x, t) = \int_{H_\gamma(x)} \lambda(\hat{x} - x) \frac{(\hat{x} - x) \otimes (\hat{x} - x)}{|\hat{x} - x|^3} (u^H(\hat{x}, t) - u^H(x, t)) d\hat{x} + l(x, t), \quad (7.3)$$

supplemented with initial data

$$u^H(x, 0) = u_0(x), \quad \partial_t u^H(x, 0) = v_0(x). \quad (7.4)$$

Here the macroscopic displacement  $u^H$  is the weak limit of the sequence of displacements  $u^\varepsilon$ . This is described by the following theorem.

**Theorem 7.1.** *Let  $u^\varepsilon$  be the solution of (6.10)-(6.12), where  $b$ ,  $u^0$ , and  $v^0$  are given by (7.2). Then as  $\varepsilon \rightarrow 0$*

$$u^\varepsilon(x, t) \rightarrow u^H(x, t) \quad \text{weakly in } L^s(\Omega \times (0, T))^3,$$

where  $u^H \in C^2([0, T]; L^s(\Omega)^3)$  is the unique solution of (7.3)-(7.4).

Moreover, assume that  $l \in C([0, T]; C(\bar{\Omega})^3)$ , and  $u_0$  and  $v_0$  are in  $C(\bar{\Omega})^3$ . Then  $u^H$  is in  $C^2([0, T]; C(\bar{\Omega})^3)$ .

### 7.1.2 The Cell-Problem

The cell-problem or the micro-level peridynamic equation is given by

$$\begin{aligned} \partial_t^2 r(y, t) &= \int_{H_\delta(y)} \alpha(y, \hat{y}) \frac{(\hat{y} - y) \otimes (\hat{y} - y)}{|\hat{y} - y|^3} (r(\hat{y}, t) - r(y, t)) d\hat{y} \\ &\quad - K r(y, t) + R(y), \end{aligned} \quad (7.5)$$

supplemented with initial conditions

$$r(y, 0) = u_1(y), \quad \partial_t r(y, 0) = v_1(y). \quad (7.6)$$

The matrix  $K$  is given by (7.1).

### 7.1.3 Downscaling

The macroscopic displacement  $u^H$  together with the rescaled solution of the cell problem provide an approximation to the actual solution  $u^\varepsilon$ . This is expressed in the following theorem.

**Theorem 7.2.** *Let  $u^\varepsilon$  be the solution of (6.10)-(6.12), where  $b$ ,  $u^0$ , and  $v^0$  are given by (7.2). Assume that  $l \in C([0, T]; C(\bar{\Omega})^3)$ , and  $u_0$  and  $v_0$  are in  $C(\bar{\Omega})^3$ . Then for almost every  $t \in (0, T)$ ,*

$$\lim_{\varepsilon \rightarrow 0} \left\| u^\varepsilon(x, t) - \left( u^H(x, t) + r \left( \frac{x}{\varepsilon}, t \right) \right) \right\|_{L^s(\Omega)^3} = 0, \quad (7.7)$$

where  $r \in C^2([0, T]; L^s_{per}(Y)^3)$  is the unique solution of (7.5)-(7.6).

Moreover, assume that  $\lambda = 0$  in equation (6.10). Then, for  $t \in (0, T)$  and  $u_0, v_0$ , and  $l(\cdot, t)$  in  $C^{0,\beta}(\bar{\Omega})^3$ , the error in (7.7) is estimated by

$$\left\| u^\varepsilon(x, t) - \left( u^H(x, t) + r \left( \frac{x}{\varepsilon}, t \right) \right) \right\|_{L^s(\Omega)^3} \leq M_1(t) \varepsilon^\beta, \quad (7.8)$$

where  $M_1(t)$  is independent of  $\varepsilon$ . The function  $M_1(t)$  is given explicitly in Section 10.2.1.

## 7.2 Second Case

In this section, the loading force and initial data are given by

$$b \left( x, \frac{x}{\varepsilon}, t \right) = F \left( \frac{x}{\varepsilon}, t \right) h(x), \quad (7.9a)$$

$$u^0 \left( x, \frac{x}{\varepsilon} \right) = 0, \quad (7.9b)$$

$$v^0 \left( x, \frac{x}{\varepsilon} \right) = 0, \quad (7.9c)$$

where  $F \in C([0, T]; L^s_{per}(Y)^{3 \times 3})$  and  $h \in L^s(\Omega)^3$ .

## 7.2.1 The Macroscopic Equation

The macroscopic peridynamic equation is given by

$$\partial_t^2 u^H(x, t) = \int_{H_\gamma(x)} \lambda(\hat{x} - x) \frac{(\hat{x} - x) \otimes (\hat{x} - x)}{|\hat{x} - x|^3} (u^H(\hat{x}, t) - u^H(x, t)) d\hat{x} + \bar{F}(t)h(x), \quad (7.10)$$

supplemented with initial data

$$u^H(x, 0) = 0, \quad \partial_t u^H(x, 0) = 0. \quad (7.11)$$

Here the macroscopic displacement  $u^H$  is the weak limit of the sequence of displacements  $u^\varepsilon$ . This is described by the following theorem.

**Theorem 7.3.** *Let  $u^\varepsilon$  be the solution of (6.10)-(6.12), where  $b$ ,  $u^0$ , and  $v^0$  are given by (7.9). Then as  $\varepsilon \rightarrow 0$*

$$u^\varepsilon(x, t) \rightarrow u^H(x, t) \quad \text{weakly in } L^s(\Omega \times (0, T))^3,$$

where  $u^H \in C^2([0, T]; L^s(\Omega)^3)$  is the unique solution of (7.10)-(7.11).

Moreover, assume that  $h \in C(\bar{\Omega})^3$ . Then  $u^H$  is in  $C^2([0, T]; C(\bar{\Omega})^3)$ .

## 7.2.2 The Cell-Problem

The micro-level peridynamics is given by the following equations. For  $j = 1, 2, 3$ ,

$$\begin{aligned} \partial_t^2 r^j(y, t) &= \int_{H_\delta(y)} \alpha(y, \hat{y}) \frac{(\hat{y} - y) \otimes (\hat{y} - y)}{|\hat{y} - y|^3} (r^j(\hat{y}, t) - r^j(y, t)) d\hat{y} \\ &\quad - K r^j(y, t) + (F^j(y, t) - \bar{F}^j(t)), \end{aligned} \quad (7.12)$$

supplemented with initial conditions

$$r^j(y, 0) = 0, \quad \partial_t r^j(y, 0) = 0. \quad (7.13)$$

In (7.12),  $F^j(y, t)$  and  $\bar{F}^j(t)$  denote the  $j^{\text{th}}$  columns of the matrices  $F(y, t)$  and  $\bar{F}(t)$ , respectively. The matrix  $K$  is given by (7.1).

### 7.2.3 Downscaling

The macroscopic displacement  $u^H$  together with the rescaled solution of the cell problem provide an approximation to the actual solution  $u^\varepsilon$ . This is expressed in the following theorem.

**Theorem 7.4.** *Let  $u^\varepsilon$  be the solution of (6.10)-(6.12), where  $b$ ,  $u^0$ , and  $v^0$  are given by (7.9). Assume that  $h \in C(\bar{\Omega})^3$ . Then for almost every  $t \in (0, T)$ ,*

$$\lim_{\varepsilon \rightarrow 0} \left\| u^\varepsilon(x, t) - \left( u^H(x, t) + \sum_{j=1}^3 r^j \left( \frac{x}{\varepsilon}, t \right) h_j(x) \right) \right\|_{L^s(\Omega)^3} = 0, \quad (7.14)$$

where  $r^j \in C^2([0, T]; L^s_{per}(Y)^3)$  is the unique solution of (7.12)-(7.13).

Moreover, assume that  $\lambda = 0$  in equation (6.10). Then, for  $t \in (0, T)$  and  $h \in C^{0,\beta}(\bar{\Omega})^3$ , the error in (7.14) is estimated by

$$\left\| u^\varepsilon(x, t) - \left( u^H(x, t) + \sum_{j=1}^3 r^j \left( \frac{x}{\varepsilon}, t \right) h_j(x) \right) \right\|_{L^s(\Omega)^3} \leq M_2(t) \varepsilon^\beta, \quad (7.15)$$

where  $M_2(t)$  is independent of  $\varepsilon$ . The function  $M_2(t)$  is given explicitly in Section 10.2.2.

## 7.3 Third Case

In this section, the loading force and initial data are given by

$$b \left( x, \frac{x}{\varepsilon}, t \right) = 0, \quad (7.16a)$$

$$u^0 \left( x, \frac{x}{\varepsilon} \right) = F \left( \frac{x}{\varepsilon} \right) h(x), \quad (7.16b)$$

$$v^0 \left( x, \frac{x}{\varepsilon} \right) = 0, \quad (7.16c)$$

where  $F \in L^s_{per}(Y)^{3 \times 3}$  and  $h \in L^s(\Omega)^3$ .

### 7.3.1 The Macroscopic Equation

The macroscopic peridynamic equation is given by

$$\partial_t^2 u^H(x, t) = \int_{H_\gamma(x)} \lambda(\hat{x} - x) \frac{(\hat{x} - x) \otimes (\hat{x} - x)}{|\hat{x} - x|^3} (u^H(\hat{x}, t) - u^H(x, t)) d\hat{x}, \quad (7.17)$$

supplemented with initial data

$$u^H(x, 0) = \bar{F}h(x), \quad \partial_t u^H(x, 0) = 0. \quad (7.18)$$

Here the macroscopic displacement  $u^H$  is the weak limit of the sequence of displacements  $u^\varepsilon$ . This is described by the following theorem.

**Theorem 7.5.** *Let  $u^\varepsilon$  be the solution of (6.10)-(6.12), where  $b$ ,  $u^0$ , and  $v^0$  are given by (7.16). Then as  $\varepsilon \rightarrow 0$*

$$u^\varepsilon(x, t) \rightarrow u^H(x, t) \quad \text{weakly in } L^s(\Omega \times (0, T))^3,$$

where  $u^H \in C^2([0, T]; L^s(\Omega)^3)$  is the unique solution of (7.17)-(7.18).

Moreover, assume that  $h \in C(\bar{\Omega})^3$ . Then  $u^H$  is in  $C^2([0, T]; C(\bar{\Omega})^3)$ .

### 7.3.2 The Cell-Problem

The micro-level peridynamics is given by the following equations. For  $j = 1, 2, 3$ ,

$$\begin{aligned} \partial_t^2 r^j(y, t) &= \int_{H_\delta(y)} \alpha(y, \hat{y}) \frac{(\hat{y} - y) \otimes (\hat{y} - y)}{|\hat{y} - y|^3} (r^j(\hat{y}, t) - r^j(y, t)) d\hat{y} \\ &\quad - K r^j(y, t), \end{aligned} \quad (7.19)$$

supplemented with initial conditions

$$r^j(y, 0) = F^j(y) - \bar{F}^j, \quad \partial_t r^j(y, 0) = 0. \quad (7.20)$$

In (7.20),  $F^j(y)$  and  $\bar{F}^j$  denote the  $j^{\text{th}}$  columns of the matrices  $F(y)$  and  $\bar{F}$ , respectively. The matrix  $K$  is given by (7.1).

### 7.3.3 Downscaling

The macroscopic displacement  $u^H$  together with the rescaled solution of the cell problem provide an approximation to the actual solution  $u^\varepsilon$ . This is expressed in the following theorem.

**Theorem 7.6.** *Let  $u^\varepsilon$  be the solution of (6.10)-(6.12), where  $b$ ,  $u^0$ , and  $v^0$  are given by (7.16). Assume that  $h \in C(\bar{\Omega})^3$ . Then for almost every  $t \in (0, T)$ ,*

$$\lim_{\varepsilon \rightarrow 0} \left\| u^\varepsilon(x, t) - \left( u^H(x, t) + \sum_{j=1}^3 r^j \left( \frac{x}{\varepsilon}, t \right) h_j(x) \right) \right\|_{L^s(\Omega)^3} = 0, \quad (7.21)$$

where  $r^j \in C^2([0, T]; L^s_{per}(Y)^3)$  is the unique solution of (7.19)-(7.20).

Moreover, assume that  $\lambda = 0$  in equation (6.10). Then, for  $t \in (0, T)$  and  $h \in C^{0,\beta}(\bar{\Omega})^3$ , the error in (7.21) is estimated by

$$\left\| u^\varepsilon(x, t) - \left( u^H(x, t) + \sum_{j=1}^3 r^j \left( \frac{x}{\varepsilon}, t \right) h_j(x) \right) \right\|_{L^s(\Omega)^3} \leq M_3(t) \varepsilon^\beta, \quad (7.22)$$

where  $M_3(t)$  is independent of  $\varepsilon$ . The function  $M_3(t)$  is given explicitly in Section 10.2.3.

## 7.4 Fourth Case

In this section, the loading force and initial data are given by

$$b \left( x, \frac{x}{\varepsilon}, t \right) = 0, \quad (7.23a)$$

$$u^0 \left( x, \frac{x}{\varepsilon} \right) = 0, \quad (7.23b)$$

$$v^0 \left( x, \frac{x}{\varepsilon} \right) = F \left( \frac{x}{\varepsilon} \right) h(x), \quad (7.23c)$$

where  $F \in L^s_{per}(Y)^{3 \times 3}$  and  $h \in L^s(\Omega)^3$ .

### 7.4.1 The Macroscopic Equation

The macroscopic peridynamic equation is given by

$$\partial_t^2 u^H(x, t) = \int_{H_\gamma(x)} \lambda(\hat{x} - x) \frac{(\hat{x} - x) \otimes (\hat{x} - x)}{|\hat{x} - x|^3} (u^H(\hat{x}, t) - u^H(x, t)) d\hat{x}, \quad (7.24)$$

supplemented with initial data

$$u^H(x, 0) = 0, \quad \partial_t u^H(x, 0) = \bar{F} h(x). \quad (7.25)$$

Here the macroscopic displacement  $u^H$  is the weak limit of the sequence of displacements  $u^\varepsilon$ . This is described by the following theorem.

**Theorem 7.7.** *Let  $u^\varepsilon$  be the solution of (6.10)-(6.12), where  $b$ ,  $u^0$ , and  $v^0$  are given by (7.23). Then as  $\varepsilon \rightarrow 0$*

$$u^\varepsilon(x, t) \rightarrow u^H(x, t) \quad \text{weakly in } L^s(\Omega \times (0, T))^3,$$

where  $u^H \in C^2([0, T]; L^s(\Omega)^3)$  is the unique solution of (7.24)-(7.25).

Moreover, assume that  $h \in C(\bar{\Omega})^3$ . Then  $u^H$  is in  $C^2([0, T]; C(\bar{\Omega})^3)$ .

### 7.4.2 The Cell-Problem

The micro-level peridynamics is given by the following equations. For  $j = 1, 2, 3$ ,

$$\begin{aligned} \partial_t^2 r^j(y, t) &= \int_{H_\delta(y)} \alpha(y, \hat{y}) \frac{(\hat{y} - y) \otimes (\hat{y} - y)}{|\hat{y} - y|^3} (r^j(\hat{y}, t) - r^j(y, t)) d\hat{y} \\ &\quad - K r^j(y, t), \end{aligned} \tag{7.26}$$

supplemented with initial conditions

$$r^j(y, 0) = 0, \quad \partial_t r^j(y, 0) = F^j(y) - \bar{F}^j. \tag{7.27}$$

In (7.27),  $F^j(y)$  and  $\bar{F}^j$  denote the  $j^{\text{th}}$  columns of the matrices  $F(y)$  and  $\bar{F}$ , respectively. The matrix  $K$  is given by (7.1).

### 7.4.3 Downscaling

The macroscopic displacement  $u^H$  together with the rescaled solution of the cell problem provide an approximation to the actual solution  $u^\varepsilon$ . This is expressed in the following theorem.

**Theorem 7.8.** *Let  $u^\varepsilon$  be the solution of (6.10)-(6.12), where  $b$ ,  $u^0$ , and  $v^0$  are given by (7.23). Assume that  $h \in C(\bar{\Omega})^3$ . Then for almost every  $t \in (0, T)$ ,*

$$\lim_{\varepsilon \rightarrow 0} \left\| u^\varepsilon(x, t) - \left( u^H(x, t) + \sum_{j=1}^3 r^j \left( \frac{x}{\varepsilon}, t \right) h_j(x) \right) \right\|_{L^s(\Omega)^3} = 0, \tag{7.28}$$

where  $r^j \in C^2([0, T]; L^s_{per}(Y)^3)$  is the unique solution of (7.26)-(7.27).

Moreover, assume that  $\lambda = 0$  in equation (6.10). Then, for  $t \in (0, T)$  and  $h \in C^{0,\beta}(\bar{\Omega})^3$ , the error in (7.28) is estimated by

$$\left\| u^\varepsilon(x, t) - \left( u^H(x, t) + \sum_{j=1}^3 r^j \left( \frac{x}{\varepsilon}, t \right) h_j(x) \right) \right\|_{L^s(\Omega)^3} \leq M_4(t) \varepsilon^\beta, \quad (7.29)$$

where  $M_4(t)$  is independent of  $\varepsilon$ . The function  $M_4(t)$  is given explicitly in Section 10.2.3.

# Chapter 8

## Existence and Uniqueness Results for the Peridynamic Equation

In this chapter, we make use of semigroup theory of operators to study the existence and uniqueness of (6.10)-(6.12). We begin by introducing the following operators.

For  $v \in L^s(\Omega)^3$ , with  $\frac{3}{2} < s < \infty$ , let

$$A_{L,1}v(x) = \int_{H_\gamma(x)} \lambda(\hat{x} - x) \frac{(\hat{x} - x) \otimes (\hat{x} - x)}{|\hat{x} - x|^3} v(\hat{x}) d\hat{x}, \quad (8.1)$$

$$A_{L,2}v(x) = \int_{H_\gamma(x)} \lambda(\hat{x} - x) \frac{(\hat{x} - x) \otimes (\hat{x} - x)}{|\hat{x} - x|^3} d\hat{x} v(x), \quad (8.2)$$

$$A_{S,1}^\varepsilon v(x) = \int_{H_{\varepsilon\delta}(x)} \frac{1}{\varepsilon^2} \alpha\left(\frac{x}{\varepsilon}, \frac{\hat{x}}{\varepsilon}\right) \frac{(\hat{x} - x) \otimes (\hat{x} - x)}{|\hat{x} - x|^3} v(\hat{x}) d\hat{x}, \quad (8.3)$$

$$A_{S,2}^\varepsilon v(x) = \int_{H_{\varepsilon\delta}(x)} \frac{1}{\varepsilon^2} \alpha\left(\frac{x}{\varepsilon}, \frac{\hat{x}}{\varepsilon}\right) \frac{(\hat{x} - x) \otimes (\hat{x} - x)}{|\hat{x} - x|^3} d\hat{x} v(x). \quad (8.4)$$

Also we set

$$A_L = A_{L,1} - A_{L,2}, \quad (8.5)$$

$$A_S^\varepsilon = A_{S,1}^\varepsilon - A_{S,2}^\varepsilon, \quad (8.6)$$

$$A^\varepsilon = A_L + A_S^\varepsilon. \quad (8.7)$$

Then by making the identifications  $u^\varepsilon(t) = u^\varepsilon(\cdot, t)$  and  $b^\varepsilon(t) = b(\cdot, \frac{\cdot}{\varepsilon}, t)$ , we can write (6.10)-(6.12) as an operator equation in  $L^s(\Omega)^3$

$$\begin{cases} \ddot{u}^\varepsilon(t) = A^\varepsilon u^\varepsilon(t) + b^\varepsilon(t), & t \in [0, T] \\ u^\varepsilon(0) = u_0^\varepsilon, \\ \dot{u}^\varepsilon(0) = v_0^\varepsilon. \end{cases} \quad (8.8)$$

or equivalently, as an inhomogeneous Abstract Cauchy Problem in

$L^s(\Omega)^3 \times L^s(\Omega)^3$

$$\begin{cases} \dot{U}^\varepsilon(t) = A^\varepsilon U^\varepsilon(t) + B^\varepsilon(t), & t \in [0, T] \\ U^\varepsilon(0) = U_0^\varepsilon. \end{cases} \quad (8.9)$$

where

$$U^\varepsilon(t) = \begin{pmatrix} u^\varepsilon(t) \\ \dot{u}^\varepsilon(t) \end{pmatrix}, \quad U_0^\varepsilon = \begin{pmatrix} u_0^\varepsilon \\ v_0^\varepsilon \end{pmatrix}, \quad B^\varepsilon(t) = \begin{pmatrix} 0 \\ b^\varepsilon(t) \end{pmatrix}, \quad \text{and } \mathbb{A}^\varepsilon = \begin{pmatrix} 0 & I \\ A^\varepsilon & 0 \end{pmatrix}.$$

Here  $I$  denotes the identity map in  $L^s(\Omega)^3$ .

**Proposition 8.1.** *Let  $\frac{3}{2} < s < \infty$  and assume that  $b^\varepsilon \in C([0, T]; L^s(\Omega)^3)$ . Then*

(a) *The operators  $A^\varepsilon$  and  $\mathbb{A}^\varepsilon$  are linear and bounded on  $L^s(\Omega)^3$  and  $L^s(\Omega)^3 \times L^s(\Omega)^3$ , respectively. Moreover, the bounds are uniform in  $\varepsilon$ .*

(b) *Equation (8.9) has a unique classical solution  $U^\varepsilon$  in  $C^1([0, T]; L^s(\Omega)^3 \times L^s(\Omega)^3)$  which is given by*

$$U^\varepsilon(t) = e^{t\mathbb{A}^\varepsilon} U_0^\varepsilon + \int_0^t e^{(t-\tau)\mathbb{A}^\varepsilon} B^\varepsilon(\tau) d\tau, \quad t \in [0, T], \quad (8.10)$$

where

$$e^{t\mathbb{A}^\varepsilon} = \sum_{n=0}^{\infty} \frac{t^n}{n!} (\mathbb{A}^\varepsilon)^n. \quad (8.11)$$

Moreover, equation (8.8) has a unique classical solution  $u^\varepsilon \in C^2([0, T]; L^s(\Omega)^3)$

which is given by

$$\begin{aligned} u^\varepsilon(t) &= \cosh\left(t\sqrt{A^\varepsilon}\right) u_0^\varepsilon + \sqrt{A^\varepsilon}^{-1} \sinh\left(t\sqrt{A^\varepsilon}\right) v_0^\varepsilon \\ &\quad + \sqrt{A^\varepsilon}^{-1} \int_0^t \sinh\left(t\sqrt{A^\varepsilon}\right) b^\varepsilon(\tau) d\tau \end{aligned} \quad (8.12a)$$

with the notation

$$\cosh\left(t\sqrt{A^\varepsilon}\right) := \sum_{n=0}^{\infty} \frac{t^{2n}}{(2n)!} (A^\varepsilon)^n \quad (8.12b)$$

$$\sqrt{A^\varepsilon}^{-1} \sinh\left(t\sqrt{A^\varepsilon}\right) := \sum_{n=0}^{\infty} \frac{t^{2n+1}}{(2n+1)!} (A^\varepsilon)^n \quad (8.12c)$$

(c) *The sequences  $(u^\varepsilon)_{\varepsilon>0}$ ,  $(\dot{u}^\varepsilon)_{\varepsilon>0}$ , and  $(\ddot{u}^\varepsilon)_{\varepsilon>0}$  are bounded in  $L^\infty([0, T]; L^s(\Omega)^3)$ .*

*Proof.* Part (a). It is clear that the operators  $A_{S,1}^\varepsilon$ ,  $A_{S,2}^\varepsilon$ ,  $A_{L,1}$ , and  $A_{L,2}$  are linear. So we begin the proof by showing that  $A_{S,1}^\varepsilon$  and  $A_{S,2}^\varepsilon$  are uniformly bounded on  $L^s(\Omega)^3$  for  $\frac{3}{2} < s < \infty$ . Let  $v \in L^s(\Omega)^3$ . Then by the change of variables  $\hat{x} = x + \varepsilon z$  in (8.3) we obtain

$$A_{S,1}^\varepsilon v(x) = \int_{H_\delta(0)} \alpha\left(\frac{x}{\varepsilon}, \frac{x}{\varepsilon} + z\right) \frac{z \otimes z}{|z|^3} v(x + \varepsilon z) dz. \quad (8.13)$$

Let  $\alpha_{\max} = \max_{y,y' \in Y} \alpha(y, y')$ . Then by taking the Euclidean norm in (8.13), we see that

$$\begin{aligned} |A_{S,1}^\varepsilon v(x)| &\leq \alpha_{\max} \int_{H_\delta(0)} \frac{1}{|z|} |v(x + \varepsilon z)| dz \\ &\leq \alpha_{\max} \left( \int_{H_\delta(0)} \frac{1}{|z|^{s'}} dz \right)^{1/s'} \left( \int_{H_\delta(0)} |v(x + \varepsilon z)|^s dz \right)^{1/s}, \end{aligned} \quad (8.14)$$

where Hölder's inequality was used in the second inequality, with  $1/s + 1/s' = 1$  and  $1 \leq s' < 3$ . By changing the variable of integration back to  $\hat{x}$  in the second integral, and then taking the limit as  $\varepsilon \rightarrow 0$ , we see that

$$\begin{aligned} \int_{H_\delta(0)} |v(x + \varepsilon z)|^s dz &= \frac{1}{\varepsilon^3} \int_{H_{\delta\varepsilon}(x)} |v(\hat{x})|^s d\hat{x} \\ &\rightarrow |H_\delta(x)| |v(x)|^s, \text{ a.e. } x, \end{aligned} \quad (8.15)$$

where we have used Lebesgue's Differentiation Theorem to evaluate this limit. On the other hand, we observe that the first integral in (8.14) is finite because  $s' < 3$ . Therefore, it follows from (8.14) and (8.15) that

$$|A_{S,1}^\varepsilon v(x)| \leq M_1 |v(x)|,$$

for some real number  $M_1 > 0$  which is independent of  $\varepsilon$ . It follows that

$$\|A_{S,1}^\varepsilon v\|_{L^s(\Omega)^3} \leq M_1 \|v\|_{L^s(\Omega)^3},$$

which shows that the operator  $A_{S,1}^\varepsilon$  is uniformly bounded. Similarly,  $A_{S,2}^\varepsilon$  can be written as

$$A_{S,2}^\varepsilon v(x) = \int_{H_\delta(0)} \alpha\left(\frac{x}{\varepsilon}, \frac{x}{\varepsilon} + z\right) \frac{z \otimes z}{|z|^3} dz v(x). \quad (8.16)$$

Thus

$$|A_{S,2}^\varepsilon v(x)| \leq \alpha_{\max} \int_{H_\delta(0)} \frac{1}{|z|} dz |v(x)|,$$

from which the boundedness of  $A_{S,2}^\varepsilon$  immediately follows. Combining these results shows that  $A_S^\varepsilon$ , which is given by  $A_{S,1}^\varepsilon - A_{S,2}^\varepsilon$ , is a uniformly bounded operator on  $L^s(\Omega)^3$ .

Next we show that the linear operator  $A_L = A_{L,1} - A_{L,2}$  is bounded on  $L^s(\Omega)^3$ .

Let  $\lambda_{\max} = \max_{\xi \in H_\gamma(0)} \lambda(\xi)$ . Then by taking the Euclidean norm in (8.1), we see that

$$\begin{aligned} |A_{L,1}v(x)| &\leq \lambda_{\max} \int_{H_\gamma(x)} \frac{1}{|\hat{x} - x|} |v(\hat{x})| d\hat{x} \\ &\leq \lambda_{\max} \left( \int_{H_\gamma(x)} \frac{1}{|\hat{x} - x|^{s'}} d\hat{x} \right)^{1/s'} \left( \int_{H_\gamma(x)} |v(\hat{x})|^s d\hat{x} \right)^{1/s}, \end{aligned} \quad (8.17)$$

where Hölder's inequality was used in the second inequality, with  $1/s + 1/s' = 1$  and  $1 \leq s' < 3$ . By the change of variables  $\xi = \hat{x} - x$ , it is easy to see that the first integral in (8.17) is independent of  $x$  and finite because  $s' < 3$ . Therefore from (8.17) we obtain

$$\|A_{L,1}v\|_{L^s(\Omega)^3} \leq \lambda_{\max} \left( \int_{H_\gamma(0)} \frac{1}{|z|^{s'}} dz \right)^{1/s'} \|v\|_{L^s(\Omega)^3}.$$

This shows that  $A_{L,1}$  is bounded on  $L^s(\Omega)^3$ . The boundedness of  $A_{L,2}$ , which is given by (8.2), is clear. Therefore  $A_L$  is bounded on  $L^s(\Omega)^3$ .

Since  $A^\varepsilon = A_L + A_S^\varepsilon$ , we conclude that

$$\|A^\varepsilon v\|_{L^s(\Omega)^3} \leq M \|v\|_{L^s(\Omega)^3}, \quad (8.18)$$

for some real number  $M > 0$  which is independent of  $\varepsilon$ .

The operator  $\mathbb{A}^\varepsilon$  is clearly linear, thus it remains to show that this operator is uniformly bounded on  $L^s(\Omega)^3 \times L^s(\Omega)^3$ . To see this, we let  $(v, w) \in L^s(\Omega)^3 \times L^s(\Omega)^3$ .

The norm in this Banach space is given by

$$\|(v, w)\|_{L^s(\Omega)^3 \times L^s(\Omega)^3} = \|v\|_{L^s(\Omega)^3} + \|w\|_{L^s(\Omega)^3}.$$

We note that

$$\mathbb{A}^\varepsilon \begin{pmatrix} v \\ w \end{pmatrix} = \begin{pmatrix} 0 & I \\ A^\varepsilon & 0 \end{pmatrix} \begin{pmatrix} v \\ w \end{pmatrix} = \begin{pmatrix} w \\ A^\varepsilon v \end{pmatrix}.$$

Thus by taking the norm, we obtain

$$\begin{aligned} \|\mathbb{A}^\varepsilon(v, w)\|_{L^s(\Omega)^3 \times L^s(\Omega)^3} &= \|w\|_{L^s(\Omega)^3} + \|A^\varepsilon v\|_{L^s(\Omega)^3} \\ &\leq \|w\|_{L^s(\Omega)^3} + \|A^\varepsilon\| \|v\|_{L^s(\Omega)^3}. \end{aligned} \quad (8.19)$$

From (8.19) and since we may assume that  $M > 1$  in (8.18), it follows that

$$\|\mathbb{A}^\varepsilon(v, w)\|_{L^s(\Omega)^3 \times L^s(\Omega)^3} \leq M \|(v, w)\|_{L^s(\Omega)^3 \times L^s(\Omega)^3}, \quad (8.20)$$

completing the argument.

Part (b). We have seen from Part (a) that  $\mathbb{A}^\varepsilon$  is a bounded linear operator on the Banach space  $L^s(\Omega)^3 \times L^s(\Omega)^3$ . Also, since  $b^\varepsilon$  is in  $C([0, T]; L^s(\Omega)^3)$  by assumption, it follows that  $B^\varepsilon = (0, b^\varepsilon)$  is in  $C([0, T]; L^s(\Omega)^3 \times L^s(\Omega)^3)$ . From these facts, it follows from the theory of semigroups that<sup>1</sup>

- (i) The operator  $\mathbb{A}^\varepsilon$  generates a uniformly continuous semigroup  $\{e^{t\mathbb{A}^\varepsilon}\}_{t \geq 0}$  on  $L^s(\Omega)^3 \times L^s(\Omega)^3$ , where  $e^{t\mathbb{A}^\varepsilon}$  is given by (8.11).
- (ii) The inhomogeneous Abstract Cauchy Problem (8.9) has a unique classical solution  $U^\varepsilon \in C^1([0, T]; L^s(\Omega)^3 \times L^s(\Omega)^3)$  which is given by (8.10).

It immediately follows from (ii) that the second order inhomogeneous Abstract Cauchy Problem (8.8) has a unique classical solution  $u^\varepsilon \in C^2([0, T]; L^s(\Omega)^3)$ . It remains to show that  $u^\varepsilon$  is given explicitly by (8.12). To see this, we begin by the following observations which can be easily shown using induction. For  $n = 0, 1, 2, \dots$ , we have

---

<sup>1</sup>see for example [57, 16].

$$\begin{pmatrix} 0 & I \\ A^\varepsilon & 0 \end{pmatrix}^{2n} = \begin{pmatrix} (A^\varepsilon)^n & 0 \\ 0 & (A^\varepsilon)^n \end{pmatrix} \quad (8.21)$$

$$\begin{pmatrix} 0 & I \\ A^\varepsilon & 0 \end{pmatrix}^{2n+1} = \begin{pmatrix} 0 & (A^\varepsilon)^n \\ (A^\varepsilon)^{n+1} & 0 \end{pmatrix} \quad (8.22)$$

From (8.11) and by using these two equations we see that

$$e^{tA^\varepsilon} = \sum_{n=0}^{\infty} \frac{t^n}{n!} \begin{pmatrix} 0 & I \\ A^\varepsilon & 0 \end{pmatrix}^n = \begin{pmatrix} \sum_{n=0}^{\infty} \frac{t^{2n}}{(2n)!} (A^\varepsilon)^n & \sum_{n=0}^{\infty} \frac{t^{2n+1}}{(2n+1)!} (A^\varepsilon)^n \\ \sum_{n=0}^{\infty} \frac{t^{2n+1}}{(2n+1)!} (A^\varepsilon)^{n+1} & \sum_{n=0}^{\infty} \frac{t^{2n}}{(2n)!} (A^\varepsilon)^n \end{pmatrix} \quad (8.23)$$

Equation (8.12) follows from equations (8.10) and (8.23), and the fact that

$$U^\varepsilon = \begin{pmatrix} u^\varepsilon \\ \dot{u}^\varepsilon \end{pmatrix}.$$

Part (c). We recall that

$$\begin{aligned} u_0^\varepsilon(x) &:= u^0(x, \frac{x}{\varepsilon}) \\ v_0^\varepsilon(x) &:= v^0(x, \frac{x}{\varepsilon}) \end{aligned}$$

Also by assumption  $u^0(x, y), v^0(x, y)$  are in  $L^s(\Omega; L^s_{per}(Y)^3)$ . Therefore we see that

$$\begin{aligned} \|u_0^\varepsilon\|_{L^s(\Omega)^3} &\leq \|u^0\|_{L^s(\Omega; L^s_{per}(Y)^3)} := \left( \int_{\Omega} \int_Y |u^0(x, y)|^s dy dx \right)^{1/s}, \\ \|v_0^\varepsilon\|_{L^s(\Omega)^3} &\leq \|v^0\|_{L^s(\Omega; L^s_{per}(Y)^3)} := \left( \int_{\Omega} \int_Y |v^0(x, y)|^s dy dx \right)^{1/s}. \end{aligned}$$

Thus  $u_0^\varepsilon$  and  $v_0^\varepsilon$  are uniformly bounded in  $L^s(\Omega)^3$ , which implies that  $U_0^\varepsilon$  is uniformly bounded in  $L^s(\Omega)^3 \times L^s(\Omega)^3$ . Similarly we can show that for  $t \in [0, T]$ ,  $b^\varepsilon(t)$  is uniformly bounded in  $L^s(\Omega)^3$ . Since  $b^\varepsilon(t)$  is continuous in  $t$ , it follows that  $b^\varepsilon$  is uniformly bounded in  $C([0, T]; L^s(\Omega)^3)$ , which implies that  $B^\varepsilon$  is uniformly bounded in  $C([0, T]; L^s(\Omega)^3 \times L^s(\Omega)^3)$ .

Next we note that

$$\begin{aligned} \|e^{t\mathbb{A}^\varepsilon}\| &\leq e^{t\|\mathbb{A}^\varepsilon\|} \\ &\leq e^{tM}, \end{aligned} \tag{8.24}$$

where in the last inequality we have used the fact that  $\mathbb{A}^\varepsilon$  is uniformly bounded. Taking the norm in both sides of (8.10) and by using (8.24), we obtain

$$\|U^\varepsilon(t)\|_{L^s(\Omega)^3 \times L^s(\Omega)^3} \leq M_1 e^{tM} + \int_0^t e^{(t-\tau)M} M_2 d\tau, \tag{8.25}$$

for some positive numbers  $M_1$ ,  $M_2$ , and  $M$ . This implies that  $U^\varepsilon$  is uniformly bounded in  $L^\infty([0, T]; L^s(\Omega)^3 \times L^s(\Omega)^3)$ . Therefore the sequences  $(u^\varepsilon)_{\varepsilon>0}$  and  $(\dot{u}^\varepsilon)_{\varepsilon>0}$  are bounded in  $L^\infty([0, T]; L^s(\Omega)^3)$ . Finally, it follows from equation (8.8) that the sequence  $(\ddot{u}^\varepsilon)_{\varepsilon>0}$  is bounded in  $L^\infty([0, T]; L^s(\Omega)^3)$ , completing the proof.  $\square$

# Chapter 9

## Two-Scale Convergence and the Two-Scale Limit Equation

The aim of this chapter is to identify the two-scale limit of the peridynamic initial-value problem (6.10)-(6.12).

### 9.1 Two-Scale Convergence

We begin by defining two-scale convergence and recalling some results from two-scale convergence. In the subsequent discussion, we will often refer to the following function spaces

$$\mathcal{K} = \{\psi \in C_c^\infty(\mathbb{R}^3 \times Y), \psi(x, y) \text{ is } Y\text{-periodic in } y\},$$

$$\mathcal{J} = \{\psi \in C_c^\infty(\mathbb{R}^3 \times Y \times \mathbb{R}^+), \psi(x, y, t) \text{ is } Y\text{-periodic in } y\},$$

$$\mathcal{Q} = \{w \in C^2([0, T]; L^s(\Omega \times Y)^3), w(x, y, t) \text{ is } Y\text{-periodic in } y, \text{ and } 3/2 < s < \infty\}.$$

Let  $p$  and  $p'$  be two real numbers such that  $1 < p < \infty$  and  $1/p + 1/p' = 1$ .

**Definition 9.1** (Two-scale convergence [53, 1]). *A sequence  $(v^\varepsilon)$  of functions in  $L^p(\Omega)$ , is said to two-scale converge to a limit  $v \in L^p(\Omega \times Y)$  if, as  $\varepsilon \rightarrow 0$*

$$\int_{\Omega} v^\varepsilon(x) \psi\left(x, \frac{x}{\varepsilon}\right) dx \rightarrow \int_{\Omega \times Y} v(x, y) \psi(x, y) dx dy \quad (9.1)$$

*for all  $\psi \in L^{p'}(\Omega; C_{per}(Y))$ . We will often use  $v^\varepsilon \xrightarrow{2} v$  to denote that  $(v^\varepsilon)$  two-scale converges to  $v$ .*

If the sequence  $(v^\varepsilon)$  is bounded in  $L^p(\Omega)$  then  $L^{p'}(\Omega; C_{per}(Y))$  can be replaced by  $\mathcal{K}$  in Definition (9.1) (see [44]).

The following are well-known results on two-scale convergence, which can be found in [44].

**Proposition 9.2.** *If  $(v^\varepsilon)$  converges to  $v$  in  $L^p(\Omega)$  then  $(v^\varepsilon)$  two-scale converges to  $\tilde{v}(x, y) = v(x)$ .*

**Proposition 9.3.** *If  $\psi \in \mathcal{K}$  then  $\psi(x, \frac{x}{\varepsilon})$  two-scale converges to  $\psi(x, y)$ .*

**Proposition 9.4.** *Let  $(v^\varepsilon)$  be a sequence in  $L^p(\Omega)$  which two-scale converges to  $v \in L^p(\Omega \times Y)$ . Then*

$$\int_{\Omega} v^\varepsilon(x) \psi \left( x, \frac{x}{\varepsilon} \right) dx \rightarrow \int_{\Omega \times Y} v(x, y) \psi(x, y) dx dy,$$

*for every  $\psi$  of the form  $\psi(x, y) = \psi_1(x) \psi_2(y)$ , where  $\psi_1 \in L^{r p'}(\Omega)$  and  $\psi_2 \in L^{r' p'}(Y)$ , with  $1 \leq r \leq \infty$  and  $1/r + 1/r' = 1$ .*

**Proposition 9.5.** *Let  $(v^\varepsilon)$  be a sequence in  $L^p(\Omega)$  which two-scale converges to  $v \in L^p(\Omega \times Y)$ . Then as  $\varepsilon \rightarrow 0$*

$$v^\varepsilon \rightarrow \int_Y v(x, y) dy \quad \text{weakly in } L^p(\Omega).$$

Definition 9.1 is motivated by the following compactness result of Nguetseng, see [53].

**Theorem 9.6.** *Let  $(v^\varepsilon)$  be a bounded sequence in  $L^p(\Omega)$ . Then there exists a subsequence and a function  $v \in L^p(\Omega \times Y)$  such that the subsequence two-scale converges to  $v$ .*

For the time-dependent problems studied in this work, we slightly modify the above two-scale convergence definition and results to allow for homogenization with a parameter, see [9, 12]. Here the parameter is denoted by  $t$ .

**Definition 9.7.** *A sequence  $(v^\varepsilon)$  of functions in  $L^p(\Omega \times (0, T))$ , is said to two-scale converge to a limit  $v \in L^p(\Omega \times Y \times (0, T))$  if, as  $\varepsilon \rightarrow 0$*

$$\int_{\Omega \times (0, T)} v^\varepsilon(x, t) \psi \left( x, \frac{x}{\varepsilon}, t \right) dx dt \rightarrow \int_{\Omega \times Y \times (0, T)} v(x, y, t) \psi(x, y, t) dx dy dt \quad (9.2)$$

*for all  $\psi \in \mathcal{J}$ .*

**Theorem 9.8.** *Let  $(v^\varepsilon)$  be a bounded sequence in  $L^p(\Omega \times (0, T))$ . Then there exists a subsequence and a function  $v \in L^p(\Omega \times Y \times (0, T))$  such that the subsequence two-scale converges to  $v$ .*

The proof of this result is essentially the same as the proof of Theorem 9.6. A slight variation of Theorem 9.8 can be found in [12] and [9].

The following is a direct consequence of Definition 9.7 and the definition of weak convergence.

**Proposition 9.9.** *Let  $(v^\varepsilon)$  be a bounded sequence in  $L^p(\Omega \times (0, T))$  that two-scale converges to  $v \in L^p(\Omega \times Y \times (0, T))$ . Then as  $\varepsilon \rightarrow 0$*

$$v^\varepsilon \rightarrow \int_Y v(x, y, t) dy \quad \text{weakly in } L^p(\Omega \times (0, T)).$$

Finally, we state the following well-known result on the weak limit of oscillatory periodic functions, which can be found in [10].

**Proposition 9.10.** *Let  $h \in L^q(\Omega)$  be a  $Y$ -periodic function, where  $1 \leq q \leq \infty$ . Set  $h^\varepsilon(x) = h(\frac{x}{\varepsilon})$  for  $x \in \Omega$ . Then as  $\varepsilon \rightarrow 0$ ,*

$$h^\varepsilon \rightarrow \bar{h} = \int_Y h(y) dy \quad \text{weakly in } L^q(\Omega), \quad (9.3)$$

if  $1 \leq q < \infty$ , and

$$h^\varepsilon \rightarrow \bar{h} \quad \text{weakly-* in } L^\infty(\Omega), \quad (9.4)$$

if  $q = \infty$ .

## 9.2 The Two-Scale Limit Equation

In this section, we use two-scale convergence to identify the limit of (6.10)-(6.12).

We observe that the loading force and initial data given by equations (7.2), (7.9),

(7.16), or (7.23), satisfy the following

$$b\left(x, \frac{x}{\varepsilon}, t\right) \xrightarrow{2} b(x, y, t), \quad (9.5a)$$

$$u^0\left(x, \frac{x}{\varepsilon}\right) \xrightarrow{2} u^0(x, y), \quad (9.5b)$$

$$v^0\left(x, \frac{x}{\varepsilon}\right) \xrightarrow{2} v^0(x, y). \quad (9.5c)$$

We note that from Proposition 8.1(c) and Theorem 9.8 it follows that, up to some subsequences,  $u^\varepsilon \xrightarrow{2} u$ ,  $\dot{u}^\varepsilon \xrightarrow{2} u^*$ , and  $\ddot{u}^\varepsilon \xrightarrow{2} u^{**}$ , where  $u$ ,  $u^*$ , and  $u^{**}$  are in  $L^s([0, T]; L^s(\Omega \times Y)^3)$ . We shall see later that  $u(x, y, t)$  is uniquely determined by an initial value problem. Therefore  $u$  is independent of the subsequence, and the whole sequence  $(u^\varepsilon)$  two-scale converges to  $u$ .

In order to identify the two-scale limit of (6.10), we multiply both sides by a test function  $\psi(x, \frac{x}{\varepsilon}, t)$ , where  $\psi(x, y, t)$  is  $Y$ -periodic in  $y$  and is such that  $\psi \in C_c^\infty(\mathbb{R}^3 \times Y \times \mathbb{R}^3)$ , and integrate on  $\Omega \times \mathbb{R}^+$

$$\begin{aligned} & \int_{\Omega \times \mathbb{R}^+} \partial_t^2 u^\varepsilon(x, t) \cdot \psi\left(x, \frac{x}{\varepsilon}, t\right) dx dt \\ &= \int_{\Omega \times \mathbb{R}^+} \left( (A_L + A_S^\varepsilon) u^\varepsilon(x, t) + b\left(x, \frac{x}{\varepsilon}, t\right) \right) \cdot \psi\left(x, \frac{x}{\varepsilon}, t\right) dx dt \end{aligned}$$

After integrating by parts twice, we obtain

$$\begin{aligned} & \int_{\Omega \times \mathbb{R}^+} u^\varepsilon(x, t) \cdot \partial_t^2 \psi\left(x, \frac{x}{\varepsilon}, t\right) dx dt - \int_{\Omega} \partial_t u^\varepsilon(x, 0) \cdot \psi\left(x, \frac{x}{\varepsilon}, 0\right) dx \\ &+ \int_{\Omega} u^\varepsilon(x, 0) \cdot \partial_t \psi\left(x, \frac{x}{\varepsilon}, 0\right) dx \\ &= \int_{\Omega \times \mathbb{R}^+} \left( (A_L + A_S^\varepsilon) u^\varepsilon(x, t) + b\left(x, \frac{x}{\varepsilon}, t\right) \right) \cdot \psi\left(x, \frac{x}{\varepsilon}, t\right) dx dt \end{aligned}$$

By letting  $\varepsilon \rightarrow 0$  we obtain

$$\begin{aligned}
& \int_{\Omega \times Y \times \mathbb{R}^+} u(x, y, t) \cdot \partial_t^2 \psi(x, y, t) \, dx dy dt - \int_{\Omega \times Y} v^0(x, y) \cdot \psi(x, y, 0) \, dx dy \\
& + \int_{\Omega \times Y} u^0(x, y) \cdot \partial_t \psi(x, y, 0) \, dx dy \\
& = \lim_{\varepsilon \rightarrow 0} \int_{\Omega \times \mathbb{R}^+} (A_L + A_S^\varepsilon) u^\varepsilon(x, t) \cdot \psi\left(x, \frac{x}{\varepsilon}, t\right) \, dx dt \\
& + \int_{\Omega \times Y \times \mathbb{R}^+} b(x, y, t) \cdot \psi(x, y, t) \, dx dy dt \tag{9.6}
\end{aligned}$$

For  $i = 1, 2, 3$ , we extend  $u_i(x, y, t)$  by periodicity from  $\Omega \times Y \times (0, T)$  to  $\Omega \times \mathbb{R}^3 \times (0, T)$ . We will use the following lemma to compute the limit on the right hand side of (9.6).

**Lemma 9.11.** *Let  $w$  be in  $L^s(\Omega; L_{per}^s(Y)^3)$  and define*

$$\begin{aligned}
B_L w(x, y) &= \int_{H_\gamma(x)} \lambda(\hat{x} - x) \frac{(\hat{x} - x) \otimes (\hat{x} - x)}{|\hat{x} - x|^3} \left( \int_Y w(\hat{x}, y') \, dy' - w(x, y) \right) \, d\hat{x}, \\
B_S w(x, y) &= \int_{H_\delta(y)} \alpha(y, \hat{y}) \frac{(\hat{y} - y) \otimes (\hat{y} - y)}{|\hat{y} - y|^3} (w(x, \hat{y}) - w(x, y)) \, d\hat{y}.
\end{aligned}$$

Then as  $\varepsilon \rightarrow 0$ ,

$$(a) \quad A_L u^\varepsilon(x, t) \xrightarrow{2} B_L u(x, y, t).$$

Moreover, the operator  $B_L$  is linear and bounded on  $L^s(\Omega; L_{per}^s(Y)^3)$ .

$$(b) \quad A_S^\varepsilon u^\varepsilon(x, t) \xrightarrow{2} B_S u(x, y, t).$$

Moreover, the operator  $B_S$  is linear and bounded on  $L^s(\Omega; L_{per}^s(Y)^3)$ .

The proof of this lemma is provided at the end of this section.

Using Lemma (9.11) and Lebesgue's dominated convergence theorem, it follows that

$$\begin{aligned}
& \lim_{\varepsilon \rightarrow 0} \int_{\Omega \times \mathbb{R}^+} (A_L + A_S^\varepsilon) u^\varepsilon(x, t) \cdot \psi\left(x, \frac{x}{\varepsilon}, t\right) \, dx dt \\
& = \int_{\Omega \times Y \times \mathbb{R}^+} (B_L + B_S) u(x, y, t) \cdot \psi(x, y, t) \, dx dy dt.
\end{aligned}$$

Thus (9.6) becomes

$$\begin{aligned}
& \int_{\Omega \times Y \times \mathbb{R}^+} u(x, y, t) \cdot \partial_t^2 \psi(x, y, t) \, dx dy dt - \int_{\Omega \times Y} v^0(x, y) \cdot \psi(x, y, 0) \, dx dy \\
& + \int_{\Omega \times Y} u^0(x, y) \cdot \partial_t \psi(x, y, 0) \, dx dy \\
& = \int_{\Omega \times Y \times \mathbb{R}^+} ((B_L + B_S)u(x, y, t) + b(x, y, t)) \cdot \psi(x, y, t) \, dx dy dt \quad (9.7)
\end{aligned}$$

We shall see from Lemma 9.13, provided before the end of this section, that  $u$  has two classical partial derivatives with respect to  $t$ , for almost every  $t$ , and the initial conditions supplementing (9.7) are given by

$$u(x, y, 0) = u^0(x, y), \quad \partial_t u(x, y, 0) = v^0(x, y). \quad (9.8)$$

Thus by integrating by parts twice, equation (9.7) becomes

$$\begin{aligned}
& \int_{\Omega \times Y \times \mathbb{R}^+} \partial_t^2 u(x, y, t) \cdot \psi(x, y, t) \, dx dy dt \\
& = \int_{\Omega \times Y \times \mathbb{R}^+} ((B_L + B_S)u(x, y, t) + b(x, y, t)) \cdot \psi(x, y, t) \, dx dy dt \quad (9.9)
\end{aligned}$$

Since this is true for any function  $\psi \in C_c^\infty(\mathbb{R}^3 \times Y \times \mathbb{R})^3$  for which  $\psi(x, y, t)$  is  $Y$ -periodic in  $y$ , we obtain that for almost every  $x, y$ , and  $t$

$$\partial_t^2 u(x, y, t) = Bu(x, y, t) + b(x, y, t), \quad (9.10)$$

where  $B = B_L + B_S$ . It follows from Lemma 9.11 that  $B$  is a bounded linear operator on  $L^s(\Omega; L_{per}^s(Y)^3)$ . Therefore, the initial value problem given by (9.10) and (9.8), interpreted as a second-order inhomogeneous abstract Cauchy problem defined on  $L^s(\Omega; L_{per}^s(Y)^3)$ , has a unique solution  $u \in \mathcal{Q}$ .

The following summarizes the results of this chapter.

**Theorem 9.12.** Let  $(u^\varepsilon)$  be the sequence of solutions of (6.10)-(6.12). Then

$u^\varepsilon \xrightarrow{2} u$  where  $u \in \mathcal{Q}$  is the unique solution of

$$\begin{aligned} \partial_t^2 u(x, y, t) &= \int_{H_\gamma(x)} \lambda(\hat{x} - x) \frac{(\hat{x} - x) \otimes (\hat{x} - x)}{|\hat{x} - x|^3} \left( \int_Y u(\hat{x}, y', t) dy' - u(x, y, t) \right) d\hat{x} \\ &+ \int_{H_\delta(y)} \alpha(y, \hat{y}) \frac{(\hat{y} - y) \otimes (\hat{y} - y)}{|\hat{y} - y|^3} (u(x, \hat{y}, t) - u(x, y, t)) d\hat{y} \\ &+ b(x, y, t), \end{aligned} \tag{9.11}$$

supplemented with initial conditions

$$u(x, y, 0) = u^0(x, y), \tag{9.12}$$

$$\partial_t u(x, y, 0) = v^0(x, y). \tag{9.13}$$

**Lemma 9.13.** Let  $t \in [0, T]$  and define

$$g(x, y, t) = \int_0^t \int_0^\tau u^{**}(x, y, l) dl d\tau + tu^*(x, y, 0) + u(x, y, 0). \tag{9.14}$$

Then  $g$  is in  $L^s(\Omega \times Y \times (0, T))^3$ , twice differentiable with respect to  $t$  almost everywhere, and satisfies

(a) For almost every  $x, y$ , and  $t$ ,  $g(x, y, t) = u(x, y, t)$ ,  $\partial_t g(x, y, t) = u^*(x, y, t)$ ,  
and  $\partial_t^2 g(x, y, t) = u^{**}(x, y, t)$ .

(b) For almost every  $x$  and  $y$

$$\begin{aligned} g(x, y, 0) &= u(x, y, 0) = u^0(x, y), \\ \partial_t g(x, y, 0) &= u^*(x, y, 0) = v^0(x, y). \end{aligned}$$

*Proof.* Part (a). Let  $\psi_1(x, y)$  be in  $C_c^\infty(\Omega \times Y)^3$  and  $Y$ -periodic in  $y$ , and let  $\phi$  be in  $C_c^\infty(\mathbb{R}^+)$ . Then by using integration by parts, we see that

$$\int_{\Omega \times \mathbb{R}^+} \partial_t u^\varepsilon(x, t) \cdot \psi_1 \left( x, \frac{x}{\varepsilon} \right) \phi(t) dx dt = - \int_{\Omega \times \mathbb{R}^+} u^\varepsilon(x, t) \cdot \psi_1 \left( x, \frac{x}{\varepsilon} \right) \dot{\phi}(t) dx dt.$$

Sending  $\varepsilon$  to 0 and using the fact that, up to a subsequence,  $\partial_t u^\varepsilon \xrightarrow{2} u^*$ , we obtain

$$\begin{aligned} & \int_{\Omega \times Y \times \mathbb{R}^+} u^*(x, y, t) \cdot \psi_1(x, y) \phi(t) dx dy dt \\ &= - \int_{\Omega \times Y \times \mathbb{R}^+} u(x, y, t) \cdot \psi_1(x, y) \dot{\phi}(t) dx dy dt. \end{aligned}$$

Since this holds for every  $\psi_1$  we conclude that

$$\int_{\mathbb{R}^+} u^*(x, y, t) \phi(t) dt = - \int_{\mathbb{R}^+} u(x, y, t) \dot{\phi}(t) dt, \quad (9.15)$$

for almost every  $x$  and  $y$  and for every  $\phi \in C_c^\infty(\mathbb{R}^+)$ . Similarly, by using the fact that, up to a subsequence,  $\partial_t^2 u^\varepsilon \xrightarrow{2} u^{**}$ , we see that

$$\int_{\mathbb{R}^+} u^{**}(x, y, t) \phi(t) dt = \int_{\mathbb{R}^+} u(x, y, t) \ddot{\phi}(t) dt, \quad (9.16)$$

for almost every  $x$  and  $y$  and for every  $\phi \in C_c^\infty(\mathbb{R}^+)$ . We note that from (9.14) it is easy to see that  $g$  is twice differentiable in  $t$  almost everywhere and satisfies

$$\partial_t g(x, y, t) = \int_0^t u^{**}(x, y, \tau) d\tau + u^*(x, y, 0), \quad (9.17)$$

$$\partial_t^2 g(x, y, t) = u^{**}(x, y, t). \quad (9.18)$$

We will use these facts together with (9.15) and (9.16) to show that  $\partial_t g = u^*$  almost everywhere and  $g = u$  almost everywhere.

For  $\phi \in C_c^\infty(\mathbb{R}^+)$ , we have

$$\begin{aligned} \int_{\mathbb{R}^+} \partial_t g(x, y, t) \dot{\phi}(t) dt &= - \int_{\mathbb{R}^+} \partial_t^2 g(x, y, t) \phi(t) dt \\ &= - \int_{\mathbb{R}^+} u^{**}(x, y, t) \phi(t) dt \\ &= - \int_{\mathbb{R}^+} u(x, y, t) \ddot{\phi}(t) dt \\ &= \int_{\mathbb{R}^+} u^*(x, y, t) \dot{\phi}(t) dt \end{aligned}$$

where (9.18) and (9.16) were used in the second and third steps, respectively. Thus we obtain

$$\int_{\mathbb{R}^+} (\partial_t g(x, y, t) - u^*(x, y, t)) \dot{\phi}(t) dt = 0, \quad (9.19)$$

for every  $\phi \in C_c^\infty(\mathbb{R}^+)$ . Since  $\partial_t g(x, y, 0) = u^*(x, y, 0)$ , we conclude from (9.19) that  $\partial_t g(x, y, t) = u^*(x, y, t)$  almost everywhere.

We also have

$$\begin{aligned} \int_{\mathbb{R}^+} g(x, y, t) \dot{\phi}(t) dt &= - \int_{\mathbb{R}^+} \partial_t g(x, y, t) \phi(t) dt \\ &= - \int_{\mathbb{R}^+} u^*(x, y, t) \phi(t) dt \\ &= \int_{\mathbb{R}^+} u(x, y, t) \dot{\phi}(t) dt \end{aligned}$$

where the fact that  $\partial_t g(x, y, t) = u^*(x, y, t)$  almost everywhere was used in the second step and (9.15) was used in the third step. Thus we see that

$$\int_{\mathbb{R}^+} (g(x, y, t) - u(x, y, t)) \dot{\phi}(t) dt = 0, \quad (9.20)$$

for every  $\phi \in C_c^\infty(\mathbb{R}^+)$ . Since  $g(x, y, 0) = u(x, y, 0)$ , we conclude from (9.20) that  $g(x, y, t) = u(x, y, t)$  almost everywhere, completing the proof of Part (a).

Part (b). Let  $\psi(x, y, t)$  be in  $C_c^\infty(\Omega \times Y \times \mathbb{R})^3$  and  $Y$ -periodic in  $y$ . Then by using integration by parts, we see that

$$\begin{aligned} \int_{\Omega \times \mathbb{R}^+} \partial_t u^\varepsilon(x, t) \cdot \psi\left(x, \frac{x}{\varepsilon}, t\right) dx dt &= - \int_{\Omega \times \mathbb{R}^+} u^\varepsilon(x, t) \cdot \partial_t \psi\left(x, \frac{x}{\varepsilon}, t\right) dx dt \\ &\quad - \int_{\Omega} u^\varepsilon(x, 0) \cdot \psi\left(x, \frac{x}{\varepsilon}, 0\right) dx. \end{aligned}$$

Sending  $\varepsilon$  to 0, we obtain

$$\begin{aligned} \int_{\Omega \times Y \times \mathbb{R}^+} u^*(x, y, t) \cdot \psi(x, y, t) dx dy dt &= - \int_{\Omega \times Y \times \mathbb{R}^+} u(x, y, t) \cdot \partial_t \psi(x, y, t) dx dy dt \\ &\quad - \int_{\Omega \times Y} u^0(x, y) \cdot \psi(x, y, 0) dx dy. \end{aligned} \quad (9.21)$$

On the other hand, using Part (a), we see that

$$\begin{aligned}
\int_{\Omega \times Y \times \mathbb{R}^+} u^*(x, y, t) \cdot \psi(x, y, t) \, dx dy dt &= \int_{\Omega \times Y \times \mathbb{R}^+} \partial_t g(x, y, t) \cdot \psi(x, y, t) \, dx dy dt \\
&= - \int_{\Omega \times Y \times \mathbb{R}^+} g(x, y, t) \cdot \partial_t \psi(x, y, t) \, dx dy dt \\
&\quad - \int_{\Omega \times Y} g(x, y, 0) \cdot \psi(x, y, 0) \, dx dy \\
&= - \int_{\Omega \times Y \times \mathbb{R}^+} u(x, y, t) \cdot \partial_t \psi(x, y, t) \, dx dy dt \\
&\quad - \int_{\Omega \times Y} u(x, y, 0) \cdot \psi(x, y, 0) \, dx dy.
\end{aligned} \tag{9.22}$$

From (9.21) and (9.22) we obtain that

$$\int_{\Omega \times Y} (u^0(x, y) - u(x, y, 0)) \cdot \psi(x, y, 0) \, dx dy = 0,$$

for every  $\psi$ . Therefore

$$u(x, y, 0) = u^0(x, y),$$

almost everywhere. Similarly we can show that

$$\partial_t u(x, y, 0) = v^0(x, y),$$

almost everywhere, completing the proof of Part (b).  $\square$

*Proof of Lemma 9.11.* Part (a). Since  $A_L = A_{L,1} - A_{L,2}$ , we will compute the two-scale limits of  $A_{L,1}u^\varepsilon$  and  $A_{L,2}u^\varepsilon$ , then combine them to show that as  $\varepsilon \rightarrow 0$ ,

$$A_L u^\varepsilon(x, t) \xrightarrow{2} B_L u(x, y, t). \tag{9.23}$$

Let  $\psi \in C_c^\infty(\mathbb{R}^3 \times Y)^3$  such that  $\psi(x, y)$  is  $Y$ -periodic in  $y$ , and  $\phi \in C_c^\infty(\mathbb{R}^+)$ . Then from the definition of  $A_{L,1}$ , equation (8.1), we see that

$$\begin{aligned}
&\int_{\Omega \times \mathbb{R}^+} A_{L,1} u^\varepsilon(x, t) \cdot \psi\left(x, \frac{x}{\varepsilon}\right) \phi(t) \, dx dt \\
&= \int_{\Omega \times \mathbb{R}^+} \int_{H_\gamma(x)} \lambda(\hat{x} - x) \frac{(\hat{x} - x) \otimes (\hat{x} - x)}{|\hat{x} - x|^3} u^\varepsilon(\hat{x}, t) \, d\hat{x} \cdot \psi\left(x, \frac{x}{\varepsilon}\right) \phi(t) \, dx dt,
\end{aligned} \tag{9.24}$$

Since  $u^\varepsilon(x, t) \xrightarrow{2} u(x, y, t)$ , we obtain using Proposition 9.9 that, as  $\varepsilon \rightarrow 0$ ,

$$u^\varepsilon \rightarrow \int_Y u(x, y, t) dy \text{ weakly in } L^s(\Omega \times (0, T))^3. \quad (9.25)$$

It follows from (9.25) that, for fixed  $x$ ,

$$\begin{aligned} & \lim_{\varepsilon \rightarrow 0} \int_{\mathbb{R}^+} \int_{H_\gamma(x)} \lambda(\hat{x} - x) \frac{(\hat{x} - x) \otimes (\hat{x} - x)}{|\hat{x} - x|^3} u^\varepsilon(\hat{x}, t) \phi(t) d\hat{x} dt \\ &= \int_{\mathbb{R}^+} \int_{H_\gamma(x)} \lambda(\hat{x} - x) \frac{(\hat{x} - x) \otimes (\hat{x} - x)}{|\hat{x} - x|^3} \left( \int_Y u(\hat{x}, y', t) dy' \right) \phi(t) d\hat{x} dt. \end{aligned} \quad (9.26)$$

We note that by replacing  $v(x)$  with  $u^\varepsilon(x, t)$  in (8.17), we obtain

$$\begin{aligned} & \left| \int_{H_\gamma(x)} \lambda(\hat{x} - x) \frac{(\hat{x} - x) \otimes (\hat{x} - x)}{|\hat{x} - x|^3} u^\varepsilon(\hat{x}, t) d\hat{x} \right| \\ & \leq \lambda_{\max} \left( \int_{H_\delta(x)} \frac{1}{|\hat{x} - x|^{s'}} d\hat{x} \right)^{1/s'} \left( \int_{H_\delta(x)} |u^\varepsilon(\hat{x}, t)|^s d\hat{x} \right)^{1/s} \\ & \leq \lambda_{\max} \left( \int_{H_\delta(x)} \frac{1}{|\hat{x} - x|^{s'}} d\hat{x} \right)^{1/s'} \|u^\varepsilon\|_{L^\infty([0, T]; L^s(\Omega)^3)}. \end{aligned} \quad (9.27)$$

From Proposition 8.1,  $\|u^\varepsilon\|_{L^\infty([0, T]; L^s(\Omega)^3)}$  is bounded. Thus from (9.26), and (9.27) and by using Lebesgue's dominated convergence theorem, we conclude that the convergence of the sequence of functions in (9.26) is not only point-wise in  $x$  convergence but also strong in  $L^s(\Omega)^3$ . Therefore we can use Proposition 9.2 and (9.26) to evaluate the limit of (9.24) as  $\varepsilon \rightarrow 0$ . We find that

$$\begin{aligned} & \lim_{\varepsilon \rightarrow 0} \int_{\Omega \times \mathbb{R}^+} A_{L,1} u^\varepsilon(x, t) \cdot \psi\left(x, \frac{x}{\varepsilon}\right) \phi(t) dx dt \\ &= \int_{\Omega \times \mathbb{R}^+} \int_{H_\gamma(x)} \lambda(\hat{x} - x) \frac{(\hat{x} - x) \otimes (\hat{x} - x)}{|\hat{x} - x|^3} \left( \int_Y u(\hat{x}, y', t) dy' \right) d\hat{x} \cdot \psi\left(x, \frac{x}{\varepsilon}\right) \phi(t) dx dt, \end{aligned} \quad (9.28)$$

Next we evaluate the two-scale limit of  $A_{L,2} u^\varepsilon$ . We recall from (8.2) that

$$A_{L,2} u^\varepsilon(x, t) = \int_{H_\gamma(x)} \lambda(\hat{x} - x) \frac{(\hat{x} - x) \otimes (\hat{x} - x)}{|\hat{x} - x|^3} d\hat{x} u^\varepsilon(x, t), \quad (9.29)$$

from which immediately follows that as  $\varepsilon \rightarrow 0$ ,

$$A_{L,2}u^\varepsilon \stackrel{2}{\rightharpoonup} \int_{H_\gamma(x)} \lambda(\hat{x} - x) \frac{(\hat{x} - x) \otimes (\hat{x} - x)}{|\hat{x} - x|^3} d\hat{x} u(x, y, t). \quad (9.30)$$

Combining equations (9.28) and (9.30), the result (9.23) follows.

The fact that the two operators  $B_L$  and  $B_S$  are linear and bounded on the Banach space  $L^s(\Omega; L^s_{per}(Y))$  can be shown by arguments similar to those used in the proof of Proposition 8.1.

Part (b). Since  $A_S^\varepsilon = A_{S,1}^\varepsilon - A_{S,2}^\varepsilon$ , we will compute the two-scale limits of  $A_{S,1}^\varepsilon u^\varepsilon$  and  $A_{S,2}^\varepsilon u^\varepsilon$ , then combine them to show that as  $\varepsilon \rightarrow 0$ ,

$$A_S^\varepsilon u^\varepsilon(x, t) \stackrel{2}{\rightharpoonup} B_S u(x, y, t). \quad (9.31)$$

Let  $\psi(x, y, t) = \psi_2(x)\psi_1(y)\phi(t)$ , where  $\psi_2 \in C_c^\infty(\mathbb{R}^3)$ ,  $\psi_1 \in C_{per}^\infty(Y)^3$ , and  $\phi \in C_c^\infty(\mathbb{R}^+)$ . Then by using (8.13), replacing  $v(x)$  with  $u^\varepsilon(x, t)$ , we see that

$$\begin{aligned} & \int_{\Omega \times \mathbb{R}^+} A_{S,1}^\varepsilon u^\varepsilon(x, t) \cdot \psi\left(x, \frac{x}{\varepsilon}, t\right) dx dt \\ &= \int_{\Omega \times \mathbb{R}^+} \int_{H_\delta(0)} \alpha\left(\frac{x}{\varepsilon}, \frac{x}{\varepsilon} + z\right) \frac{z \otimes z}{|z|^3} u^\varepsilon(x + \varepsilon z, t) dz \cdot \psi\left(x, \frac{x}{\varepsilon}, t\right) dx dt. \end{aligned} \quad (9.32)$$

We recall that  $\alpha\left(\frac{x}{\varepsilon}, \frac{x}{\varepsilon} + z\right)$  is defined by equation (6.5). Without loss of generality, we may assume that  $\alpha\left(\frac{x}{\varepsilon}, \frac{x}{\varepsilon} + z\right)$  is given by

$$\alpha\left(\frac{x}{\varepsilon}, \frac{x}{\varepsilon} + z\right) = \chi_f\left(\frac{x}{\varepsilon}\right) \chi_f\left(\frac{x}{\varepsilon} + z\right).$$

Thus after a change in the order of integration in the right hand side of equation (9.32), we see that

$$\begin{aligned} & \int_{\Omega \times \mathbb{R}^+} A_{S,1}^\varepsilon u^\varepsilon(x, t) \cdot \psi\left(x, \frac{x}{\varepsilon}, t\right) dx dt \\ &= \int_{H_\delta(0)} \frac{1}{|z|^3} \int_{\Omega \times \mathbb{R}^+} \chi_f\left(\frac{x}{\varepsilon}\right) \chi_f\left(\frac{x}{\varepsilon} + z\right) u^\varepsilon(x + \varepsilon z, t) \cdot z \psi_1\left(\frac{x}{\varepsilon}\right) \cdot z \psi_2(x)\phi(t) dx dt dz. \end{aligned} \quad (9.33)$$

Now we focus on evaluating the limit as  $\varepsilon \rightarrow 0$  of the inner integral in (9.33). By the change of variables  $r = x + \varepsilon z$  we obtain

$$\begin{aligned} & \int_{\Omega \times \mathbb{R}^+} \chi_f\left(\frac{x}{\varepsilon}\right) \chi_f\left(\frac{x}{\varepsilon} + z\right) u^\varepsilon(x + \varepsilon z, t) \cdot z \psi_1\left(\frac{x}{\varepsilon}\right) \cdot z \psi_2(x) \phi(t) dx dt \\ &= \int_{\mathbb{R}^3 \times \mathbb{R}^+} \chi_\Omega(r - \varepsilon z) \chi_f\left(\frac{r}{\varepsilon} - z\right) \chi_f\left(\frac{r}{\varepsilon}\right) u^\varepsilon(r, t) \cdot z \psi_1\left(\frac{r}{\varepsilon} - z\right) \cdot z \psi_2(r - \varepsilon z) \phi(t) dr dt \end{aligned} \quad (9.34)$$

$$:= a^\varepsilon(z),$$

where  $\chi_\Omega$  denotes the indicator function of  $\Omega$ . We will show that for  $z \in H_\delta(0)$ ,

$$\lim_{\varepsilon \rightarrow 0} a^\varepsilon(z) = \int_{\Omega \times Y \times \mathbb{R}^+} \chi_f(y - z) \chi_f(y) u(r, y, t) \cdot z \psi_1(y - z) \cdot z \psi_2(r) \phi(t) dr dy dt. \quad (9.35)$$

To see this, we approximate  $\chi_\Omega$  by smooth functions  $\zeta_n$  such that as  $n \rightarrow \infty$ ,  $\zeta_n(r) \rightarrow \chi_\Omega(r)$  almost everywhere and  $\zeta_n \rightarrow \chi_\Omega$  in  $L_{loc}^{s'}(\Omega)$ , with  $1/s + 1/s' = 1$ . Then by adding and subtracting  $\zeta_n(r - \varepsilon z)$  to and from  $\chi_\Omega(r - \varepsilon z)$  in (9.34), we obtain that

$$a^\varepsilon(z) = a_1^{n,\varepsilon}(z) + a_2^{n,\varepsilon}(z), \quad (9.36)$$

where,

$$\begin{aligned} a_1^{n,\varepsilon}(z) &:= \int_{\mathbb{R}^3 \times \mathbb{R}^+} (\chi_\Omega(r - \varepsilon z) - \zeta_n(r - \varepsilon z)) \times \\ &\quad \chi_f\left(\frac{r}{\varepsilon} - z\right) \chi_f\left(\frac{r}{\varepsilon}\right) u^\varepsilon(r, t) \cdot z \psi_1\left(\frac{r}{\varepsilon} - z\right) \cdot z \psi_2(r - \varepsilon z) \phi(t) dr dt, \end{aligned} \quad (9.37)$$

$$\begin{aligned} a_2^{n,\varepsilon}(z) &:= \int_{\mathbb{R}^3 \times \mathbb{R}^+} \zeta_n(r - \varepsilon z) \times \\ &\quad \chi_f\left(\frac{r}{\varepsilon} - z\right) \chi_f\left(\frac{r}{\varepsilon}\right) u^\varepsilon(r, t) \cdot z \psi_1\left(\frac{r}{\varepsilon} - z\right) \cdot z \psi_2(r - \varepsilon z) \phi(t) dr dt. \end{aligned} \quad (9.38)$$

From (9.37) and by using Hölder's inequality, we see that

$$\begin{aligned}
|a_1^{n,\varepsilon}(z)| &\leq \left( \int_{\mathbb{R}^3} |\chi_\Omega(r - \varepsilon z) - \zeta_n(r - \varepsilon z)|^{s'} dr \right)^{1/s'} \times \\
&\int_{\mathbb{R}^+} \left( \int_{\mathbb{R}^3} \chi_f\left(\frac{r}{\varepsilon} - z\right) \chi_f\left(\frac{r}{\varepsilon}\right) \left| u^\varepsilon(r, t) \cdot z \psi_1\left(\frac{r}{\varepsilon} - z\right) \cdot z \psi_2(r - \varepsilon z) \right|^s dr \right)^{1/s} \times \\
&\phi(t) dt. \tag{9.39}
\end{aligned}$$

We note that the second term on the right hand side of (9.39) is bounded above uniformly in  $\varepsilon$ . This follows from Hölder's inequality applied to the inner integral and the fact that  $(u^\varepsilon)_{\varepsilon>0}$  is bounded in  $L_{loc}^\infty(\mathbb{R}^+; L^s(\Omega)^3)$ . On the other hand, by the change of variables  $r' = r - \varepsilon z$ , the first term on the right hand side of (9.39) becomes

$$\left( \int_{\mathbb{R}^3} |\chi_\Omega(r') - \zeta_n(r')|^{s'} dr' \right)^{1/s'},$$

which goes to zero as  $n \rightarrow \infty$ . From these two facts and (9.39), we conclude that for all  $\varepsilon > 0$  and  $z \in H_\delta(0)$ ,

$$\lim_{n \rightarrow \infty} a_1^{n,\varepsilon}(z) = 0. \tag{9.40}$$

Now for fixed  $n$ , since  $\zeta_n$  and  $\psi_2$  are smooth functions, we see that as  $\varepsilon \rightarrow 0$ ,  $\zeta_n(r - \varepsilon z)\psi_2(r - \varepsilon z) \rightarrow \zeta_n(r)\psi_2(r)$  uniformly. Therefore, we see from (9.38) that

$$\begin{aligned}
&\lim_{\varepsilon \rightarrow 0} a_2^{n,\varepsilon}(z) \\
&= \lim_{\varepsilon \rightarrow 0} \int_{\mathbb{R}^3 \times \mathbb{R}^+} \zeta_n(r) \chi_f\left(\frac{r}{\varepsilon} - z\right) \chi_f\left(\frac{r}{\varepsilon}\right) u^\varepsilon(r, t) \cdot z \psi_1\left(\frac{r}{\varepsilon} - z\right) \cdot z \psi_2(r) \phi(t) dr dt \\
&= \int_{\mathbb{R}^3 \times Y \times \mathbb{R}^+} \zeta_n(r) \chi_f(y - z) \chi_f(y) u(r, y, t) \cdot z \psi_1(y - z) \cdot z \psi_2(r) \phi(t) dr dy dt, \tag{9.41}
\end{aligned}$$

where in the last step the fact that  $(u^\varepsilon)_{\varepsilon>0}$  two-scale converges to  $u(r, y, t)$  was used. By taking the limit as  $n \rightarrow \infty$  in (9.41), we obtain

$$\begin{aligned}
&\lim_{n \rightarrow \infty} \lim_{\varepsilon \rightarrow 0} a_2^{n,\varepsilon}(z) \\
&= \int_{\Omega \times Y \times \mathbb{R}^+} \chi_f(y - z) \chi_f(y) u(r, y, t) \cdot z \psi_1(y - z) \cdot z \psi_2(r) \phi(t) dr dy dt. \tag{9.42}
\end{aligned}$$

From (9.40) and (9.42) and since

$$\lim_{\varepsilon \rightarrow 0} a^\varepsilon(z) = \lim_{n \rightarrow \infty} \lim_{\varepsilon \rightarrow 0} (a_1^{n,\varepsilon}(z) + a_2^{n,\varepsilon}(z)),$$

equation (9.35) follows.

From (9.33) and (9.35), and by using Lebesgue's dominated convergence theorem, we obtain

$$\begin{aligned} & \lim_{\varepsilon \rightarrow 0} \int_{\Omega \times \mathbb{R}^+} A_{S,1}^\varepsilon u^\varepsilon(x, t) \cdot \psi\left(x, \frac{x}{\varepsilon}, t\right) dx dt \\ &= \int_{H_\delta(0)} \frac{1}{|z|^3} \int_{\Omega \times Y \times \mathbb{R}^+} \chi_f(y-z) \chi_f(y) u(r, y, t) \cdot z \psi_1(y-z) \cdot z \psi_2(r) \phi(t) dr dy dt dz \\ &= \int_{\Omega \times \mathbb{R}^+} \int_{H_\delta(0)} \frac{1}{|z|^3} \int_Y \chi_f(y-z) \chi_f(y) u(r, y, t) \cdot z \psi_1(y-z) \cdot z dy dz \psi_2(r) \phi(t) dr dt, \end{aligned} \quad (9.43)$$

where we have changed the order of integration in the last step. After shifting the domain of integration in the inner integral of the right hand side of equation (9.43), we obtain

$$\begin{aligned} & \int_Y \chi_f(y-z) \chi_f(y) u(r, y, t) \cdot z \psi_1(y-z) \cdot z dy \\ &= \int_{Y-z} \chi_f(y) \chi_f(y+z) u(r, y+z, t) \cdot z \psi_1(y) \cdot z dy \\ &= \int_Y \chi_f(y) \chi_f(y+z) u(r, y+z, t) \cdot z \psi_1(y) \cdot z dy, \end{aligned} \quad (9.44)$$

where in the last step the fact that the integrand is  $Y$ -periodic in  $y$  was used. Substituting (9.44) in equation (9.43), then by changing the order of integration we obtain

$$\begin{aligned} & \lim_{\varepsilon \rightarrow 0} \int_{\Omega \times \mathbb{R}^+} A_{S,1}^\varepsilon u^\varepsilon(x, t) \cdot \psi\left(x, \frac{x}{\varepsilon}, t\right) dx dt \\ &= \int_{\Omega \times \mathbb{R}^+} \int_Y \int_{H_\delta(0)} \chi_f(y) \chi_f(y+z) \frac{z \otimes z}{|z|^3} u(r, y+z, t) dz \cdot \psi_1(y) dy \psi_2(r) \phi(t) dr dt \\ &= \int_{\Omega \times Y \times \mathbb{R}^+} \int_{H_\delta(y)} \chi_f(y) \chi_f(\hat{y}) \frac{(\hat{y}-y) \otimes (\hat{y}-y)}{|\hat{y}-y|^3} u(r, \hat{y}, t) d\hat{y} \cdot \psi(r, y, t) dr dy dt. \end{aligned} \quad (9.45)$$

In the last equality the change of variables  $\hat{y} = y + z$  was used.

Next we evaluate the two-scale limit of  $A_{S,2}^\varepsilon u^\varepsilon$ . Let  $\psi$  be a test function in  $\mathcal{J}$ .

Then by using (8.16), replacing  $v(x)$  with  $u^\varepsilon(x, t)$ , we obtain

$$\begin{aligned} & \int_{\Omega \times \mathbb{R}^+} A_{S,2}^\varepsilon u^\varepsilon(x, t) \cdot \psi\left(x, \frac{x}{\varepsilon}, t\right) dx dt \\ &= \int_{\Omega \times \mathbb{R}^+} \int_{H_\delta(0)} \alpha\left(\frac{x}{\varepsilon}, \frac{x}{\varepsilon} + z\right) \frac{z \otimes z}{|z|^3} dz u^\varepsilon(x, t) \cdot \psi\left(x, \frac{x}{\varepsilon}, t\right) dx dt. \end{aligned} \quad (9.46)$$

The right hand side of (9.46), after changing the order of integration, is equal to

$$\int_{H_\delta(0)} \frac{1}{|z|^3} \int_{\Omega \times \mathbb{R}^+} \alpha\left(\frac{x}{\varepsilon}, \frac{x}{\varepsilon} + z\right) u^\varepsilon(x, t) \cdot z \psi\left(x, \frac{x}{\varepsilon}, t\right) \cdot z dx dt dz. \quad (9.47)$$

Using the fact that  $(u^\varepsilon)_{\varepsilon>0}$  two-scale converges to  $u(x, y, t)$ , we see that for

$z \in H_\delta(0)$ ,

$$\begin{aligned} & \lim_{\varepsilon \rightarrow 0} \int_{\Omega \times \mathbb{R}^+} \alpha\left(\frac{x}{\varepsilon}, \frac{x}{\varepsilon} + z\right) u^\varepsilon(x, t) \cdot z \psi\left(x, \frac{x}{\varepsilon}, t\right) \cdot z dx dt \\ &= \int_{\Omega \times Y \times \mathbb{R}^+} \alpha(y, y + z) u(x, y, t) \cdot z \psi(x, y, t) \cdot z dx dy dt. \end{aligned} \quad (9.48)$$

From (9.46), (9.47) and (9.48), and by using Lebesgue's dominated convergence theorem, we obtain

$$\begin{aligned} & \lim_{\varepsilon \rightarrow 0} \int_{\Omega \times \mathbb{R}^+} A_{S,2}^\varepsilon u^\varepsilon(x, t) \cdot \psi\left(x, \frac{x}{\varepsilon}, t\right) dx dt \\ &= \int_{H_\delta(0)} \frac{1}{|z|^3} \int_{\Omega \times Y \times \mathbb{R}^+} \alpha(y, y + z) u(x, y, t) \cdot z \psi(x, y, t) \cdot z dx dy dt dz \end{aligned} \quad (9.49)$$

By changing the order of integration and then using the change of variables

$\hat{y} = y + z$ , we conclude that

$$\begin{aligned} & \lim_{\varepsilon \rightarrow 0} \int_{\Omega \times \mathbb{R}^+} A_{S,2}^\varepsilon u^\varepsilon(x, t) \cdot \psi\left(x, \frac{x}{\varepsilon}, t\right) dx dt \\ &= \int_{\Omega \times Y \times \mathbb{R}^+} \int_{H_\delta(y)} \alpha(y, \hat{y}) \frac{(\hat{y} - y) \otimes (\hat{y} - y)}{|\hat{y} - y|^3} d\hat{y} u(x, y, t) \cdot \psi(x, y, t) dx dy dt. \end{aligned} \quad (9.50)$$

Equation (9.31) follows from combining (9.45) and (9.50), completing the proof.

□

# Chapter 10

## The Macroscopic Equation and Downscaling

The aim of this chapter is to justify the main results of Chapter 7.

### 10.1 Derivation of the Macroscopic Equation

We begin this section with the following observation. Let  $\phi$  be a function in  $L^s_{per}(Y)^3$ . Then

$$\int_Y \int_{H_\delta(y)} \alpha(y, \hat{y}) \frac{(\hat{y} - y) \otimes (\hat{y} - y)}{|\hat{y} - y|^3} (\phi(\hat{y}) - \phi(y)) d\hat{y} dy = 0. \quad (10.1)$$

To see this, we note that using Fubini's theorem and the assumption that  $\phi$  is  $Y$ -periodic, the double integral in (10.1) can be written as

$$\begin{aligned} & \int_Y \int_{H_\delta(\hat{y})} \alpha(y, \hat{y}) \frac{(\hat{y} - y) \otimes (\hat{y} - y)}{|\hat{y} - y|^3} (\phi(\hat{y}) - \phi(y)) dy d\hat{y} \\ &= - \int_Y \int_{H_\delta(\hat{y})} \alpha(\hat{y}, y) \frac{(y - \hat{y}) \otimes (y - \hat{y})}{|(y - \hat{y})|^3} (\phi(y) - \phi(\hat{y})) dy d\hat{y}, \end{aligned} \quad (10.2)$$

where in the last equality we have used the fact  $\alpha(y, \hat{y}) = \alpha(\hat{y}, y)$ . Comparing the double integral in (10.1) with (10.2) the result follows.

Now let

$$u^H(x, t) = \int_Y u(x, y, t) dy.$$

Then from Proposition 9.9, we have that  $u^H(x, t)$  is the weak limit of  $u^\varepsilon(x, t)$  in  $L^p(\Omega \times (0, T))^3$ . To identify the equation that  $u^H$  solves, we integrate (9.11) over

$Y$  to obtain

$$\begin{aligned}
\partial_t^2 u^H(x, t) &= \int_{H_\gamma(x)} \lambda(\hat{x} - x) \frac{(\hat{x} - x) \otimes (\hat{x} - x)}{|\hat{x} - x|^3} (u^H(\hat{x}, t) - u^H(x, t)) d\hat{x} \\
&+ \int_Y \int_{H_\delta(y)} \alpha(y, \hat{y}) \frac{(\hat{y} - y) \otimes (\hat{y} - y)}{|\hat{y} - y|^3} (u(x, \hat{y}, t) - u(x, y, t)) d\hat{y} dy \\
&+ \int_Y b(x, y, t) dy.
\end{aligned} \tag{10.3}$$

Using (10.1), the second integral on right hand side of (10.3) is equal to zero for all  $x \in \Omega$  and  $t \in (0, T)$ . Thus  $u^H$  solves

$$\partial_t^2 u^H(x, t) = \int_{H_\gamma(x)} \lambda(\hat{x} - x) \frac{(\hat{x} - x) \otimes (\hat{x} - x)}{|\hat{x} - x|^3} (u^H(\hat{x}, t) - u^H(x, t)) d\hat{x} + \int_Y b(x, y, t) dy, \tag{10.4}$$

supplemented with initial data

$$u^H(x, 0) = \int_Y u^0(x, y) dy, \quad \partial_t u^H(x, 0) = \int_Y v^0(x, y) dy. \tag{10.5}$$

The initial value problem (10.4)-(10.5) can be written as the following operator equation in  $L^s(\Omega)^3$

$$\begin{cases} \ddot{u}^H(t) &= A_L u^H(t) + \bar{b}(t), & t \in [0, T] \\ u^H(0) &= \bar{u}^0, \\ \dot{u}^H(0) &= \bar{v}^0. \end{cases} \tag{10.6}$$

where

$$\begin{aligned}
\bar{b}(x, t) &= \int_Y b(x, y, t) dy, \\
\bar{u}^0(x) &= \int_Y u^0(x, y) dy, \text{ and} \\
\bar{v}^0(x) &= \int_Y v^0(x, y) dy.
\end{aligned}$$

We have seen from the proof of Proposition 8.1 that  $A_L$  is a bounded linear operator on  $L^s(\Omega)^3$ , thus  $u^H \in C^2([0, T]; L^s(\Omega)^3)$  is the unique solution of 10.6.

To complete the proof of Theorems 7.1, 7.3, 7.5, and 7.7, we show that  $u^H$  is in  $C^2([0, T]; C(\bar{\Omega})^3)$ , when the initial data  $\bar{u}^0$  and  $\bar{v}^0$  are in  $C(\bar{\Omega})^3$ , and the loading force  $\bar{b}$  is in  $C([0, T]; C(\bar{\Omega})^3)$ . In fact, it suffices to show that the linear operator  $A_L$  is bounded on the Banach space of continuous functions  $C(\bar{\Omega})^3$  equipped with the uniform norm. So we let  $v \in C(\bar{\Omega})^3$  and denote the uniform norm on  $C(\bar{\Omega})^3$  by  $\|\cdot\|_{C(\bar{\Omega})^3}$ . Then, we recall from (8.5) that  $A_L = A_{L,1} + A_{L,2}$ , where  $A_{L,1}$  and  $A_{L,2}$  can be written as

$$A_{L,1}v(x) = \int_{H_\gamma(0)} \lambda(\xi) \frac{\xi \otimes \xi}{|\xi|^3} v(x + \xi) d\xi, \quad (10.7)$$

$$A_{L,2}v(x) = \int_{H_\gamma(0)} \lambda(\xi) \frac{\xi \otimes \xi}{|\xi|^3} d\xi v(x), \quad (10.8)$$

respectively. Taking the norm in (10.7) we see that

$$\begin{aligned} \|A_{L,1}v\|_{C(\bar{\Omega})^3} &= \max_{x \in \bar{\Omega}} \left| \int_{H_\gamma(0)} \lambda(\xi) \frac{\xi \otimes \xi}{|\xi|^3} v(x + \xi) d\xi \right| \\ &\leq \left( \max_{\xi \in H_\gamma(0)} \lambda(\xi) \right) \max_{x \in \bar{\Omega}} \int_{H_\gamma(0)} \frac{1}{|\xi|} |v(x + \xi)| d\xi \\ &\leq \left( \max_{\xi \in H_\gamma(0)} \lambda(\xi) \right) \int_{H_\gamma(0)} \frac{1}{|\xi|} d\xi \|v\|_{C(\bar{\Omega})^3}. \end{aligned}$$

Thus  $A_{L,1}$  is bounded on  $C(\bar{\Omega})^3$ . It is clear that  $A_{L,2}$  is also bounded on  $C(\bar{\Omega})^3$ , and therefore  $A_L$  is bounded completing the argument.

## 10.2 Justifying the Downscaling Step

In this section we prove Theorems 7.2, 7.4, 7.6, and 7.8. We begin by showing that for fixed  $t \in (0, T)$ ,

$$\lim_{\varepsilon \rightarrow 0} \left\| u^\varepsilon(x, t) - u\left(x, \frac{x}{\varepsilon}, t\right) \right\|_{L^s(\Omega)^3} = 0.$$

By shifting the domains of integration, equation (9.11) can be written as follows

$$\begin{aligned}
\partial_t^2 u(x, y, t) &= \int_{H_\gamma(0)} \lambda(\xi) \frac{\xi \otimes \xi}{|\xi|^3} \left( \int_Y u(x + \xi, y', t) dy' - u(x, y, t) \right) d\xi \\
&+ \int_{H_\delta(0)} \alpha(y, y + z) \frac{z \otimes z}{|z|^3} (u(x, y + z, t) - u(x, y, t)) dz \\
&+ b(x, y, t).
\end{aligned} \tag{10.9}$$

Since  $u(x, y, t)$  is in  $\mathcal{Q}$  and solves (10.9) with initial conditions (9.12) and (9.13), then  $u(x, \frac{x}{\varepsilon}, t)$  is in  $C^2([0, T]; L^s(\Omega)^3)$  and solves

$$\begin{aligned}
\partial_t^2 u \left( x, \frac{x}{\varepsilon}, t \right) &= \int_{H_\gamma(0)} \lambda(\xi) \frac{\xi \otimes \xi}{|\xi|^3} \left( \int_Y u(x + \xi, y', t) dy' - u \left( x, \frac{x}{\varepsilon}, t \right) \right) d\xi \\
&+ \int_{H_\delta(0)} \alpha \left( \frac{x}{\varepsilon}, \frac{x}{\varepsilon} + z \right) \frac{z \otimes z}{|z|^3} \left( u \left( x, \frac{x}{\varepsilon} + z, t \right) - u \left( x, \frac{x}{\varepsilon}, t \right) \right) dz \\
&+ b \left( x, \frac{x}{\varepsilon}, t \right),
\end{aligned} \tag{10.10}$$

supplemented with initial conditions

$$u(x, y, 0) = u^0 \left( x, \frac{x}{\varepsilon} \right), \tag{10.11}$$

$$\partial_t u(x, y, 0) = v^0 \left( x, \frac{x}{\varepsilon} \right). \tag{10.12}$$

We let  $e^\varepsilon(x, t) = u^\varepsilon(x, t) - u(x, \frac{x}{\varepsilon}, t)$ . Then by subtracting (10.10) from (6.10), we find that  $e^\varepsilon \in C^2([0, T]; L^s(\Omega)^3)$  solves

$$\partial_t^2 e^\varepsilon(x, t) = A^\varepsilon e^\varepsilon(x, t) + d^\varepsilon(x, t), \tag{10.13}$$

$$e^\varepsilon(x, 0) = 0, \tag{10.14}$$

$$\partial_t e^\varepsilon(x, 0) = 0. \tag{10.15}$$

where  $A^\varepsilon$  is given by (8.7) and  $d^\varepsilon(x, t)$  is given by

$$d^\varepsilon(x, t) = d_L^\varepsilon(x, t) + d_S^\varepsilon(x, t), \quad (10.16)$$

$$d_L^\varepsilon(x, t) = \int_{H_\gamma(0)} \lambda(\xi) \frac{\xi \otimes \xi}{|\xi|^3} \left( u \left( x + \xi, \frac{x + \xi}{\varepsilon}, t \right) - \int_Y u(x + \xi, y', t) dy' \right) d\xi, \quad (10.17)$$

$$d_S^\varepsilon(x, t) = \int_{H_\delta(0)} \alpha \left( \frac{x}{\varepsilon}, \frac{x}{\varepsilon} + z \right) \frac{z \otimes z}{|z|^3} \left( u \left( x + \varepsilon z, \frac{x}{\varepsilon} + z, t \right) - u \left( x, \frac{x}{\varepsilon} + z, t \right) \right) dz. \quad (10.18)$$

Since  $A^\varepsilon$  is bounded, the solution of (10.13)-(10.15) is explicitly given by

$$e^\varepsilon(x, t) = \int_0^t \sum_{n=0}^{\infty} \frac{(t - \tau)^{2n+1}}{(2n + 1)!} (A^\varepsilon)^n d^\varepsilon(x, \tau) d\tau.$$

Thus

$$\begin{aligned} \|e^\varepsilon(\cdot, t)\|_{L^s(\Omega)^3} &\leq \int_0^t \sum_{n=0}^{\infty} \frac{(t - \tau)^{2n+1}}{(2n + 1)!} \|(A^\varepsilon)^n\| \|d^\varepsilon(\cdot, \tau)\|_{L^s(\Omega)^3} d\tau \\ &\leq \int_0^t \frac{1}{\sqrt{M}} \sinh \left( \sqrt{M}(t - \tau) \right) \|d^\varepsilon(\cdot, \tau)\|_{L^s(\Omega)^3} d\tau \end{aligned} \quad (10.19)$$

where in the second inequality we have used the fact that  $A^\varepsilon$  is bounded above by an  $M > 0$  independent of  $\varepsilon$ .

In the following sections we will show that for  $t \in (0, T)$ ,

$$\lim_{\varepsilon \rightarrow 0} \|d^\varepsilon(\cdot, t)\|_{L^s(\Omega)^3} = 0, \quad (10.20)$$

for each of the four cases of initial and loading conditions that has been introduced in Chapter 7. On the other hand, from (10.16)-(10.18) and the fact that  $u$  is continuous on  $[0, T]$ , it follows that  $d^\varepsilon(\cdot, \tau)$  is continuous on  $[0, t]$  for  $t \leq T$ . Thus, from equations (10.19) and (10.20), and Lebesgue's convergence theorem, we see that

$$\lim_{\varepsilon \rightarrow 0} \|e^\varepsilon(\cdot, t)\|_{L^s(\Omega)^3} = 0,$$

from which the result follows.

In order to prove (10.20), we will make use of the following observation:

*The solution of each cell-problem of Chapter 7 has zero average over the unit cell.*

To see this, we integrate equation (7.5) over  $Y$  to obtain

$$\ddot{\bar{r}}(t) = \int_Y \int_{H_\delta(y)} \alpha(y, \hat{y}) \frac{(\hat{y} - y) \otimes (\hat{y} - y)}{|\hat{y} - y|^3} (r(\hat{y}, t) - r(y, t)) d\hat{y} dy - K \bar{r}(t) \quad (10.21)$$

supplemented with initial conditions

$$\bar{r}(0) = 0, \quad \dot{\bar{r}}(0) = 0. \quad (10.22)$$

Using (10.1), the integral on the right hand side of (10.21) is equal to zero for all  $t \in (0, T)$ . Thus  $\bar{r}$  solves

$$\ddot{\bar{r}}(t) = -K \bar{r}(t), \quad (10.23)$$

supplemented with zero initial conditions. Obviously the solution of (10.23) is given by

$$\int_Y r(y, t) dy = \bar{r}(t) = 0, \quad (10.24)$$

for all  $t \in (0, T)$ . Similarly we can show that

$$\int_Y r^j(y, t) dy = \bar{r}^j(t) = 0, \quad (10.25)$$

for all  $t \in (0, T)$ , where  $r^j$  is the solution of (7.12), (7.19), or (7.26).

### 10.2.1 First Case

In this section we complete the proof of Theorem 7.2 by showing that equation (10.20) holds true when  $b$ ,  $u^0$ , and  $v^0$  are given by (7.2). We also prove the error estimate (7.8).

Using the fact that  $r(y, t)$ , the solution of the cell problem (7.5)-(7.6), has zero average over  $Y$ , and by linearity, it is easy to check that  $u^H(x, t) + r(y, t)$  solves (9.11)-(9.13), where  $u^H$  is the solution of (7.3)-(7.4). Thus by uniqueness we conclude that

$$u(x, y, t) = u^H(x, t) + r(y, t). \quad (10.26)$$

Using this representation of  $u(x, y, t)$  and from equations (10.17) and (10.18), we see that  $d_L^\varepsilon(x, t)$  and  $d_S^\varepsilon(x, t)$  are now given by

$$d_L^\varepsilon(x, t) = \int_{H_\gamma(0)} \lambda(\xi) \frac{\xi \otimes \xi}{|\xi|^3} r\left(\frac{x + \xi}{\varepsilon}, t\right) d\xi, \quad (10.27)$$

$$d_S^\varepsilon(x, t) = \int_{H_\delta(0)} \alpha\left(\frac{x}{\varepsilon}, \frac{x}{\varepsilon} + z\right) \frac{z \otimes z}{|z|^3} (u^H(x + \varepsilon z, t) - u^H(x, t)) dz, \quad (10.28)$$

respectively.

Changing variables of integration, equation (10.27) becomes

$$d_L^\varepsilon(x, t) = \int_{H_\gamma(x)} \lambda(\hat{x} - x) \frac{(\hat{x} - x) \otimes (\hat{x} - x)}{|\hat{x} - x|^3} r\left(\frac{\hat{x}}{\varepsilon}, t\right) d\hat{x}. \quad (10.29)$$

Since  $r(y, t)$  is  $Y$ -periodic in  $y$  and from Proposition 9.10, we see that for fixed  $t$ , as  $\varepsilon \rightarrow 0$

$$r\left(\frac{\hat{x}}{\varepsilon}, t\right) \rightarrow \int_Y r(y, t) dt = 0 \quad \text{weakly in } L^s(\Omega)^3.$$

Thus from (10.29) we obtain that

$$\lim_{\varepsilon \rightarrow 0} d_L^\varepsilon(x, t) = 0,$$

for  $x \in \Omega$  and  $t \in (0, T)$ . It follows from Lebesgue's convergence theorem that

$$\lim_{\varepsilon \rightarrow 0} \|d_L^\varepsilon(\cdot, t)\|_{L^s(\Omega)^3} = 0, \quad (10.30)$$

for  $t \in (0, T)$ . On the other hand, by taking the Euclidean norm of  $d_S^\varepsilon(x, t)$  in (10.28), we obtain

$$|d_S^\varepsilon(x, t)| \leq \alpha_{\max} \int_{H_\delta(0)} \frac{1}{|z|} |u^H(x + \varepsilon z, t) - u^H(x, t)| dz, \quad (10.31)$$

where  $\alpha_{\max} = \max_{y, y' \in Y} \alpha(y, y')$ . Since  $u^H \in C^2([0, T]; C(\bar{\Omega})^3)$  (see Section 10.1), it follows that for  $x \in \Omega$  and  $t \in (0, T)$

$$\lim_{\varepsilon \rightarrow 0} |d_S^\varepsilon(x, t)| = 0. \quad (10.32)$$

Thus using Lebesgue's convergence theorem, we obtain

$$\lim_{\varepsilon \rightarrow 0} \|d_S^\varepsilon(\cdot, t)\|_{L^s(\Omega)^3} = 0, \quad (10.33)$$

for  $t \in (0, T)$ . Equation (10.20) follows from equations (10.30) and (10.33).

Now we prove the error estimate (7.8). By setting  $\lambda = 0$  in equation (7.3), we see that its solution  $u^H$  is given explicitly by

$$u^H(x, t) = u_0(x) + t v_0(x) + \int_0^t (t - \tau) l(x, \tau) d\tau. \quad (10.34)$$

By assumption  $u_0, v_0$ , and  $l(\cdot, t)$  are in  $C^{0,\beta}(\bar{\Omega})$ . Thus for  $z \in H_\delta(0)$ , we see from (10.34) that

$$\begin{aligned} |u^H(x + \varepsilon z, t) - u^H(x, t)| &\leq C|\varepsilon z|^\beta + t C|\varepsilon z|^\beta + \int_0^t (t - \tau) C|\varepsilon z|^\beta d\tau \\ &= C \left(1 + t + \frac{t^2}{2}\right) |z|^\beta \varepsilon^\beta, \end{aligned} \quad (10.35)$$

for some  $C > 0$ . We use this bound in inequality (10.31) to obtain

$$|d_S^\varepsilon(x, t)| \leq C \left(1 + t + \frac{t^2}{2}\right) \alpha_{\max} \int_{H_\delta(0)} |z|^{\beta-1} dz \varepsilon^\beta. \quad (10.36)$$

Since  $\lambda = 0$  we see from (10.16)-(10.18) that  $d^\varepsilon = d_S^\varepsilon$ . Therefore from (10.36), after a simple calculation, we obtain

$$\|d^\varepsilon(\cdot, t)\|_{L^s(\Omega)^3} \leq 4\pi C \alpha_{\max} |\Omega|^{1/s} \frac{\delta^{\beta+2}}{\beta+2} \left(1 + t + \frac{t^2}{2}\right) \varepsilon^\beta. \quad (10.37)$$

By using (10.37) to bound  $\|d^\varepsilon(\cdot, \tau)\|_{L^s(\Omega)^3}$  in (10.19), the error estimate (7.8) follows.

### 10.2.2 Second Case

In this section we complete the proof of Theorem 7.4 by showing that equation (10.20) holds true when  $b, u^0$ , and  $v^0$  are given by (7.9). We also prove the error estimate (7.15).

Using the fact that  $r(y, t)$ , the solution of the cell problem (7.12)-(7.13), has zero average over  $Y$ , and by linearity, it is easy to check that  $u^H(x, t) + \sum_{j=1}^3 r^j(y, t) h_j(x)$

solves (9.11)-(9.13), where  $u^H$  is the solution of (7.10)-(7.11). Thus by uniqueness we conclude that

$$u(x, y, t) = u^H(x, t) + \sum_{j=1}^3 r^j(y, t)h_j(x). \quad (10.38)$$

Using this representation of  $u(x, y, t)$  and from equations (10.17) and (10.18), we see that  $d_L^\varepsilon(x, t)$  is now given by

$$d_L^\varepsilon(x, t) = \int_{H_\gamma(0)} \lambda(\xi) \frac{\xi \otimes \xi}{|\xi|^3} \sum_{j=1}^3 r^j \left( \frac{x + \xi}{\varepsilon}, t \right) h_j(x + \xi) d\xi, \quad (10.39)$$

and  $d_S^\varepsilon(x, t)$  can be written as

$$d_S^\varepsilon(x, t) = d_{S,1}^\varepsilon(x, t) + d_{S,2}^\varepsilon(x, t), \quad (10.40)$$

where,

$$d_{S,1}^\varepsilon(x, t) = \int_{H_\delta(0)} \alpha \left( \frac{x}{\varepsilon}, \frac{x}{\varepsilon} + z \right) \frac{z \otimes z}{|z|^3} (u^H(x + \varepsilon z, t) - u^H(x, t)) dz, \quad (10.41)$$

$$d_{S,2}^\varepsilon(x, t) = \int_{H_\delta(0)} \alpha \left( \frac{x}{\varepsilon}, \frac{x}{\varepsilon} + z \right) \frac{z \otimes z}{|z|^3} \sum_{j=1}^3 r^j \left( \frac{x}{\varepsilon} + z, t \right) (h_j(x + \varepsilon z) - h_j(x)) dz. \quad (10.42)$$

Applying the methods developed in Section 10.2.1 for (10.30) and (10.33), we can show that for  $t \in (0, T)$ ,

$$\lim_{\varepsilon \rightarrow 0} \|d_L^\varepsilon(\cdot, t)\|_{L^s(\Omega)^3} = 0, \quad (10.43)$$

and

$$\lim_{\varepsilon \rightarrow 0} \|d_{S,1}^\varepsilon(\cdot, t)\|_{L^s(\Omega)^3} = 0. \quad (10.44)$$

It remains to show that for  $t \in (0, T)$ ,

$$\lim_{\varepsilon \rightarrow 0} \|d_{S,2}^\varepsilon(\cdot, t)\|_{L^s(\Omega)^3} = 0. \quad (10.45)$$

From equation (10.42), we see that

$$|d_{S,2}^\varepsilon(x, t)| \leq \alpha_{\max} \int_{H_\delta(0)} \frac{1}{|z|} \sum_{j=1}^3 \left| r^j \left( \frac{x}{\varepsilon} + z, t \right) \right| |h_j(x + \varepsilon z) - h_j(x)| dz, \quad (10.46)$$

where  $\alpha_{\max} = \max_{y, y' \in Y} \alpha(y, y')$ . Since  $\frac{3}{2} < s < \infty$ , we can choose  $s'$ , with  $\frac{3}{2} < s' < \infty$ , and  $s''$ , with  $1 \leq s'' < 3$ , such that  $1/s + 1/s' + 1/s'' = 1$ . By Hölder's inequality we obtain

$$\begin{aligned} |d_{S,2}^\varepsilon(x, t)| &\leq \alpha_{\max} \left( \int_{H_\delta(0)} \frac{1}{|z|^{s''}} dz \right)^{1/s''} \sum_{j=1}^3 \left( \int_{H_\delta(0)} \left| r^j \left( \frac{x}{\varepsilon} + z, t \right) \right|^{s'} dz \right)^{1/s'} \\ &\quad \times \left( \int_{H_\delta(0)} |h_j(x + \varepsilon z) - h_j(x)|^s dz \right)^{1/s}. \end{aligned} \quad (10.47)$$

It is easy to see that

$$\left( \int_{H_\delta(0)} \left| r^j \left( \frac{x}{\varepsilon} + z, t \right) \right|^{s'} dz \right)^{1/s'} \leq \|r^j(\cdot, t)\|_{L^{s'}(\Omega)^3}. \quad (10.48)$$

Thus from (10.47) and (10.48), and by using the triangle inequality in  $L^s$ , we obtain

$$\begin{aligned} \|d_{S,2}^\varepsilon(\cdot, t)\| &\leq \alpha_{\max} \left( \int_{H_\delta(0)} \frac{1}{|z|^{s''}} dz \right)^{1/s''} \sum_{j=1}^3 \|r^j(\cdot, t)\|_{L^{s'}(\Omega)^3} \\ &\quad \times \left( \int_{\Omega} \int_{H_\delta(0)} |h_j(x + \varepsilon z) - h_j(x)|^s dz dx \right)^{1/s}. \end{aligned} \quad (10.49)$$

Since  $h_j$  is continuous on  $\bar{\Omega}$ , we obtain from Lebesgue's convergence theorem that

$$\lim_{\varepsilon \rightarrow 0} \int_{\Omega} \int_{H_\delta(0)} |h_j(x + \varepsilon z) - h_j(x)|^s dz dx = 0. \quad (10.50)$$

Equation (10.45) follows from (10.49) and (10.50). This shows that (10.20) holds true for this case.

Now we prove the error estimate (7.15). By setting  $\lambda = 0$  in equation (7.10), we see that its solution  $u^H$  is given explicitly by

$$u^H(x, t) = \int_0^t (t - \tau) \bar{F}(\tau) d\tau h(x). \quad (10.51)$$

By assumption  $h$  is in  $C^{0,\beta}(\bar{\Omega})$ . Thus for  $z \in H_\delta(0)$ , we see from (10.51) that

$$|u^H(x + \varepsilon z, t) - u^H(x, t)| \leq C|\varepsilon z|^\beta \int_0^t (t - \tau) \bar{F}(\tau) d\tau, \quad (10.52)$$

for some  $C > 0$ . Taking the Euclidean norm in both sides of (10.41) and using the bound (10.52), we see that

$$|d_{S,1}^\varepsilon(x, t)| \leq C\alpha_{\max} \int_0^t (t - \tau) \bar{F}(\tau) d\tau \int_{H_\delta(0)} |z|^{\beta-1} dz \varepsilon^\beta, \quad (10.53)$$

and it follows that

$$\|d_{S,1}^\varepsilon(\cdot, t)\|_{L^s(\Omega)^3} \leq 4\pi C\alpha_{\max} |\Omega|^{1/s} \frac{\delta^{\beta+2}}{\beta+2} \left( \int_0^t (t - \tau) \bar{F}(\tau) d\tau \right) \varepsilon^\beta. \quad (10.54)$$

On the other hand from (10.49), after a straight forward calculation, we obtain

$$\|d_{S,2}^\varepsilon(\cdot, t)\|_{L^s(\Omega)^3} \leq C\alpha_{\max} \left( 4\pi \frac{\delta^{3-s''}}{3-s''} \right)^{1/s''} \left( 4\pi |\Omega| \frac{\delta^{s\beta+3}}{s\beta+3} \right)^{1/s} \sum_{j=1}^3 \|r^j(\cdot, t)\|_{L^{s'}(\Omega)^3} \varepsilon^\beta. \quad (10.55)$$

Since  $\lambda = 0$  we see that  $d^\varepsilon = d_{S,1}^\varepsilon + d_{S,2}^\varepsilon$ . Therefore by combining (10.54) and (10.55) to bound  $\|d^\varepsilon(\cdot, \tau)\|_{L^s(\Omega)^3}$  in (10.19), the error estimate (7.15) follows.

### 10.2.3 Third and Fourth Cases

Arguments similar to those presented in Section 10.2.2 show that equation (10.20) holds true when the loading and initial conditions are given by (7.16) or (7.23). Also, the proofs of the error estimates (7.22) and (7.29) are similar to the proof of (7.15) provided in Section 10.2.2. For completeness, we explicitly provide the functions  $M_3(t)$  and  $M_4(t)$  of Theorems 7.6 and 7.6, respectively. The function  $M_3(t)$  is given by

$$M_3(t) = \int_0^t \frac{1}{\sqrt{M}} \sinh\left(\sqrt{M}(t - \tau)\right) f_3(\tau) d\tau$$

where

$$f_3(t) = C\alpha_{\max} |\Omega|^{1/s} \left( 4\pi |\bar{F}| \frac{\delta^{\beta+2}}{\beta+2} + \left( 4\pi \frac{\delta^{3-s''}}{3-s''} \right)^{1/s''} \left( 4\pi \frac{\delta^{s\beta+3}}{s\beta+3} \right)^{1/s} \sum_{j=1}^3 \|r^j(\cdot, t)\|_{L^{s'}(\Omega)^3} \right)$$

and  $r^j$  solves (7.19)-(7.20).

The function  $M_4(t)$  is given by

$$M_4(t) = \int_0^t \frac{1}{\sqrt{M}} \sinh \left( \sqrt{M}(t - \tau) \right) f_4(\tau) d\tau$$

where

$$f_4(t) = C\alpha_{\max}|\Omega|^{1/s} \left( 4\pi|\bar{F}| \frac{\delta^{\beta+2}}{\beta+2} t + \left( 4\pi \frac{\delta^{3-s''}}{3-s''} \right)^{1/s''} \left( 4\pi \frac{\delta^{s\beta+3}}{s\beta+3} \right)^{1/s} \sum_{j=1}^3 \|r^j(\cdot, t)\|_{L^{s'}(\Omega)^3} \right)$$

and  $r^j$  solves (7.26)-(7.27).

This completes the proofs of Theorems 7.6 and 7.8.

# Chapter 11

## Fluctuating Long-Range Bond Model

In this chapter, we present a new multiscale analysis method for computing the deformation of fiber-reinforced composites modeled by the peridynamic formulation. This is done for the Fluctuating Long-Range Bond model described in Section 6.3. The method provides a computationally inexpensive multiscale numerical method. This is described by Theorem 11.1. A homogenization result for this model is expressed in Theorem 11.2.

We begin by recalling the peridynamic equation of motion for this model. By expanding  $\alpha_L^\varepsilon$  in equation (6.15), then collecting the  $\chi_f^\varepsilon$  terms, we obtain

$$\begin{aligned} \partial_t^2 u^\varepsilon(x, t) &= \chi_f^\varepsilon(x) \int_{I_\delta^n(x)} (C_f - \varepsilon C_m) \frac{(\hat{x} - x) \otimes (\hat{x} - x)}{|\hat{x} - x|^2} (u^\varepsilon(\hat{x}, t) - u^\varepsilon(x, t)) dl_{\hat{x}} \\ &+ \int_{H_\delta(x)} \varepsilon C_m \frac{(\hat{x} - x) \otimes (\hat{x} - x)}{|\hat{x} - x|^2} (u^\varepsilon(\hat{x}, t) - u^\varepsilon(x, t)) d\hat{x}, \end{aligned} \quad (11.1)$$

where the first integral in (11.1) is a line integral over the set

$$I_\delta^n(x) = \{\hat{x} \in H_\delta(x) \text{ such that } \hat{x} - x \text{ is parallel to } n\}.$$

The initial conditions supplementing this equation are given by

$$u^\varepsilon(x, 0) = u^0(x), \quad (11.2)$$

$$\partial_t u^\varepsilon(x, 0) = v^0(x). \quad (11.3)$$

The well-posedness of equation (11.1)-(11.3) is provided in Section 11.1 (Proposition 11.4).

**Theorem 11.1** (Downscaling). *Let  $u^\varepsilon \in C^2([0, T]; L^p(\Omega)^3)$  be the solution of (11.1)-(11.3), where  $1 \leq p < \infty$ . Then for  $t \in [0, T]$ ,*

$$\lim_{\varepsilon \rightarrow 0} \|u^\varepsilon(x, t) - (\chi_f^\varepsilon(x)w(x, t) + u^0(x) + tv^0(x))\|_{L^p(\Omega)^3} = 0, \quad (11.4)$$

where  $w \in C^2([0, T]; L^p(\Omega)^3)$  is the solution of

$$\begin{aligned} \partial_t^2 w(x, t) &= \int_{I_\delta^n(x)} C_f \frac{(\hat{x} - x) \otimes (\hat{x} - x)}{|\hat{x} - x|^2} (w(\hat{x}, t) - w(x, t)) dl_{\hat{x}} \\ &+ \int_{I_\delta^n(x)} C_f \frac{(\hat{x} - x) \otimes (\hat{x} - x)}{|\hat{x} - x|^2} (u^0(\hat{x}) + tv^0(\hat{x}) - (u^0(x) + tv^0(x))) dl_{\hat{x}} \end{aligned} \quad (11.5)$$

supplemented with the initial conditions

$$w(x, 0) = 0, \quad (11.6)$$

$$\partial_t w(x, 0) = 0. \quad (11.7)$$

Moreover, for  $t \in [0, T]$  the error in (11.4) is estimated by

$$\|u^\varepsilon(x, t) - (\chi_f^\varepsilon(x)w(x, t) + u^0(x) + tv^0(x))\|_{L^p(\Omega)^3} \leq \varepsilon M_5(t), \quad (11.8)$$

where

$$M_5(t) = \left( \|u^0\|_{L^p(\Omega)^3} \cosh \sqrt{M}t + \|v^0\|_{L^p(\Omega)^3} \frac{1}{\sqrt{M}} \sinh \sqrt{M}t \right),$$

and where  $M$  is a positive constant.

Theorem 11.1 is proved in Section 11.2.

The macroscopic peridynamic equation for this model is given by

$$\begin{aligned} \partial_t^2 u^H(x, t) &= \int_{I_\delta^n(x)} C_f \frac{(\hat{x} - x) \otimes (\hat{x} - x)}{|\hat{x} - x|^2} (u^H(\hat{x}, t) - u^H(x, t)) dl_{\hat{x}} \\ &+ (\theta_f - 1) \int_{I_\delta^n(x)} C_f \frac{(\hat{x} - x) \otimes (\hat{x} - x)}{|\hat{x} - x|^2} (u^0(\hat{x}) + tv^0(\hat{x}) - (u^0(x) + tv^0(x))) dl_{\hat{x}}, \end{aligned} \quad (11.9)$$

supplemented with initial conditions

$$u^H(x, 0) = u^0(x), \quad (11.10)$$

$$\partial_t u^H(x, 0) = v^0(x). \quad (11.11)$$

Here the macroscopic displacement  $u^H$  is the weak limit of the sequence of displacements  $u^\varepsilon$ . This is described by the following theorem.

**Theorem 11.2** (Homogenization). *Let  $u^\varepsilon \in C^2([0, T]; L^p(\Omega)^3)$  be the solution of (11.1)-(11.3), where  $1 \leq p < \infty$ . Then for  $t \in [0, T]$ , as  $\varepsilon \rightarrow 0$ ,*

$$u^\varepsilon(\cdot, t) \rightarrow u^H(\cdot, t) \quad \text{weakly in } L^p(\Omega)^3,$$

where  $u^H \in C^2([0, T]; L^p(\Omega)^3)$  is the solution of (11.9)-(11.11). Equivalently,  $u^H$  can be computed as follows

$$u^H(x, t) = \theta_f w(x, t) + u^0(x) + t v^0(x), \quad (11.12)$$

where  $w$  solves (11.5)-(11.7).

Theorem 11.2 is proved in Section 11.2.

**Remark 11.0.** We observe that the macroscopic peridynamic equation (11.9) has a nonzero loading force, although the original peridynamic equation (11.1) has no loading force. The physical interpretation for this phenomenon is not well-understood up to this point.

## 11.1 Existence and Uniqueness Results

Without loss of generality, we may choose the fiber direction to be parallel to the  $x_1$ -axis. So let  $n = (1, 0, 0)$ . We note that the matrix multiplying  $(u^\varepsilon(\hat{x}, t) - u^\varepsilon(x, t))$  in the first integral of (11.1) is now given by

$$\frac{(\hat{x} - x) \otimes (\hat{x} - x)}{|\hat{x} - x|^2} = \begin{pmatrix} 1 & 0 & 0 \\ 0 & 0 & 0 \\ 0 & 0 & 0 \end{pmatrix}$$

for  $\hat{x}_1 \neq x_1$ . Thus equation (11.1), after shifting the domain of integration in the first integral, becomes

$$\begin{aligned} \partial_t^2 u^\varepsilon(x, t) &= (C_f - \varepsilon C_m) \chi_f^\varepsilon(x) \int_{-\delta}^{\delta} (u_1^\varepsilon(x + (l, 0, 0), t) - u_1^\varepsilon(x, t)) dl \\ &+ \int_{H_\delta(x)} \varepsilon C_m \frac{(\hat{x} - x) \otimes (\hat{x} - x)}{|\hat{x} - x|^2} (u^\varepsilon(\hat{x}, t) - u^\varepsilon(x, t)) d\hat{x}. \end{aligned} \quad (11.13)$$

Let  $v = (v_1, v_2, v_3) \in L^p(\Omega)^3$  with  $1 \leq p < \infty$ . Then we define the following operators

$$A_f v(x) = C_f \int_{-\delta}^{\delta} (v_1(x + (l, 0, 0)) - v_1(x)) dl, \quad (11.14)$$

$$A_f^\varepsilon v(x) = \chi_f^\varepsilon(x) A_f v(x), \quad (11.15)$$

$$A_m v(x) = \int_{H_\delta(x)} C_m \frac{(\hat{x} - x) \otimes (\hat{x} - x)}{|\hat{x} - x|^2} (v(\hat{x}) - v(x)) d\hat{x}, \quad (11.16)$$

$$A^\varepsilon = A_f^\varepsilon + \varepsilon \left( A_m - \frac{C_m}{C_f} A_f^\varepsilon \right). \quad (11.17)$$

The initial value problem (11.1)-(11.3) can be written as the following operator equation in  $L^p(\Omega)^3$

$$\begin{cases} \ddot{u}^\varepsilon(t) = A^\varepsilon u^\varepsilon(t), & t \in [0, T] \\ u^\varepsilon(0) = u^0, \\ \dot{u}^\varepsilon(0) = v^0. \end{cases} \quad (11.18)$$

Existence and uniqueness of solution of (11.18) is given by the following proposition.

**Proposition 11.4.** *Let  $1 \leq p < \infty$ . Then*

(a) *The operator  $A^\varepsilon$  is linear and uniformly bounded on  $L^p(\Omega)^3$ .*

(b) *Equation (11.18) has a unique classical solution  $u^\varepsilon \in C^2([0, T]; L^p(\Omega)^3)$*

*which is given by*

$$u^\varepsilon(t) = \sum_{n=0}^{\infty} \frac{t^{2n}}{(2n)!} (A^\varepsilon)^n u^0 + \sum_{n=0}^{\infty} \frac{t^{2n+1}}{(2n+1)!} (A^\varepsilon)^n v^0. \quad (11.19)$$

*Proof.* Part (a). First, we show that the linear operator  $A_m$  is bounded on  $L^p(\Omega)^3$ .

Let  $v \in L^p(\Omega)^3$ . Then from (11.16),  $A_m$  can be written as

$$A_m = C_m(A_{m,1} - A_{m,2}),$$

where

$$A_{m,1}v(x) = \int_{H_\delta(x)} \frac{(\hat{x} - x) \otimes (\hat{x} - x)}{|\hat{x} - x|^2} v(\hat{x}) d\hat{x}, \quad (11.20)$$

$$A_{m,2}v(x) = \int_{H_\delta(x)} \frac{(\hat{x} - x) \otimes (\hat{x} - x)}{|\hat{x} - x|^2} d\hat{x} v(x). \quad (11.21)$$

From equation (11.20) we see that

$$\begin{aligned} \|A_{m,1}v\|_{L^p(\Omega)^3}^p &\leq \int_{\Omega} \left( \int_{H_\gamma(x)} |v(\hat{x})| d\hat{x} \right)^p dx \\ &\leq |\Omega| \|v\|_{L^p(\Omega)^3}^p, \end{aligned} \quad (11.22)$$

where the fact that  $\|v\|_{L^1(\Omega)^3} \leq \|v\|_{L^p(\Omega)^3}$  was used in the last step. This shows that  $A_{m,1}$  is bounded on  $L^p(\Omega)^3$ . The boundedness of  $A_{m,2}$  is clear. Therefore  $A_m$  is bounded on  $L^p(\Omega)^3$ .

Next we note that  $A_f$  is bounded on  $L^p(\Omega)^3$ , which is a consequence of Lemma 11.5 given at the end of this section. Thus it follows from (11.15) that  $A_f^\varepsilon$  is uniformly bounded on  $L^p(\Omega)^3$ .

Combining these results with equation (11.17), it follows that  $A^\varepsilon$  is uniformly bounded on  $L^p(\Omega)^3$ , completing the proof of Part (a).

The proof of Part (b) is similar to the proof of Part (b) of Proposition 8.1.

□

**Lemma 11.5.** *Let  $v$  be in  $L^p(\Omega)^3$ , where  $1 \leq p < \infty$ , and define*

$$\check{v}(x) = \int_{-\delta}^{\delta} v(x + (l, 0, 0)) dl.$$

*Then  $\check{v}$  is in  $L^p(\Omega)^3$  and*

$$\|\check{v}\|_{L^p(\Omega)^3} \leq 2\gamma \|v\|_{L^p(\Omega)^3}. \quad (11.23)$$

*Proof.* From the definition of  $\check{v}$  it is easy to see that

$$\int_{\Omega} |\check{v}(x)|^p dx \leq \int_{\Omega} \left( \int_{-\delta}^{\delta} |v(x_1 + l, x_2, x_3)| dl \right)^p dx_1 dx_2 dx_3. \quad (11.24)$$

Using Hölder's inequality in the inner integral with  $v \in L^p(\Omega)^3$  and  $1 \in L^{p'}(\Omega)^3$ , where  $1/p + 1/p' = 1$ , we obtain

$$\begin{aligned} \int_{\Omega} |\check{v}(x)|^p dx &\leq (2\delta)^{p/p'} \int_{\Omega} \int_{-\delta}^{\delta} |v(x_1 + l, x_2, x_3)|^p dl dx_1 dx_2 dx_3 \\ &= (2\delta)^{p/p'} \int_{-\delta}^{\delta} \int_{\Omega} |v(x_1 + l, x_2, x_3)|^p dx_1 dx_2 dx_3 dl, \end{aligned} \quad (11.25)$$

by Fubini's theorem. We extend  $v$  to  $\mathbb{R}^3$  by setting  $v = 0$  outside  $\Omega$ . Then by the change of variables  $\hat{x}_1 = x_1 + l$  in the inner integral of (11.25), we obtain

$$\int_{\Omega} |v(x_1 + l, x_2, x_3)|^p dx_1 \leq \int_{\Omega} |v(x_1, x_2, x_3)|^p dx_1.$$

Using this estimate in (11.25), we conclude that

$$\int_{\Omega} |\check{v}(x)|^p dx \leq (2\delta)^{p/p'} (2\delta) \int_{\Omega} |v(x)|^p dx, \quad (11.26)$$

and (11.23) follows, completing the proof.  $\square$

## 11.2 Multiscale Analysis Using the Semigroups Approach

The aim of this section is to prove Theorems 11.1 and 11.2. Our approach is summarized by the following steps:

- (i) Compute the two-scale limit  $u(x, y, t)$  of the sequence  $(u^\varepsilon)$  using the explicit representation of  $u^\varepsilon$ , equation (11.19). We show that for fixed  $t \in [0, T]$ , as  $\varepsilon \rightarrow 0$ ,

$$u^\varepsilon(x, t) \xrightarrow{2} u(x, y, t), \quad (11.27)$$

where  $u$  is given by

$$\begin{aligned} u(x, y, t) &= u^0(x) + tv^0(x) + \chi_f(y) \sum_{n=1}^{\infty} \frac{t^{2n}}{(2n)!} (A_f)^n u^0(x) \\ &\quad + \chi_f(y) \sum_{n=1}^{\infty} \frac{t^{2n+1}}{(2n+1)!} (A_f)^n v^0(x). \end{aligned} \quad (11.28)$$

(ii) Compute  $\partial_t^2 u$  in (11.28) then use it to identify the two-scale limit equation.

We find that  $u \in C^2([0, T]; L^p(\Omega)^3)$  uniquely solves

$$\begin{cases} \partial_t^2 u(x, y, t) &= \tilde{A}_f u(x, y, t) + b(x, y, t), \\ u(x, y, 0) &= u^0(x), \\ \partial u(x, y, 0) &= v^0(x), \end{cases} \quad (11.29)$$

where  $b$  is given by

$$b(x, y, t) = (\chi_f(y) - 1)A_f(u^0 + tv^0)(x).$$

Here the operator  $\tilde{A}_f$  is defined as follows. For  $\tilde{v} \in L^p(\Omega \times Y)^3$ ,

$$\tilde{A}_f \tilde{v}(x, y) = C_f \int_{-\delta}^{\delta} (\tilde{v}_1(x + (l, 0, 0), y) - \tilde{v}_1(x, y)) dl. \quad (11.30)$$

(iii) The macroscopic equation is found by integrating (11.29) over  $Y$ . We find that the macroscopic displacement  $u^H$  solves

$$\begin{cases} \partial_t^2 u^H(x, t) &= A_f u^H(x, t) + \bar{b}(x, t), \\ u^H(x, 0) &= u^0(x), \\ \partial u^H(x, 0) &= v^0(x), \end{cases} \quad (11.31)$$

where  $\bar{b}$  is given by

$$\bar{b}(x, t) = (\theta_f - 1)A_f(u^0 + tv^0)(x).$$

Here for fixed  $t \in [0, T]$ , as  $\varepsilon \rightarrow 0$ ,

$$u^\varepsilon(\cdot, t) \rightarrow u^H(\cdot, t) \text{ weakly in } L^p(\Omega)^3. \quad (11.32)$$

(iv) The two-scale limit  $u$  can also be computed by the following method. This method is numerically inexpensive.

$$u(x, y, t) = \chi_f(y)w(x, t) + u^0(x) + tv^0(x), \quad (11.33)$$

where  $w \in C^2([0, T]; L^p(\Omega)^3)$  solves

$$\begin{cases} \partial_t^2 w(x, t) &= A_f w(x, t) + A_f(u^0 + tv^0)(x), \\ w(x, 0) &= 0, \\ \partial w(x, 0) &= 0. \end{cases} \quad (11.34)$$

It follows from integrating (11.33) over  $Y$  that  $u^H$  can also be computed by

$$u^H(x, t) = \theta_f w(x, t) + u^0(x) + tv^0(x). \quad (11.35)$$

(v) Extend  $u$  by periodicity from  $\Omega \times Y \times (0, T)$  to  $\Omega \times \mathbb{R}^3 \times (0, T)$ . Then we use the explicit representations of  $u^\varepsilon$  and  $u$ , equations (11.19) and (11.28), respectively, to show that for fixed  $t \in [0, T]$ ,

$$\lim_{\varepsilon \rightarrow 0} \left\| u^\varepsilon(x, t) - u\left(x, \frac{x}{\varepsilon}, t\right) \right\|_{L^p(\Omega)^3} = 0. \quad (11.36)$$

Now we justify steps (i)-(v).

Proof of (i). Let  $v \in L^p(\Omega)^3$ , where  $1 \leq p < \infty$ . Then we first show that

$$(A_f^\varepsilon)^n v(x) = \chi_f^\varepsilon(x) (A_f)^n v(x) \quad \text{for all } n \in \mathbb{N}. \quad (11.37)$$

The proof is by induction on  $n$ . The formula (11.37) holds for  $n = 1$  by the definition of  $A_f^\varepsilon$ . Assume that it holds for  $n = k$ . Then for  $n = k + 1$ ,

$$\begin{aligned} (A_f^\varepsilon)^{k+1} v(x) &= \chi_f^\varepsilon(x) C_f \int_{-\delta}^{\delta} \left( (A_f^\varepsilon)^k v_1(x + (l, 0, 0)) - (A_f^\varepsilon)^k v_1(x) \right) dl \\ &= \chi_f^\varepsilon(x) C_f \int_{-\delta}^{\delta} \left( \chi_f^\varepsilon(x + (l, 0, 0)) (A_f)^k v_1(x + (l, 0, 0)) \right. \\ &\quad \left. - \chi_f^\varepsilon(x) (A_f)^k v_1(x) \right) dl. \end{aligned} \quad (11.38)$$

Note that since  $x$  lies in a fiber if and only if  $x + (l, 0, 0)$  lies in the same fiber, then  $\chi_f^\varepsilon(x + (l, 0, 0)) = \chi_f^\varepsilon(x)$ . On the other hand  $(\chi_f^\varepsilon)^2 = \chi_f^\varepsilon$ , thus (11.38) becomes

$$\begin{aligned} (A_f^\varepsilon)^{k+1} v(x) &= \chi_f^\varepsilon(x) \left( C_f \int_{-\delta}^{\delta} \left( (A_f)^k v_1(x + (l, 0, 0)) - (A_f)^k v_1(x) \right) dl \right) \\ &= \chi_f^\varepsilon(x) (A_f)^{k+1} v(x). \end{aligned}$$

Therefore (11.37) follows. Since  $(A_f)^n v \in L^p(\Omega)$ , it follows from Propositions 9.3 and 9.4 of Section 9.1 that

$$\chi_f^\varepsilon(x)(A_f)^n v(x) \xrightarrow{2} \chi_f(y)(A_f)^n v(x). \quad (11.39)$$

Next we show that

$$(A^\varepsilon)^n v(x) \xrightarrow{2} \chi_f(y)(A_f)^n v(x). \quad (11.40)$$

To see this, we note that from (11.17), the operator  $(A^\varepsilon)^n$ ,  $n \in \mathbb{N}$ , can be written in the following form

$$(A^\varepsilon)^n = (A_f^\varepsilon)^n + \varepsilon D_n^\varepsilon, \quad (11.41)$$

where the operator  $D_n^\varepsilon$  is bounded on  $L^p(\Omega)^3$  and satisfies

$$\|D_n^\varepsilon\| < M^n \quad (11.42)$$

for some  $M > 0$  independent of  $\varepsilon$ . It follows that for fixed  $n \in \mathbb{N}$ ,

$$\lim_{\varepsilon \rightarrow 0} \varepsilon D_n^\varepsilon v = 0, \quad \text{in } L^p(\Omega)^3, \quad (11.43)$$

and thus by Proposition 9.2, the sequence  $(\varepsilon D_n^\varepsilon v)_{\varepsilon > 0}$  two-scale converges to 0.

Therefore the result follows by combining (11.41), (11.39), and (11.37).

Now we recall from (11.19) that  $u^\varepsilon(x, t)$  is given by

$$u^\varepsilon(x, t) = u^0(x) + tv^0(x) + \sum_{n=1}^{\infty} \frac{t^{2n}}{(2n)!} (A^\varepsilon)^n u^0(x) + \sum_{n=1}^{\infty} \frac{t^{2n+1}}{(2n+1)!} (A^\varepsilon)^n v^0(x). \quad (11.44)$$

Using (11.40), we will show in Section 11.2.1 that for  $\psi \in \mathcal{K}$ ,

$$\begin{aligned} \lim_{\varepsilon \rightarrow 0} \int_{\Omega} \sum_{n=1}^{\infty} \frac{t^{2n}}{(2n)!} (A^\varepsilon)^n u^0(x) \cdot \psi\left(x, \frac{x}{\varepsilon}\right) dx \\ = \int_{\Omega} \int_Y \sum_{n=1}^{\infty} \frac{t^{2n}}{(2n)!} \chi_f(y) (A_f)^n u^0(x) \cdot \psi(x, y) dy dx, \end{aligned} \quad (11.45)$$

$$\begin{aligned} \lim_{\varepsilon \rightarrow 0} \int_{\Omega} \sum_{n=1}^{\infty} \frac{t^{2n+1}}{(2n+1)!} (A^\varepsilon)^n v^0(x) \cdot \psi\left(x, \frac{x}{\varepsilon}\right) dx \\ = \int_{\Omega} \int_Y \sum_{n=1}^{\infty} \frac{t^{2n+1}}{(2n+1)!} \chi_f(y) (A_f)^n v^0(x) \cdot \psi(x, y) dy dx. \end{aligned} \quad (11.46)$$

It follows from (11.45) and (11.46) that for fixed  $t \in [0, T]$ , as  $\varepsilon \rightarrow 0$ ,  $u^\varepsilon(x, t) \xrightarrow{2} u(x, y, t)$ , where  $u$  is given by (11.28).

Proof of (ii). We can see from (11.28) that  $u \in C^2([0, T]; L^p(\Omega \times Y)^3)$ . Then by taking the second time derivative of both sides (11.28), we obtain

$$\begin{aligned} \partial_t^2 u(x, y, t) &= \chi_f(y) \sum_{n=0}^{\infty} \frac{t^{2n}}{(2n)!} (A_f)^{n+1} u^0(x) + \chi_f(y) \sum_{n=0}^{\infty} \frac{t^{2n+1}}{(2n+1)!} (A_f)^{n+1} v^0(x) \\ &= \chi_f(y) A_f (u^0 + t v^0)(x) \\ &\quad + \chi_f(y) A_f \sum_{n=1}^{\infty} \frac{t^{2n}}{(2n)!} (A_f)^n u^0(x) + \chi_f(y) A_f \sum_{n=1}^{\infty} \frac{t^{2n+1}}{(2n+1)!} (A_f)^n v^0(x) \end{aligned} \quad (11.47)$$

From (11.28) and the definition of  $\tilde{A}_f$ , given by (11.30), we see that

$$\begin{aligned} \tilde{A}_f u(x, y, t) - A_f (u^0 + t v^0)(x) &= \chi_f(y) A_f \sum_{n=1}^{\infty} \frac{t^{2n}}{(2n)!} (A_f)^n u^0(x) \\ &\quad + \chi_f(y) A_f \sum_{n=1}^{\infty} \frac{t^{2n+1}}{(2n+1)!} (A_f)^n v^0(x) \end{aligned} \quad (11.48)$$

Thus from (11.47) and (11.48) we obtain that

$$\partial_t^2 u(x, y, t) = \tilde{A}_f u(x, y, t) + (\chi_f(y) - 1) A_f (u^0 + t v^0)(x), \quad (11.49)$$

and hence (11.29) follows. The linear operator  $\tilde{A}_f$  is bounded on  $L^p(\Omega \times Y)^3$ . Thus  $u$  is the unique solution of (11.29).

Proof of (iii). From (11.27) and Proposition 9.9, we obtain that for fixed  $t \in [0, T]$ , as  $\varepsilon \rightarrow 0$ ,

$$u^\varepsilon(\cdot, t) \rightarrow \int_Y u(\cdot, y, t) dy \text{ weakly in } L^p(\Omega)^3.$$

By definition  $u^H(x, t) = \int_Y u(x, y, t) dy$ , thus (11.32) follows. It is clear that (11.31) follows from integrating (11.29) over  $Y$ .

Proof of (iv). Define

$$w(x, t) = \sum_{n=1}^{\infty} \frac{t^{2n}}{(2n)!} (A_f)^n u^0(x) + \sum_{n=1}^{\infty} \frac{t^{2n+1}}{(2n+1)!} (A_f)^n v^0(x). \quad (11.50)$$

Combining this equation with (11.28) gives (11.33). On the other hand, equation (11.50) implies that  $w \in C^2([0, T]; L^p(\Omega)^3)$ . Thus by taking the second time derivative of both sides of (11.50) gives

$$\begin{aligned} \partial_t^2 w(x, t) &= \sum_{n=0}^{\infty} \frac{t^{2n}}{(2n)!} (A_f)^{n+1} u^0(x) + \sum_{n=0}^{\infty} \frac{t^{2n+1}}{(2n+1)!} (A_f)^{n+1} v^0(x) \\ &= A_f(u^0 + tv^0)(x) + A_f \left( \sum_{n=1}^{\infty} \frac{t^{2n}}{(2n)!} (A_f)^n u^0 + \sum_{n=1}^{\infty} \frac{t^{2n+1}}{(2n+1)!} (A_f)^n v^0 \right) (x) \\ &= A_f(u^0 + tv^0)(x) + A_f w(x, t). \end{aligned} \quad (11.51)$$

Note that from (11.50) it is easy to see that  $w(x, 0) = 0$  and  $\partial_t w(x, 0) = 0$ . Combining this fact with (11.51), equation (11.34) follows. The fact that  $A_f$  is linear and bounded on  $L^p(\Omega)^3$  implies that  $w$  is the unique solution of (11.34).

Proof of (v). Extend  $\chi_f$  from  $Y$  to  $\mathbb{R}^3$  by periodicity. Then by making the substitution  $y = \frac{x}{\varepsilon}$  in (11.28), we obtain

$$\begin{aligned}
u\left(x, \frac{x}{\varepsilon}, t\right) &= u^0(x) + tv^0(x) + \chi_f^\varepsilon(x) \sum_{n=1}^{\infty} \frac{t^{2n}}{(2n)!} (A_f)^n u^0(x) \\
&\quad + \chi_f^\varepsilon(x) \sum_{n=1}^{\infty} \frac{t^{2n+1}}{(2n+1)!} (A_f)^n v^0(x) \\
&= u^0(x) + tv^0(x) + \sum_{n=1}^{\infty} \frac{t^{2n}}{(2n)!} (A_f^\varepsilon)^n u^0(x) \\
&\quad + \sum_{n=1}^{\infty} \frac{t^{2n+1}}{(2n+1)!} (A_f^\varepsilon)^n v^0(x), \tag{11.52}
\end{aligned}$$

where in the last equality we have used equation (11.37).

Now we compute the difference  $u^\varepsilon(x, t) - u(x, \frac{x}{\varepsilon}, t)$  using equations (11.19) and (11.52). We see that

$$\begin{aligned}
u^\varepsilon(x, t) - u\left(x, \frac{x}{\varepsilon}, t\right) &= \sum_{n=1}^{\infty} \frac{t^{2n}}{(2n)!} ((A^\varepsilon)^n - (A_f^\varepsilon)^n) u^0(x) \\
&\quad + \sum_{n=1}^{\infty} \frac{t^{2n+1}}{(2n+1)!} ((A^\varepsilon)^n - (A_f^\varepsilon)^n) v^0(x) \\
&= \sum_{n=1}^{\infty} \frac{t^{2n}}{(2n)!} (\varepsilon D_n^\varepsilon) u^0(x) + \sum_{n=1}^{\infty} \frac{t^{2n+1}}{(2n+1)!} (\varepsilon D_n^\varepsilon) v^0(x), \tag{11.53}
\end{aligned}$$

where in the last equality we have used equation (11.41). By taking the  $L^p$  norm in (11.53) and by using (11.42), we see that

$$\begin{aligned}
\|u^\varepsilon(x, t) - u\left(x, \frac{x}{\varepsilon}, t\right)\|_{L^p(\Omega)^3} &\leq \varepsilon \sum_{n=1}^{\infty} \frac{t^{2n}}{(2n)!} M^n \|u^0\|_{L^p(\Omega)^3} \\
&\quad + \varepsilon \sum_{n=1}^{\infty} \frac{t^{2n+1}}{(2n+1)!} M^n \|v^0\|_{L^p(\Omega)^3} \\
&= \varepsilon \left( \|u^0\|_{L^p(\Omega)^3} \cosh \sqrt{Mt} + \|v^0\|_{L^p(\Omega)^3} \frac{1}{\sqrt{M}} \sinh \sqrt{Mt} \right)
\end{aligned}$$

thus (11.36) follows, completing the proof.

### 11.2.1 Proof of (11.45) and (11.46)

In this section we prove (11.45). Equation (11.46) can be derived similarly.

We begin by the following observation

$$\sum_{n=1}^{\infty} \int_{\Omega} \left| \frac{t^{2n}}{(2n)!} (A^\varepsilon)^n u^0(x) \cdot \psi \left( x, \frac{x}{\varepsilon} \right) \right| dx < \infty. \quad (11.54)$$

To see this, we use Cauchy-Schwarz inequality to obtain

$$\int_{\Omega} \left| (A^\varepsilon)^n u^0(x) \cdot \psi \left( x, \frac{x}{\varepsilon} \right) \right| dx \leq \| (A^\varepsilon)^n u^0 \|_{L^2(\Omega)^3} \left\| \psi \left( x, \frac{x}{\varepsilon} \right) \right\|_{L^2(\Omega)^3}. \quad (11.55)$$

From Part (a) of Proposition 11.4, the operator  $A^\varepsilon$  is uniformly bounded on  $L^2(\Omega)^3$ .

Also, it is easy to see that

$$\left\| \psi \left( x, \frac{x}{\varepsilon} \right) \right\|_{L^2(\Omega)^3} \leq \| \psi \|_{L^2(\Omega; C_{per}(Y)^3)} := \left( \int_{\Omega} \sup_{y \in Y} |\psi(x, y)|^2 dx \right)^{1/2}.$$

We use these two facts in (11.55) to obtain

$$\int_{\Omega} \left| (A^\varepsilon)^n u^0(x) \cdot \psi \left( x, \frac{x}{\varepsilon} \right) \right| dx \leq M^n \| u^0 \|_{L^2(\Omega)^3} \| \psi \|_{L^2(\Omega; C_{per}(Y)^3)}, \quad (11.56)$$

for some  $M > 0$ . Therefore

$$\sum_{n=1}^{\infty} \int_{\Omega} \left| \frac{t^{2n}}{(2n)!} (A^\varepsilon)^n u^0(x) \cdot \psi \left( x, \frac{x}{\varepsilon} \right) \right| dx \leq \| u^0 \|_{L^2(\Omega)^3} \| \psi \|_{L^2(\Omega; C_{per}(Y)^3)} \sum_{n=1}^{\infty} \frac{t^{2n}}{(2n)!} M^n,$$

from which (11.54) follows.

Now from (11.54) and by using Lebesgue's dominated convergence theorem, it is straightforward to show that

$$\int_{\Omega} \sum_{n=1}^{\infty} \frac{t^{2n}}{(2n)!} (A^\varepsilon)^n u^0(x) \cdot \psi \left( x, \frac{x}{\varepsilon} \right) dx = \sum_{n=1}^{\infty} \int_{\Omega} \frac{t^{2n}}{(2n)!} (A^\varepsilon)^n u^0(x) \cdot \psi \left( x, \frac{x}{\varepsilon} \right) dx. \quad (11.57)$$

For  $n \in \mathbb{N}$ , we define

$$S_{N,\varepsilon} = \sum_{n=1}^N \frac{t^{2n}}{(2n)!} \int_{\Omega} (A^\varepsilon)^n u^0(x) \cdot \psi \left( x, \frac{x}{\varepsilon} \right) dx.$$

Then using (11.40) we see that

$$\lim_{\varepsilon \rightarrow 0} S_{N,\varepsilon} = \sum_{n=1}^N \frac{t^{2n}}{(2n)!} \int_{\Omega \times Y} \chi_f(y) (A_f)^n u^0(x) \cdot \psi(x, y) \, dx dy, \quad (11.58)$$

and hence

$$\lim_{N \rightarrow \infty} \lim_{\varepsilon \rightarrow 0} S_{N,\varepsilon} = \sum_{n=1}^{\infty} \frac{t^{2n}}{(2n)!} \int_{\Omega \times Y} \chi_f(y) (A_f)^n u^0(x) \cdot \psi(x, y) \, dx dy. \quad (11.59)$$

Below we will show that the order of the limits in (11.59) can be interchanged, i.e.,

$$\lim_{\varepsilon \rightarrow 0} \lim_{N \rightarrow \infty} S_{N,\varepsilon} = \lim_{N \rightarrow \infty} \lim_{\varepsilon \rightarrow 0} S_{N,\varepsilon}. \quad (11.60)$$

Combining this with (11.57) we obtain

$$\begin{aligned} \lim_{\varepsilon \rightarrow 0} \int_{\Omega} \sum_{n=1}^{\infty} \frac{t^{2n}}{(2n)!} (A^\varepsilon)^n u^0(x) \cdot \psi\left(x, \frac{x}{\varepsilon}\right) \, dx \\ = \sum_{n=1}^{\infty} \frac{t^{2n}}{(2n)!} \int_{\Omega \times Y} \chi_f(y) (A_f)^n u^0(x) \cdot \psi(x, y) \, dx dy. \end{aligned} \quad (11.61)$$

Applying arguments similar to those used in obtaining (11.57), we can show that

$$\begin{aligned} \sum_{n=1}^{\infty} \int_{\Omega \times Y} \frac{t^{2n}}{(2n)!} \chi_f(y) (A_f)^n u^0(x) \cdot \psi(x, y) \, dx dy \\ = \int_{\Omega \times Y} \sum_{n=1}^{\infty} \frac{t^{2n}}{(2n)!} \chi_f(y) (A_f)^n u^0(x) \cdot \psi(x, y) \, dx dy. \end{aligned} \quad (11.62)$$

From (11.61) and (11.62), the result (11.45) follows.

To complete the proof, it remains to justify (11.60). It is sufficient to show the double sequence  $(S_{N,\varepsilon})$  is Cauchy. So assume that  $N, L \in \mathbb{N}$  such that  $N \geq L$ . Then

$$\begin{aligned} |S_{N,\varepsilon} - S_{L,\varepsilon}| &= \left| \sum_{n=L+1}^N \frac{t^{2n}}{(2n)!} \int_{\Omega} (A^\varepsilon)^n u^0(x) \cdot \psi\left(x, \frac{x}{\varepsilon}\right) \, dx \right| \\ &\leq \sum_{n=L+1}^N \frac{t^{2n}}{(2n)!} \int_{\Omega} \left| (A^\varepsilon)^n u^0(x) \cdot \psi\left(x, \frac{x}{\varepsilon}\right) \right| \, dx \\ &\leq \|u^0\|_{L^2(\Omega)^3} \|\psi\|_{L^2(\Omega; C_{per}(Y)^3)} \sum_{n=L+1}^N \frac{t^{2n}}{(2n)!} M^n, \end{aligned} \quad (11.63)$$

where (11.56) was used in the last step. We note that the term  $\sum_{n=L+1}^N \frac{t^{2n}}{(2n)!} M^n$  in (11.63) can be made arbitrarily small by choosing large values of  $N$  and  $L$ . We conclude that for given  $\zeta > 0$ , there exists a positive integer  $K(\zeta)$  such that for  $N, L > K(\zeta)$  and all  $\varepsilon > 0$ ,

$$|S_{N,\varepsilon} - S_{L,\varepsilon}| < \zeta. \quad (11.64)$$

From (11.58) and (11.64), and by using Lemma 11.6 below, it follows that the double sequence  $(S_{N,\varepsilon})$  is Cauchy.

**Lemma 11.6.** *Let  $(a_{n,k})$  be a double sequence in  $\mathbb{R}^d$ ,  $d \in \mathbb{N}$ , such that*

(a) *For each  $n \in \mathbb{N}$ ,*

$$\lim_{k \rightarrow \infty} a_{n,k} = \bar{a}_n.$$

(b) *Given  $\zeta > 0$ , there exists a positive integer  $N = N(\zeta)$  such that for  $n, l > N$  and all  $k \in \mathbb{N}$ ,*

$$|a_{n,k} - a_{l,k}| < \zeta. \quad (11.65)$$

*Then the double sequence  $(a_{n,k})$  is Cauchy, and hence convergent.*

*Proof.* Let  $\zeta > 0$  and assume that  $N \in \mathbb{N}$  satisfies Part (b). Then consider the sequence  $(a_{N,k})_{k \in \mathbb{N}}$ . It follows from Part (a) that this sequence is convergent, and hence Cauchy. Thus there exists a positive integer  $K = K(N, \zeta)$  such that for  $k, m > K$ ,

$$|a_{N,k} - a_{N,m}| < \zeta. \quad (11.66)$$

Let  $J = \max\{N, K\}$ . Then from (11.65) and (11.66) we obtain that for  $n, l, k, m > J$ ,

$$\begin{aligned} |a_{n,k} - a_{l,m}| &\leq |a_{n,k} - a_{N,k}| + |a_{N,k} - a_{N,m}| + |a_{N,m} - a_{l,m}| \\ &\leq 3\zeta, \end{aligned}$$

and therefore the double sequence  $(a_{n,k})$  is Cauchy.  $\square$

# References

- [1] Allaire, G. (1992). “Homogenization and two-scale convergence.” *SIAM Journal on Mathematical Analysis* **23**, No. 6, pp. 1482–1518.
- [2] Allaire, G. and R.V. Kohn (1993). “Explicit optimal bounds on the elastic energy of a two-phase composite in two space dimensions.” *Quart. Appl. Math.* **51**, pp. 675 - 699.
- [3] Bazant, Z. and Planas, J. (1998). *Fracture and Size Effect in Concrete and Other Quasibrittle Materials*. CRC Press, Boca Raton, FL.
- [4] Bobaru, F. and Silling, S. A. (2004). “Peridynamic 3D problems of nanofiber networks and carbon nanotube-reinforced composites.” *Materials and Design: Proceedings of Numiform, American Institute of Physics*, pp. 1565 – 1570.
- [5] Bobaru, F., Silling, S. A., and Jiang, H. (2005). “Peridynamic fracture and damage modeling of membranes and nanofiber networks.” *Proceedings of the XI International Conference on Fracture, Turin, Italy*, 5748: 1–6.
- [6] Bobaru, F., Yang, M, Alves, L. F., Silling, S. A., Askari, E., and Xu, J. (2007). “Convergence, adaptive refinement, and scaling in 1D peridynamics.” [submitted].
- [7] Bonnetier, E. and Vogelius, M. (2000). “An elliptic regularity result for a composite medium with “touching” fibers of circular cross-section.” *SIAM J. Math. Anal.* **31**, pp. 651–677.
- [8] Caffarelli, L.A. and Peral, I. (1998). “On  $W^{1,p}$  estimates for elliptic equations in divergence form.” *Comm. Pure App. Math.* **51**, pp. 1–21.
- [9] Clark, G. W. and Showalter, R.E. (1999). “Two-scale convergence of a model for flow in a partially fissured medium.” *Electronic Journal of Differential Equations* **1999**, No. 02, pp. 1–20.
- [10] Dacorogna, B. (1989). *Direct Methods in the Calculus of Variations*. Springer-Verlag, Berlin, New York.
- [11] Dayal, K. and Bhattacharya, K. (2006). “Kinetics of phase transformations in the peridynamic formulation of continuum mechanics.” *Journal of the Mechanics and Physics of Solids* **54**, pp. 1811 - 1842.
- [12] E,W. (1992). “Homogenization of linear and nonlinear transport equations.” *Communications on Pure and Applied Mathematics* **45**, No. 3, pp. 301 - 326.

- [13] Emmrich, E. and Weckner, O. (2005). “Analysis and numerical approximation of an integrodifferential equation modelling non-local effects in linear elasticity.” *Mathematics and Mechanics of Solids*, published online first, DOI: 10.1177/1081286505059748.
- [14] Emmrich, E. and Weckner, O. (2006). “The peridynamic equation of motion in non-local elasticity theory.” In: C. A. Mota Soares et al. (eds.), III European Conference on Computational Mechanics. Solids, Structures and Coupled Problems in Engineering ,Lisbon, , Springer, 19 p.
- [15] Emmrich, E. and Weckner, O. (2007). “On the well-posedness of the linear peridynamic model and its convergence towards the Navier equation of linear elasticity.” [submitted].
- [16] Engel, K.-J. and Nagel, R. (2000). *One-Parameter Semigroups for Linear Evolution Equations*, Springer-Verlag, New York.
- [17] Faraco, D. (2003). “Milton’s conjecture on the regularity of solutions to isotropic equations.” *Annales de L’Institute Henri Poincare (c) Nonlinear Analysis* **20**, pp. 889–909.
- [18] Fattorini, H. O. (1983). *The Cauchy Problem*. Addison-Wesley. MR 84g:34003
- [19] Garroni A., Nesi, V. and Ponsiglione, M. (2001). “Dielectric breakdown: optimal bounds.” *Proc. R. Soc. Lond. A* **457** pp. 2317–2335.
- [20] Gerstle, W., Sau, N., and Silling, S. A. (2005). “Peridynamic modeling of plain and reinforced concrete structures.” SMiRT18: 18th Int. Conf. Struct. Mech. React. Technol., Beijing.
- [21] Golden K. and Papanicolaou G. (1983). “Bounds for effective parameters of heterogeneous media by analytic continuation.” *Comm. Math. Phys.* **90**, pp. 473–491.
- [22] Goldsztein, G.H. (2001). “Rigid-perfectly-plastic two-dimensional polycrystals.” *Proc. R. Soc. Lond.* **457**, pp. 2789–2798.
- [23] Gosse, J.H. and Christensen, S. (2001). “Strain invariant failure criteria for polymers in composite materials.” AIAA-2001–1184.
- [24] Grabovsky, Y. and Kohn, R. V. (1995). “Microstructures minimizing the energy of a two phase elastic composite in two space dimensions. II: The Vigdergauz microstructure.” *J. Mech. Phys. Solids.* **43**, pp. 949–972.
- [25] Hashin, Z. (1983). “Analysis of composite materials – a survey.” *Journal of Applied Mechanics* **50**, pp. 481–505.
- [26] Hashin, Z. (1962). “The elastic moduli of heterogeneous materials.” *Journal of Applied Mechanics* **29**, pp. 143–150.

- [27] Hashin, Z. and Shtrikman, S. (1962). “A variational approach to the theory of the effective magnetic permeability of multiphase materials.” *Journal of Applied Physics* **33**, pp. 3125–3131.
- [28] He, Q.C. (2007). “Lower bounds in the stress and strain fields inside random two-phase elastic media.” *Acta Mechanica* **188**, pp. 123–137.
- [29] Hill, R. (1963). “Elastic properties of reinforced solids: Some theoretical principles.” *J. Mech. Phys. Solids* **11**, pp. 357–372.
- [30] Jikov, V.V., Kozlov, S.M., and Oleinik, O.A. (1994). *Homogenization of Differential Operators and Integral Functionals*. Springer-Verlag, Berlin.
- [31] Jeulin, D. (2001). “Random structure models for homogenization and fracture statistics.” *Mechanics of Random and Multiscale Microstructures*, D. Jeulin and M. Ostoja-Starzewski, eds., CISM Courses and Lectures No. 430. Springer, Wien, New York, pp., 33–91.
- [32] Kelly, A. and Macmillan, N.H. (1986). *Strong Solids*. Monographs on the Physics and Chemistry of Materials. Clarendon Press, Oxford.
- [33] Kohn, R.V. and Little, T.D. (1998). “Some model problems of polycrystal plasticity with deficient basic crystals.” *SIAM J. Appl. Math.* **59**, pp. 172–197.
- [34] Kunstmann, P. C. (1999). “Distribution semigroups and abstract Cauchy problems.” *Transactions of the American Mathematical Society* **351**, No. 2, pp. 837 – 856.
- [35] Leonetti, F. and Nesi, V. (1997). “Quasiconformal solutions to certain first order systems and the proof of a conjecture of G.W. Milton.” *J. Math. Pures. Appl.* **76**, pp. 109–124.
- [36] Levy, O. and Bergman, D.J. (1994). “Critical behavior of the weakly nonlinear conductivity and flicker noise of two-component composites.” *Phys. Rev. B* **50**, pp. 3652–3660.
- [37] Li., Y. S. and Duxbury, P. M. (1989). “From moduli scaling to breakdown scaling: A moment-spectrum analysis.” *Phys. Rev. B* **40**, pp. 4889–4897.
- [38] Li., Y. and Nirenberg, L. (2003). “Estimates for elliptic systems from composite material.” *Communications on Pure and Applied Mathematics LVI*, pp. 892–925.
- [39] Li, Y.Y. and Vogelius, M. (2000). “Gradient estimates for solutions to divergence form elliptic equations with discontinuous coefficients.” *Arch. rational Mech. Anal.* **153**, pp. 91-151.

- [40] Lipton, R. (2004). “Optimal lower bounds on the electric-field concentration in composite media.” *Journal of Applied Physics* **96**, pp. 2821–2827.
- [41] Lipton, R. (2006). “Optimal lower bounds on the dilatational strain inside random two-phase elastic composites subjected to hydrostatic loading.” *Mechanics of Materials* **38**, pp. 833–839.
- [42] Lipton, R. (2005). “Optimal lower bounds on the hydrostatic stress amplification inside random two-phase elastic composites.” *Journal of the Mechanics and Physics of Solids* **53**, pp. 2471–2481.
- [43] Lipton, R. (2001). “Optimal inequalities for gradients of solutions of elliptic equations occurring in two-phase heat conductors. *SIAM J. Math. Analysis* **32**, pp. 1081–1093.
- [44] Lukkassen, D., Nguetseng, G., and Wall, P. (2002). “Two-scale convergence.” *International Journal of Pure and Applied Mathematics* **2**, No. 1, pp. 35–86.
- [45] Markov, K. and Preziosi, L. (2000). *Heterogeneous Media: Micromechanics Modeling Methods and Simulations (Modeling and Simulation in Science, Engineering and Technology)*. Birkhäuser Boston.
- [46] Maxwell Garnett, J.C. (1904). “Colours in metal glasses and in metallic films. *Philosophical Transactions of the Royal Society of London* **203**, pp. 385–420.
- [47] Melnikova, I. V. (1997). “Properties of Lions’s d-semigroups and generalized well-posedness of the Cauchy Problem.” *Functional Analysis and Its Applications* **31**, No. 3, pp. 167 - 175.
- [48] Milton, G.W. (2002). *The Theory of Composites*. Cambridge University Press, Cambridge.
- [49] Milton, G.W. (1986). “Modeling the properties of composites by laminates.” In: *Homogenization and Effective Moduli of Materials and Media*. Edited by J. Erickson, D. Kinderlehrer, R.V. Kohn, and J.L. Lions. *IMA Volumes in Mathematics and Its Applications* 1, pp. 150–174. Springer-Verlag, New York.
- [50] Nemat–Nasser, S. and Hori, M. (1999). *Micromechanics: Overall Properties of Heterogeneous Materials*. Elsevier, Amsterdam.
- [51] Nesi, V., Smyshlyaev, V.P. and Willis, J.R. (2000). “Improved bounds for the yield stress of a model polycrystalline material.” *J. Mech. Phys. Solids* **48**, pp. 1799–1825.
- [52] Neubrandner, F. (1988). “Integrated semigroups and their application to the abstract Cauchy problem.” *Pacific Journal of Mathematics* **135**, No. 1, pp. 111 – 157.

- [53] Nguetseng, G. (1989). “A general convergence result for a functional related to the theory of homogenization.” *SIAM Journal on Mathematical Analysis* **20**, No. 3, pp. 608 - 623.
- [54] Olsen, T. (1994). “Improvements on Taylor’s upper bounds for rigid–plastic composites.” *Materials Science and Engineering A175*, pp. 15–20.
- [55] Papanicolaou G. and S. R. S. Varadhan, S.R.S. (1982). “Boundary value problems with rapidly oscillating random coefficients, *Colloquia Mathematica Societatis Janos Bolyai* **27**, pp. 835–873.
- [56] Paul, B. (1960). “Prediction of elastic constants of multiphase materials.” *Trans. Metall. Soc. AIME* **218**, pp. 36–41.
- [57] Pazy, A. (1983). *Semigroups of Linear Operators and Applications to Partial Differential Equations*, Springer Verlag.
- [58] Ponte Castañeda, P. and Suquet, P. (1998). “Nonlinear Composites.” *Advances in Applied Mechanics* **34**, pp. 171–302.
- [59] Ponte Castaneda, P. and DeBotton, G. (1992). “On the homogenized yield strength of two-phase composites.” *Proc. Roy. Soc. Lond. A* **438**, pp. 419–431.
- [60] Rayleigh, L. (1892). “On the influence of obstacles arranged in rectangular order upon the properties of a medium.” *Philosophical Magazine* **34**, pp. 481–502.
- [61] Sachs, G. (1928). “Zur abeilung einer fleissbedingung.” *Z. Ver. Dtsch. Ing.* **72**, pp. 734–736.
- [62] Silling, S.A. (2000). “Reformulation of elasticity theory for discontinuities and long-range forces.” *Journal of the Mechanics and Physics of Solids* **48**, pp. 175 - 209.
- [63] Silling, S.A. (2003). “Dynamic fracture modeling with a meshfree peridynamic code.” In: Bathe KJ, editor. *Computational Fluid and Solid Mechanics*, Elsevier, Amsterdam, pp. 641 - 644.
- [64] Silling, S.A. and Askari, E. (2004). “Peridynamic modeling of impact damage.” In: Moody FJ, editor. *PVP-Vol. 489*, American Society of Mechanical Engineers, New York, pp. 197 - 205.
- [65] Silling, S.A. and Askari, E. (2005). “A meshfree method based on the peridynamic model of solid mechanics.” *Computers & Structures* **83** pp. 1526 - 1535.
- [66] Silling, S.A. and Bobaru, F. (2005). “Peridynamic modeling of membranes and fibers.” *International Journal of Nonlinear Mechanics* **40**, pp. 395 - 409.

- [67] Silling, S. A., Zimmermann, M., and Abeyaratne, R. (2003). “Deformation of a peridynamic bar.” *Journal of Elasticity* **73**, pp. 173 – 190.
- [68] Tartar, L. (1985). “Estimation Fine des Coefficients Homogénéisés.” in P. Kree (ed.), *E. De Giorgi colloquium (Paris, 1983)*, Pitman Publishing Ltd., London, pp. 168–187.
- [69] Taylor, G. (1938). “Plastic strains in metals.” *J. Inst. Metals* **62**, pp. 307–324.
- [70] Taylor, G.I. (1954). “The two coefficients of viscosity for an incompressible fluid containing air bubbles. Proceedings of the Royal society of London Series A **226**, pp. 34–39.
- [71] Torquato, S. (2002). *Random Heterogeneous Materials Microstructure and Macroscopic Properties*. Springer, New York.
- [72] Vigdergauz, S. B. (1994). “Two-dimensional grained composites of extreme rigidity.” *ASME J. Appl. Mech.* **61**, pp. 390–394.
- [73] Weckner, O. and Abeyaratne, R. (2005). “The effect of long-range forces on the dynamics of a bar.” *Journal of Mechanics and Physics of Solids* **53**, 3, pp. 705 – 728.
- [74] Wheeler, L. T. (1993). “Inhomogeneities of minimum stress concentration.” *Anisotropy and Inhomogeneity in Elasticity and Plasticity* (ed. Y. C. Angel), Vol. AMD–158. ASME, pp. 1–6.
- [75] Zimmermann, M. (2005). “A continuum theory with long-range forces for solids.” PhD Thesis, Massachusetts Institute of Technology, Department of Mechanical Engineering.

# Vita

Bacim Alali was born in December 1975, in Irbid, Jordan. He grew up in Ramtha, Jordan, and graduated from Ramtha High School in 1993. He completed his undergraduate studies in mathematics with minor in physics at Yarmouk University in 1998. From 1998 to 2002, he worked at Zeine Technological Applications, Jordan. In 2002 he came to Louisiana State University, where he completed a Master of Science degree in mathematics in 2005. Under the direction of Professor Robert Lipton, this dissertation is the culmination of his graduate study at Louisiana State University for the degree of Doctor of Philosophy.